Hypoxic Methane Oxidation Coupled to Denitrification in a Membrane Biofilm Reactor

by

Wael Saeed Alrashed

A thesis

presented to the University of Waterloo

in fulfillment of the

thesis requirement for the degree of

Doctor of Philosophy

in

Civil Engineering

Waterloo, Ontario, Canada, 2020

Examining Committee Membership

The following served on the Examining Committee for this thesis. The decision of the Examining Committee is by majority vote.

External Examiner   NAME: Yang Liu
Title: Professor

Supervisor   NAME: Hyung-Sool Lee
Title: Professor

Internal Member   NAME: Peter Huck
Title: Professor

Internal-external Member   NAME: Bonwoo Koo
Title: Professor

Other Member(s)   NAME: Ann Pham
Title: Professor

Author's declaration

This thesis consists of material all of which I authored or co-authored: see Statement of Contributions included in the thesis. This is a true copy of the thesis, including any required final revisions, as accepted by my examiners.

I understand that my thesis may be made electronically available to the public.

Abstract

Nitrate removal has become a necessity in Canada and around the globe as a means to mitigate harmful effects from nitrogen compounds, such as eutrophication, which pose toxic hazards to both aquatic life as well as human health. Nitrogen compounds, among other contaminants, will be or already have been regulated for drinking water and wastewater effluent. Thus, to aid in compliance with regulations, biological nitrogen removal has been thoroughly investigated using numerous bioreactor configurations and electron donors with consideration given to minimizing carbon footprint and finding cost-efficient methods. The membrane biofilm reactor (MBfR) is a bio-technique that has been investigated for the removal of various contaminants from water bodies and wastewater. This approach uses a gaseous substrate that serves as an electron donor (e.g., methane or hydrogen), which is supplied via a hollow-fiber membrane lumen to the acclimated biofilm on the outer surface. This technology is an option for efficient nitrate removal with methane as the primary electron donor and carbon source. This treatment is both practical and eco-friendly because methane can be produced on-site in wastewater treatment plants at a lower cost than methanol that is widely used for denitrification. Hence, the objectives of this study was to gain an advanced understanding of the process of methane oxidation coupled to denitrification (MOD) in a methane-based membrane biofilm reactor. The study also aimed to systematically characterize and optimize the effects of operating conditions, hydraulic retention time (HRT), nitrate loading rate (NLR), methane flux at high and low methane pressures. In addition, nitrite removal via methane-based MBfR was also explored to evaluate the sustainability of nitrite reduction compared to nitrate reduction in the denitrification process under hypoxic conditions. In addition, the microbial population in the MBfR was studied under different operating scenarios.

An MBfR with gas-permeable hydrophobic polyethylene fibers, enriched with MOD culture was operated while applying high methane pressures (7, 5, and 2 psig), and total specific surface area of 35 m^2/m^3, have showed a relatively low nitrate removal rate, with 1.2 – 1.3 mg N/L-h at methane pressure of 2-7 psig and HRT 12 h, while the dissolved methane was as high as (8 -13 mg CH_4/L). These results suggest that the methane oxidation and nitrate reduction are limited by the microorganism's kinetics, rather than methane transfer to the biofilm. The sequencing

analysis showed *Methylocystaceae* was dominant, with 21% of bacterial SSU rRNA genes. Moreover, there were no traces of archaea in the community in either biofilm or planktonic samples. An MBfR enriched with *Methylocystaceae* using a hydrophobic polyvinylidene difluoride (PVDF) gas permeable membranes, with total surface area of 188.5 cm^2, was operated at low methane pressures (0.05 – 0.25 psig) to monitor the impact on the dissolved methane concentrations and nitrate reduction. The nitrate concentration in the effluent was 4.0 mg NO_3^-/L, with a minimal methane concentration in the effluent of 3.3 mg CH_4/L with a hydraulic retention time of 4 hours. These results imply that the implication of this type of gas permeable membranes have proven to be more efficient in methane gas delivery, in which the nitrate removal flux was as high as 412.2 mg N/m^2-d, and successfully managed to decrease the dissolved methane in the effluent. The dissolved oxygen in the MBfR recorded an average of 0.04 mg O_2/L. The 16S rRNA gene sequencing analysis detected *Methylococcus* bacteria that are able to oxidize methane coupled to denitrification. The results indicated syntrophic microbial interaction in a consortium of aerobic methanotrophs and denitrifiers in the active biofilm of a methane-based MBfR under hypoxic conditions. A methane-based MBfR inoculated with 21% *Methylocystaceae* in bacterial SSU rRNA genes, evidenced to have the ability to remove nitrite; with a removal flux was up to 885 mg N/m^2-d, at a relatively low methane pressure of 2.4 kPa (0.35 psig); indicating that nitrite reduction step is not the main rate limiting step in the denitrification process inside the biofilm. The microbial community sequencing showed the existence of *Methylococcus capsulatus*, a *Type I methanotroph*, at relative abundance of 78% for the maximum HRT of 12 hours and a methane pressure of 0.35 kPa (0.05 psig), while the relative abundance decreased when the HRT was 4 and 2 hours at the same methane pressure. This implies that we cannot correlate *Methylococcus capsulatus* abundance to the electron donor (methane) flux in this particular experimental set. The study outcomes support that methane-based MBfRs can be a proficient and sustainable biotechnology approach to meet strict nitrogen standards in wastewater effluent, under hypoxic conditions with insignificant methane buildup.

Acknowledgments

In the beginning, I wish to sincerely express my gratitude to my supervisor Prof. Hyung-Sool Lee, for allowing me to join his research group. During the last few years, I have gained a tremendous amount of experience, both scientific and broad knowledge, that I have already benefited from, and I will continue to do so in the future. His support and guidance were unlimited, even in the harshest and stressful periods. I extended my thanks to the Ph.D. committee members: Prof. Huck, Prof. Koo, Prof. Pham, and Prof. Yang Liu. for their helpful guidance and valuable feedback. I wish to thank our research collaborators Prof. Josh, and Katjia from the Biology department for their genuine help. I am very appreciative to all previous and current members at Waterloo Environmental Biotechnology Laboratory (WEBL). Special thanks to Dr. Lee, Jangho, for his research collaboration and assistance. I also wish to thank Dr. Bipro Dhar for his generous aid, especially when I first came to Waterloo; he was always supportive; also, I want to thank and Dr. Chandra, Rashmi, for her support and useful remarks. I must thank the civil engineering department technical staff; both Mark Merlau and Mark Sobon, they went above and beyond in aiding me in many laboratory tasks. Finally, I wish to express my deepest gratitude to my parents for their support, even during these turbulent times. I also express my thanks to my wife and my son Faisal Alrashed. Lastly, I wish to thank every person who believed in me.

Dedication

To my parents, my wife, and my son.

Table of Contents

List of Figures

microorganisms.

flux and fixed methane pressure of 0.05 psig (0.35 kPa) for 8, 4, and 2 h HRTs.
(a) at influent concentration of 20 mg NO_2^--N/L. (b) at influent concentration of
40 mg NO_2^--N/L.

List of Tables

Nomenclature

AnMBR	Anaerobic membrane bioreactor
MOD	Methane oxidation coupled to denitrification
b	Endogenous-decay coefficient
BOD	Biochemical oxygen demand
COD	Chemical oxygen demand
CSTR	Continuously Stirred Tank Reactor
DB	Denitrifying bacteria
DI	Deionized Water
ECD	Electron Capture Detector
GC	Gas Chromatography
GC-TCD	Gas Chromatography –Thermal Conductivity Detector
HRT	Hydraulic Residence Time
IC	Ion Chromatography
K_H	Henry's Law constant
Ks	Half saturation constant
MBfR	Membrane biofilm reactor
NB	Nitrifying bacteria
NLR	Nitrate Loading Rate
T	Operating temperature (K)
TCD	Thermal Conductivity Detector
VSS	Volatile suspended solids
X_a	Active biomass
R	Ideal gas constant (8.314 J/mol-K)
S	Substrate concentration (g COD/m^3)
J_{CH4}	specific mass flux (g/m^3. s)

Chapter 1

Introduction

1.1 Background

The global community faces a variety of environmental issues related to energy consumption, water security, and climate change, which drives the development of more sustainable wastewater treatment. Numerous studies that address these issues have produced innovative technologies that manage to recover energy in addition to removing undesirable contaminates via optimum utilization of biologically based technology. One of these biotechnologies is anaerobic and anoxic wastewater treatment, where oxygen levels are maintained at extremely trivial levels. Moreover, this biotechnology improves energy efficiency and sustainability because of energy recovery and re-use, reduced sludge production, and lack of aeration. For instance, anaerobic membrane bioreactors (AnMBRs) show promise in that dilute wastewater, such as municipal wastewater, facilitate treatment in an energy-neutral manner (Bq et al., 2006; Yeo & Lee, 2013). Several studies have reported that the removal of the biochemical oxygen demand (BOD), chemical oxygen demand (COD), and total suspended solids (TSS) concentrations from the permeate in AnMBRs treating domestic wastewater were less than 88%, 90%, and 98%, respectively (Saddoud et al., 2007; Huang et al., 2011). However, there are several limitations to be addressed when deploying anaerobic wastewater treatment in the field, and one of the most important challenges is nitrogen control. Compared to activated sludge (AS) processes, anaerobic wastewater treatment lacks an oxidation step for organic and ammonium nitrogen, which is essential for biological nitrogen removal. Nitrogen recovery using adsorption or ion exchange might be sustainable, and operating costs for adsorption/ion exchange processes are not high. However, re-utilization of recovered nitrogen requires further purification steps that inevitably end up increasing costs. In addition to this, there are no solid markets for nitrogen recovered from wastewater. Hence, there is a need for

new economic nitrogen control processes that complement anaerobic wastewater treatment and fully utilize the benefits of anaerobic wastewater treatment, thus improving the sustainability of wastewater management.

Conventional heterotrophic denitrification that employs an exogenous electron donor (e.g., methanol) is not an economical solution for nitrogen removal in anaerobic wastewater treatment processes due to the expensive cost of methanol at ~CAD 450/MT (Methanex, 2019). Anaerobic wastewater treatment using fermentation and methanogenesis generates methane gas. If the methane produced from wastewater can be used as the electron donor for denitrification, the process will help remove nitrogen without incurring any significant costs. Thus, the benefits of anaerobic wastewater treatment (energy, less sludge production, and lack of aeration) can be retained, along with ensuring high effluent quality. In this dissertation, a new denitrification bioprocess is presented that uses methane gas as an electron donor and carbon source under hypoxic conditions. The idea is to improve denitrification rates through a unique and advanced technology utilizing a special biofilm reactor that employs gas-permeable membranes as media for biofilm formation and the provision of methane gas for methane oxidation coupled with denitrification (MOD) microorganisms. This biofilm reactor, known as a membrane biofilm reactor (MBfR), was first developed for autotrophic denitrification in a hydrogen-based MBfR (Lee & Rittmann, 2002). MBfRs have two distinct advantages over other biofilm processes. The first advantage is the maintenance of high biofilm density in bioreactors by simply increasing the membrane-packing density (m^2 of membrane surface area/m^3 of bioreactor) without creating significant suspended solids in the bioreactor's effluent (Martin & Nerenberg, 2012). The second advantage is the supply of a high concentration of electron donor (e.g., methane molecules) to target the microorganisms growing on the surface of the membranes. This unique supply of electron donor through gas-permeable membranes allows the microorganisms to be more active

throughout the biofilms on the membrane's surface (Martin & Nerenberg, 2012; Tang, 2012). These two features of MBfRs can improve the denitrification rate and efficiency as compared to other bioprocesses (Martin & Nerenberg, 2012). The advantages and features of this process will be further elaborated upon in the literature review chapter.

1.2 Scope and Objectives

The principal objective of this study was to obtain an advanced understanding of the applicability of methane oxidation coupled to denitrification process in methane-based MBfRs under hypoxic conditions. The explicit objectives were to optimize MBfR performance for MOD by assessing the following parameters: hydraulic retention time (HRT), nitrate loading rate (NLR), methane pressure, and flux at high and low methane pressures. Nitrite removal via methane-based MBfR was also investigated to assess the nitrite reduction kinetics. Also investigated were the dynamics of microbial communities in the biofilm of the MBfRs under various operating scenarios. This provides deep insights into the syntrophic interactions within the microbial consortium and improves the identification of the optimum operating conditions for the MBfR.

1.3 Thesis Outline

This thesis comprises of six chapters, references, and appendices. Chapter one (current chapter) provides background information on the research topic and a summary of the goals of this research. Chapter two presents an overview of the existing literature related to the thesis research. Chapter three, four and five are the main dissertation chapters, presented in an article format. Chapter six summarizes the findings with keen focus on scientific and engineering implications of the results and provides recommendations for future research.

Chapter 2
Literature Review

2.1 Implications of Nitrogen Removal in Wastewater Treatment

Throughout the literature, it has been well-established that human activities such as excessive utilization of nitrogen fertilizers and combustion by-products have increased the amount of nitrogen discharged to the environment. Subsequently, this nitrogen flows to bodies of water, causing contamination that threatens aquatic ecosystems and human health, both directly and indirectly (Erisman et al., 2015; Mosier et al., 2013; Townsend et al., 2003; Zeng et al., 2016). In fact, human alteration of the nitrogen balance in nature has had an impact on the nitrogen cycle. For example, the concentration of gaseous nitrogen forms in the atmosphere has been augmented, leading to the accumulation of toxic fog (Vitousek et al., 1997). Nonetheless, nitrogen is vital for all living species because it is one of the constituents of nucleic acids and proteins (Bothe et al., 2007). The nitrogen cycle refers to the conversion of nitrogen to different forms via physical or biological processes such as fixation or through bacterial influence, including ammonification, nitrification, and denitrification, as illustrated in Figure 2.1 (Bothe et al., 2007; Harrison, 2003).

Among other nitrogen species (e.g., ammonium and nitrite), the nitrate ion (NO_3^-) can be formed as a product of the nitrification process whereby ammonium nitrogen is oxidized to nitrite via nitrifying bacteria (NB). Nitrate is a naturally existing anion found in the soil and groundwater (Bothe et al., 2007; Pinar et al., 1997). Factors such as soil characteristics, the aging of water in the aquifers, and geochemistry have contributed to increased nitrate concentrations in groundwater (Dubrovsky & Hamilton, 2010).
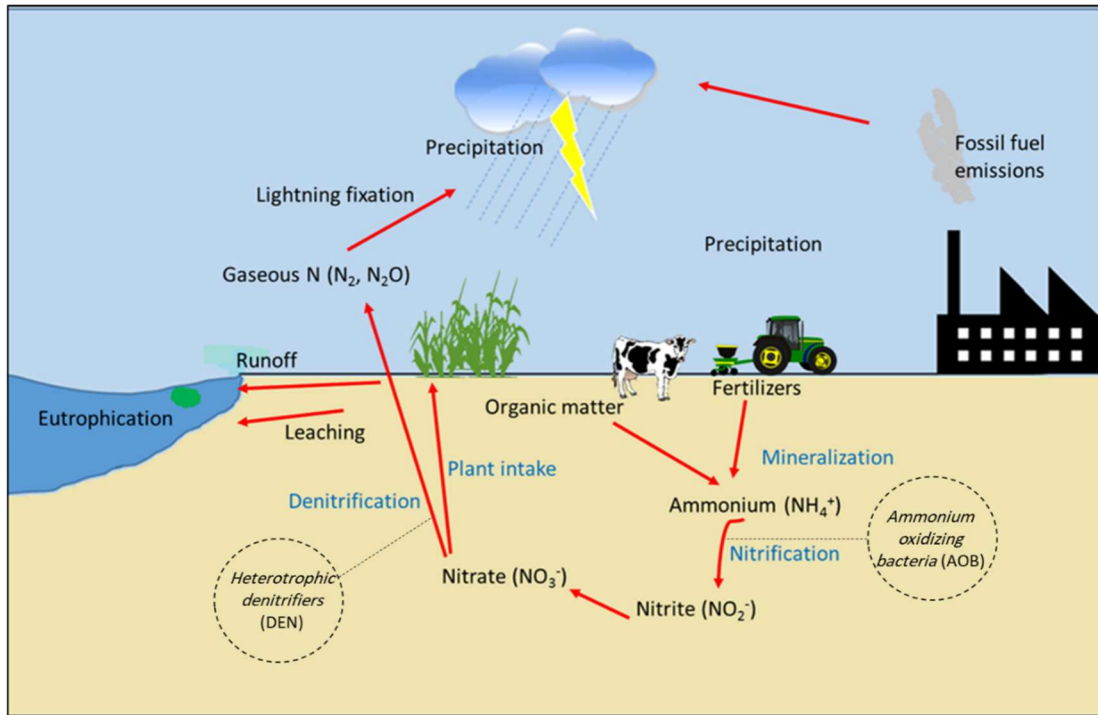
Figure 2-1. The nitrogen cycle, illustrating the biochemical pathways (Scott et al., 2006).

It has been reported that uptake of high concentrations of nitrates by humans through drinking water or by consuming vegetables is related to several serious diseases (Fann et al., 1993; Powlson et al., 2008; Santamaria et al., 2006). For example, methemoglobinemia (blue baby syndrome), a disease that is most dominant in communities that depend on groundwater for their daily supply of drinking water, is caused by water that is contaminated with elevated levels of nitrates (Fewtrell, 2004; Knobeloch et al., 2000). Nitrate intake correlates with gastrointestinal cancer and cardiovascular system complications (Habermeyer et al., 2015; Hord et al., 2009). Beyond human disease, it has been reported that elevated concentrations of nitrate nitrogen, among other ionic forms of nitrogen, negatively impacts the ecosystem. Effects include eutrophication of water bodies, which has a direct impact on oxygen depletion; acidification as a result of the increase of hydrogen ions due to multiple chemical reactions in the absence of adequate buffering capacity;

and deleterious impacts on the growth of aquatic life due to the impairment caused by toxic algae overgrowth (Camargo & Alonso, 2006; Dodds et al., 2002; Schindler et al., 1996).

Beyond the direct impact on human health, the impact of elevated nitrate concentrations on the ecosystem and aquatic life has been widely recognized and has influenced the implementation of regulations governing wastewater treatment plants. Thus, guidelines have been established to regulate acceptable nitrate levels. According to the World Health Organization (WHO), the maximum allowable nitrate content in drinking water is 50 mg/L. The Canadian regulation for nitrate in drinking water is 45 mg/L as nitrate, which is equivalent to 10 mg/L as (NO_3^-N) (Health Canada, 2013). This limit was the driving force for researchers to develop adequate and reliable nitrate removal methods. Subsequently, various removal techniques have been developed, including physical, chemical, and biological processes, to mitigate the adverse effects of nitrate on aquatic ecosystems and human health. These techniques include ion exchange and biological denitrification (the reduction of nitrate to nitrogen gas). Furthermore, treatment via bioreactor membranes has been researched extensively using various configurations in order to reach optimum nitrate removal.

The physical and chemical properties of nitrate have made treatment via conventional methods, such as coagulation, sedimentation, and filtration, challenging. Thus, advanced treatment techniques, including ion exchange and reverse osmosis, have been used for nitrate removal (Fonseca, 2000; McAdam & Judd, 2006). Ion exchange; membrane filtration using nano-filtration, or reverse osmosis; and electrodialysis are typical physicochemical nitrate removal methods. The high efficacy of the ion exchange process for nitrate removal has made this type of treatment one of the most commonly applied in treatment plants. The ion exchange removes nitrate by replacing it with counter anions such as chloride and bicarbonate (Cl^- or HCO_3^-) in an exchange bed with high

levels of a strong base. Accordingly, the bed will be saturated and require a further process of regeneration or replacement (Clifford & Liu, 1993), adding cost. On the other hand, physical treatment such as reverse osmosis (RO), which can be defined as the application of high pressure through a dense membrane that only allows water molecules to pass through, retains all dissolved salts and ions in the raw water, including nitrate ions (Missimer et al., 2013). However, membrane fouling limits the performance of RO membranes, in which case additional pre-treatment and post-treatment is required. As a result, the additional processes will increase both capital and operational costs (Fangang et al., 2008). Moreover, it has been recognized that RO operational and maintenance costs are much higher than the ion exchange process, which makes it less feasible and, therefore, less frequently used only for nitrate control. Electrodialysis is another treatment technology in which a combination of electrical and chemical processes is applied for the removal of various ions by forcing the polluted water to pass through a membrane stacked with alternative anions and cations driven by a direct current (DC) force in addition to the high pressure (Sahli et al., 2008). Subsequently, the ion exchange membrane removes nitrate and washes it out as a waste product (Brylev et al., 2007; Elmidaoui et al., 2001). However, this technique also has shortcomings. The complex operational features of the system may hinder performance in full-scale applications, and the highly contaminated waste by-products require additional treatment. Furthermore, pH control may be considered an operational disadvantage (Health Canada, 2013; Kapoor & Viraraghaven, 1997). When considering economic efficiency in nitrate removal, it appears that biological methods would be the best solution. The next section will discuss biological nitrogen removal processes.

2.2 Biological Nitrogen Removal

Biological nitrogen removal (BNR) is a popular process in wastewater treatment that includes both nitrification and denitrification steps. Nitrification is a nitrogen oxidation reaction in which reduced forms of nitrogenous compounds (e.g., ammonium nitrogen) are oxidized to nitrite and nitrate. Denitrification is a nitrogen reduction reaction in which nitrate is reduced to nitrogen gas. Eq. (2.1) describe nitrification reactions using oxygen molecules as the terminal electron acceptor: ammonium nitrogen to nitrite, and nitrite to nitrate, respectively (Howards et al., 1985).

$$NH_4^+ + \frac{3}{2} O_2 \rightarrow NO_2^- + 2H^+ + H_2O \tag{2.1}$$

In denitrification, nitrate acts as the terminal electron acceptor, which means that the denitrifying bacteria need an electron donor for denitrification. Typically, denitrification is considered as a cascade of reduction reactions, as shown in Eq. (2.2), and the full denitrification route can be expressed in the half-reaction in Eq. (2.3) (Knowles, 1982; Metcalf & Eddy, 2003).

$$NO_3^- \rightarrow NO_2^- \rightarrow NO \rightarrow N_2O \rightarrow N_2 \tag{2.2}$$

$$2NO_3^- + 10\ e^- + 12H^+ \rightarrow N_2 + 6H_2O \tag{2.3}$$

Organic carbon sources such as methanol are widely used as electron donors to perform denitrification in the field. In this case, denitrifying bacteria use the organic matter as carbon sources, and hence, this denitrification is referred to as heterotrophic denitrification. The carbon and electron sources can be separated. For example, hydrogen gas or elemental sulfur can be used as electron donors for denitrifying bacteria (Xia et al., 2010). These types of bacteria can use inorganic carbon (e.g., carbon dioxide) as a carbon source, and hence this type of denitrification is called autotrophic denitrification. Next, the two denitrification processes are compared.

2.2.1 Heterotrophic and Autotrophic Denitrification

Heterotrophic denitrification can be defined as the biological removal of nitrate (terminal electron acceptor) in the presence of an external organic (electron donor) carbon source such as methanol (Liessens et al., 1993). Table 2.1 lists the stoichiometry for methanol, ethanol, and acetic acid for denitrification, and it can be seen that methanol has the uppermost C/N molar ratio (Mateju et al., 1992; McAdam & Judd, 2006; Zhou, 2007).

Table 2-1. Heterotrophic denitrification using various carbonaceous substrates

Substrate *(electron donor & carbon source)*	Stoichiometric reaction
Methanol	$1.08\ CH_3OH + NO_3- + 0.24\ H_2CO_3 \rightarrow 0.056\ C_5H_7O_2N + 0.47\ N_2 + 1.68\ H_2O + HCO_3^-$
Ethanol	$0.69\ C_2H_5OH + NO_3^- + H^+ \rightarrow 0.14\ C_5H_7O_2N + 0.43\ N_2 + 0.67\ CO_2 + 2.07\ H_2O$
Acetic Acid	$0.819\ CH_3COOH + NO_3 \rightarrow 0.068\ C_5H_7NO_2 + HCO_3 + 0.30\ CO_2 + 0.902\ H_2O + 0.466\ N_2$

The high performance of heterotrophic denitrification in wastewater treatment underlies its frequent use among biological treatment methods (Nerenberg, 2003). One of the disadvantages inherent to heterotrophic denitrification is the production of residual amounts of organic carbon in the treatment effluent, and as a result, issues such as taste and odor, corrosion, and contamination may occur (Rittmann & Huck, 1989). In comparison, the organic matter concentration can be less, such as in groundwater, which may hinder the denitrification process. Furthermore, the presence of alcoholic compounds (methanol and ethanol) raises some health concerns if their concentration in the effluents exceeds the regulated levels.

Unlike the heterotrophic denitrification process, autotrophic denitrifiers such as *Thiomicrospira*

denitrificans obtain their energy source from inorganic compounds by reducing nitrate to nitrogen

gas. Compounds such as hydrogen gas, elemental sulfur, and hydrogen sulfide are utilized as

external electron donors (Kim et al., 2008). Autotrophic denitrifiers also extract their carbon

requirements from inorganic compounds of carbon dioxide and bicarbonate (Lamp & Zhang, 1996;

Syed et al., 2006). Therefore, autotrophic denitrification offers the advantage of avoiding the need

for an exogenous organic carbon source (e.g., ethanol and methanol), which is ideal for nitrate

control in groundwater. A summary of the advantages and disadvantages of both heterotrophic and

autotrophic denitrification is provided in Table 2.2.

Table 2-2. Comparison of heterotrophic denitrification versus autotrophic denitrification

	Advantages	Disadvantages
Heterotrophic Denitrification	High efficiency of nitrate removal.	The need for external organic carbon source (e.g., methanol).
Autotrophic denitrification	• External carbon source is not required. • Minimization of sludge production.	The usage of inorganic electron donor (e.g., H_2 gas), which is relatively expensive and challenging to handle.

2.2.2 Anaerobic Ammonium Oxidation

In addition to the previously mentioned biological removal approaches, there is one unique

biological denitrification process: anammox. In this process, ammonium is partially oxidized to

nitrite anaerobically, and the nitrite is reduced to dinitrogen by using residual ammonium as the

electron donor (Schmidt & Bock, 2002). Anammox within the context of engineered systems was

first discovered in 1995 at a denitrifying reactor (Mulder et al., 1995; Strous et al., 1998), and it has

gained tremendous levels of attention from engineers and scientists as energy and sustainable

issues became significant in water and wastewater treatment. Anammox processes can be more

economical than existing BNR systems in that the electron donor is free (existing ammonium in wastewater), especially for wastewater with high ammonium concentrations (Ali et al., 2013; Kartal et al., 2010). However, anammox seems unsuitable for areas with cold winter seasons, such as Canada, because anammox bacteria (e.g., *Candidatus Brocadia anammoxidans*) are very sensitive to low temperatures (Awata et al., 2015; Lackner et al., 2015). Table 2.3 summarizes the advantages and drawbacks of this process.

Table 2-3. Advantages and disadvantages of anammox process

Advantages	Disadvantages	Reference
• The supply for additional organic carbon is not needed.	• Low microbial growth rate (0.07/day).	Strous et al., 1998
• Reduced energy consumption used in WWTPs.	• Long operating retention time.	Fernández et al., 2008
• Lower mass of sludge produced.	• Sensitivity to high concentration of nitrite and heavy metals.	Jin et al., 2012
• Cost efficient.	• Poor performance at low temperatures.	Awata et al., 2015
	• pH control is required.	Tao et al., 2012

2.3 Aerobic Methane Oxidation Coupled to Denitrification

The process of aerobic methane oxidation coupled to denitrification has been thoroughly investigated in both batch and continuously operated reactors (Ettwig et al., 2010; Liu et al., 2014; Modin et al., 2008). In this process, methane is oxidized via aerobic methanotrophs releasing organic compounds that are then utilized by denitrifying bacteria as electron donors and carbon sources to complete the denitrification process. In the presence of oxygen, aerobic methanotrophs are able to oxidize methane to carbon dioxide. Furthermore, aerobic methanotrophs are classified into groups based on properties of their morphology, membrane structure and the assimilation of

formaldehyde pathway (Jing et al., 2016; Trotsenko et al., 2005). The type I methanotrophs belongs to the *Methylococcaceae* family and the formaldehyde generated from methane or methanol oxidation is assimilated via the ribulose monophosphate (RuMP) pathway. While in type II methanotrophs that belong to the *Methylocystaceae* family, formaldehyde is assimilated through the serine pathway. In addition, type I methanotrophs have higher methane oxidation rate, possibly leading to more organic intermediates produced. As a result, denitrifies can utilize the intermediates to complete denitrification rapidly coupled to methane oxidation (Liu et al., 2014). Furthermore, it is reported in a recent study that type I methanotrophs (e.g., *Methylococcus*) had a maximum specific growth rate of 0.36/h (Alsayed et a., 2018), which is higher than that for the type II methanotrophs. For instance, the maximum specific growth rates for *Methylosinus sporium* and *Methylosinus trichosporium* OB3b were reported at 0.093/h and 0.29/h, respectively (Ordaz et al., 2014; Rostkowski et al., 2013). Table 2-4 compares type I and II methanotrophs properties, morphology and microbial growth kinetics. In addition, Figure 2-2 illustrates the presumed aerobic methane oxidation coupled to denitrification pathway
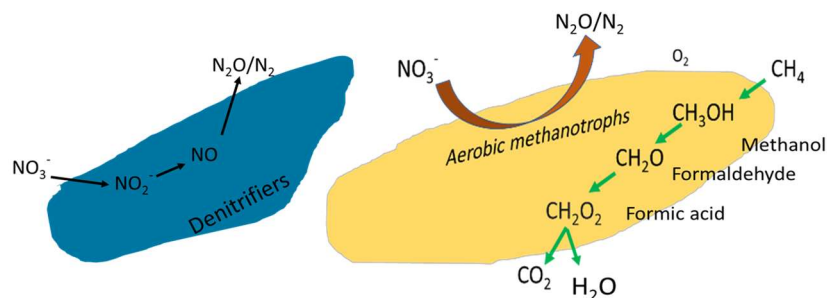
Figure 2-2. The proposed pathway of aerobic methane oxidation coupled to denitrification via aerobic methanotrophs.

Table 2-4: Comparison between type I and II aerobic methanotrophic bacteria characteristics.

Characteristics	Type I methanotrophs	Type II methanotrophs
Morphological features	Cocci, short rods	Crescent rods
Formaldehyde assimilation pathway	Ribulose monophosphate (RuMP) pathway	Serine pathway
Maximum specific growth rate (1/h)	0.36	0.09-0.29
pH growth span	4.0 – 9.5	4.2 – 9.0
Fixation of N_2	Capable	Not capable
Growth Temperature	(0-72 °C)	(1-40 °C)

2.4 Anaerobic and Hypoxic Methane Oxidation Coupled to Denitrification

The oxidation of methane under anaerobic conditions and extremely low oxygen concentrations has attained tremendous attention to better understand the global methane efflux. Anaerobic methane oxidation (AMO) was initially discovered in sulfate- and methane-rich environments (Valentine & Reeburgh, 2000), in which marine sediments exhibited the microbial consortium of methane-oxidizing archaea and sulfate-reducing bacteria (SRB). From a metagenomic perspective, reverse methanogenesis, which is the capability of methanotrophic archaea to consume methane anaerobically and produce carbon dioxide, was investigated, and verified using marine sediment samples (He et al., 2015).

Even though sulfate is considered the terminal electron acceptor coupled to AMO, other electron acceptors exhibit the ability to be coupled with AMO, such as nitrite or nitrate. Eq. (2.4) and (2.5) show overall reactions of AMO coupled with nitrate and nitrite and their standard Gibbs free energy, which highlights that both reactions were thermodynamically favorable. Raghoebarsing et al. (2006) reported successful nitrate reduction to nitrogen gas (21.5 µmol N_2/h) coupled with AMO.

$$5CH_4 + 8NO_3^- + 8H^+ \rightarrow 5CO_2 + 4N_2 + 14H_2O \quad \Delta G^{\circ\prime} = -765 \frac{KJ}{mol\ CH_4} \quad\quad (2.4)$$

$$3CH_4 + 8NO_2^- + 8H^+ \rightarrow 3CO_2 + 4N_2 + 10H_2O \quad \Delta G^{\circ\prime} = -928 \frac{KJ}{mol\ CH_4} \quad\quad (2.5)$$
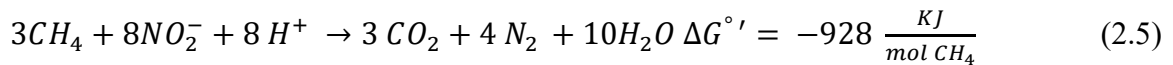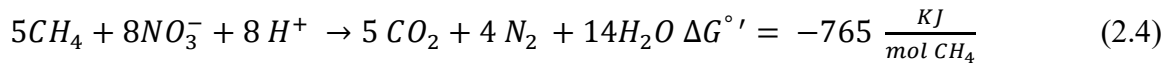
Figure 2.3 summarizes the proposed AMO mechanisms. First, the anaerobic methanotroph archaea (ANME-1) are coupled with SRB to anaerobically oxidize methane to carbon dioxide. Second, AMO coupling with nitrate reduction is facilitated by the consortium of anaerobic methanotroph archaea (ANME-2d) and anammox bacteria. The final mechanism is similar to the second mechanism except that nitrite reduction is accomplished by NC10 bacteria (*Candidatus* Methylomirabilis oxyfera), which compete for methane with the anaerobic methanotroph archaea (Hu et al., 2009; Raghoebarsing et al., 2006; Ettwig et al., 2010). NC10 bacteria is unique in that NO is split to N_2 and O_2. This internal O_2 is the source to aerobic methane oxidation pathway, which is the same to aerobic methanotroph pathway.
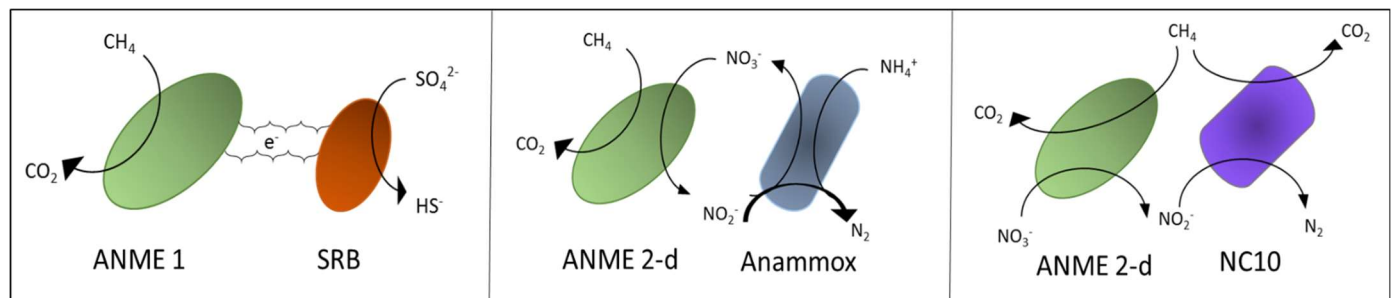
Figure 2-3. Mechanisms of anaerobic methane oxidation (adapted from McGlynn et al., 2015; Wegener et al., 2015).

Table 2-5 provides an insightful comparison between various denitrification reactors coupled to anaerobic and aerobic methane oxidation. It can be seen that anaerobic methane oxidation coupled to denitrification (AMO-D) has lower removal rates than aerobic methane oxidation coupled to denitrification, which can be attributed to the highly kinetic features of aerobic methanotrophs: Intermediates (e.g., methanol or formate) accumulated by the methanotrophs can be used by

denitrifiers for nitrate reduction to dinitrogen (Eisentraeger et al., 2001; Modin et al., 2007). It is apparent that it is necessary to improve AMO-D kinetics for engineering AMO-D systems in the field, and unfortunately, there is limited information on AMO-D reaction rates in the literature. Furthermore, Wang (2014) studied the microbial population dynamics for denitrification in activated sludge process under hypoxic and anoxic conditions. However, methanol was used as the main carbon source in this research. The study finding showed that maintaining DO levels under 0.10 mg O_2/L has proven to be optimum for efficient denitrification.

Table 2-5: Comparison between various denitrification reactors coupled to anaerobic and aerobic methane oxidation

Type of experiment	Type of methane	Denitrification rate		References
		mg N	mg N/ g. VSS-h	
Batch reactor (0.5 L)	AMO	–	0.20	Islas-Lima et al. (2004)
Batch reactor (1.0 L)	AMO	–	0.4	Raghoebarsing et al. (2006)
Batch reactor (0.4 L)	Aerobic-MO	2.0	–	Thalasso et al. (1997)
Batch reactor (5.0 L)	Aerobic-MO	3.30	–	Houbron et al. (1999)
MBfR (0.8 L)	Aerobic-MO	–	1.8/VS	Modin, et al. (2008)
MBfR (4.5 L)	Aerobic-MO	–	64.5–74.2	Sun et al. (2013)

MO: methane oxidation.

2.5 Membrane Biofilm Reactors (MBfRs)

Membrane biofilm reactors (MBfRs) take advantage of coupling the delivery of a gaseous substrate through the membrane lumen and the attached biofilm that has accumulated on the outer surface of the membrane fiber (Nerenberg, 2003; Rittmann et al., 2004;). Figure 2.4 illustrates the operating

principle of the MBfR system, highlighting the gaseous substrate diffusion through hollow-fiber membranes, which are mainly fabricated using hydrophobic microporous materials (i.e., polyethylene, polyvinylidene difluoride) (Sun et al., 2013; Zhou et al., 2018). The biofilm starts to accumulate on the membrane's outer surface, where the methane is oxidized to carbon dioxide, and nitrate is reduced to nitrogen gas via a syntrophic consortium between methanotrophs and denitrifiers.
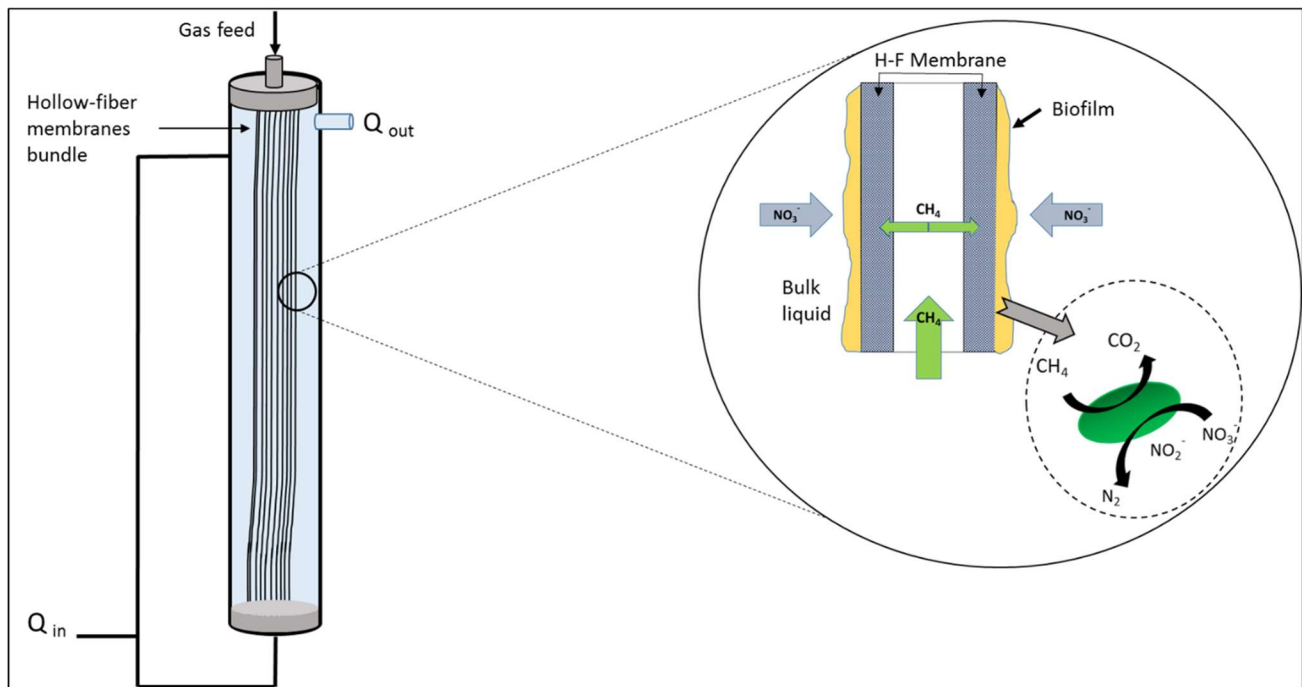
Figure 2-4. The concept of the MBfR working principle, where the microbial consortium in the biofilm active layer are utilized to reduce nitrate and oxidize methane.

MBfRs are considered to be one of the technologies studied for the reduction of various oxidized contaminants such as nitrate (NO_3^-) and other ions, including selenate Se (VI), in wastewater or groundwater (Chung et al., 2006). Hydrogen-based MBfRs for denitrification have been extensively investigated and widely discussed in the literature (Nerenberg & Rittmann, 2004). Numerous studies have tested autotrophic denitrification by a hydrogen-based MBfR on groundwater and wastewater (Celmer et al., 2008; Li, 2014; Rittmann, 2007; Rittmann et al., 2002;

Terada et al., 2006; Valencia, 2012; Zhao et al., 2013; Zhao et al., 2014). H_2 is a universal electron donor for anaerobic microorganisms to reduce many types of oxidized contaminants (Lee & Rittmann, 2000; Rittmann, 2004).

One of the most important advantages of the MBfR is gas delivery, where the gaseous substrate (e.g., methane, hydrogen) is delivered to the biofilm directly, minimizing gas loss from bioreactors (Rittmann, 2007). This type of bubble-less gas delivery mitigates the issue of dissipation of the sparging gases that are used in wastewater treatment, which has a significant impact on operational cost. The efficiency of gas delivery by the bubble-less membranes is almost 100% achieved through self-regulation, in which the active bacteria/archaea draw the required gaseous substrate according to the reduction reactions. This creates a substrate concentration gradient in both the membrane wall and the biofilm (Rittmann, 2007; Rittmann et al., 2004). In addition to the already listed advantages, MBfRs have the advantage of creating a large surface area for biofilm formation on the external surface of the bubble-less membrane, which enhances the efficiency of removal of the targeted contaminants (Martin & Nerenberg, 2012).

Biological removal of nitrate necessitates an exogenous electron donor. Like methanol in Eq (2.6), methane can serve as an electron donor and a carbon source in wastewater treatment plants (Timmermans & Van Haute, 1983). Islas-Lima et al. (2004) demonstrated the utilization of methane oxidation in anoxic conditions and as the sole electron donor for denitrification in a batch bioreactor. Their report confirmed the existence of a consortium of methanotrophs and denitrifying bacteria that were responsible for nitrate reduction to N_2, adapting the theoretical stoichiometry (2.7).

$$1.10 \ CH_3 \ OH + NO_3^- + H^+ = 0.46 \ N_2 + 0.078 \ C_5H_7O_2N + 2.42 \ H_2O + 0.71 \ CO_2 \qquad (2.6)$$

$$5CH_4 + 8NO_3^- = 4N_2 + 8 \ OH^- + 6 \ H_2O + 5CO_2 \qquad (2.7)$$
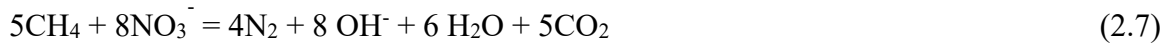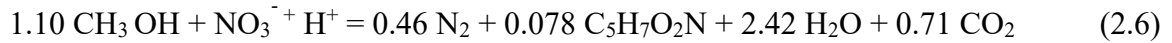
where $\Delta G^{o\prime}$ has a value of -767 KJ mol/CH_4, which is thermodynamically favorable under standard conditions. Here, methane is oxidized to carbon dioxide, and nitrate is reduced to nitrogen gas. Moreover, the denitrification rate results showed a positive correlation with the corresponding methane partial pressure, where the denitrification rate ranged between 0.25 and 0.004 g NO_3-N/g VSS.d, respectively. The utilization of methane gas in MBfR systems have been investigated for nitrate reduction and for the purpose of other contaminants removal, and it showed a potential to be a successive biotechnology approach (Long et al., 2017; Zhong et al., 2017; Luo et al., 2018; Cai et al., 2018; Chen et al., 2016 & Xie et al., 2018) Modin et al. (2008) first investigated aerobic denitrification in a methane-based MBfR, where they supplied methane and oxygen to the MBfR. Their study reported that a high degree of nitrate and nitrite removal was observed (93 mg N/m^2-h), where the membrane surface area and the liquid volume was 28.3 cm^2, and 800 ml, respectively (Modin et al., 2008).Utilization of the bubble-less gas transfer membrane in an MBfR could establish optimum conditions for anaerobic methane oxidation coupled to denitrification due to the high level of control over the gaseous substrate. Shi et al. (2013) investigated the removal of nitrogen in MBfRs via the utilization of a consortium of anammox and denitrifying anaerobic methane oxidation microorganisms using methane as a gaseous substrate, reporting nitrate and ammonium removal at 86 and 27 mg N/m^2 d, respectively. They claimed that denitrifying anaerobic methane oxidation archaea and bacteria were responsible for the reduction of nitrate to nitrogen gas by utilizing methane and ammonium as electron donors. This interesting interaction was revealed via a fluorescence *in situ* hybridization (FISH) analysis, and all previously mentioned archaea and bacteria were found to exist in abundance in the microbial community. Although the

proposed syntrophy might be prevalent in MBfRs, there are still other microorganisms and biochemical reactions for AMO-D, such as the involvement of the reverse-methanogenesis archaea (Haroon et al., 2013) discussed above.

2.5.1 Provision of Gas Through Gas-Permeable Membranes as Electron Donor

Since the 1970s, several researchers have investigated and developed hollow-fiber membranes for gas separation or provision purposes (Kammermeyer, 1976), until Mitsubishi Rayon Aqua, a Japanese-based manufacturer, developed a series of hollow-fiber membranes that were first marketed in 1992 (Mitsubishi Rayon, 2000). MBfRs were distinct from other biofilm reactors, such as packed bed and fluidized-bed reactors, in that a gas phase electron donor is delivered to biofilms grown on membrane outer surfaces (Rittmann & McCarty, 2001).

The materials that hollow-fiber membranes are generally made from are either hydrophilic or hydrophobic. Hydrophobic membranes outcompete hydrophilic membranes for gaseous mass transfer, in which gas molecules have the advantage of diffusion through a gas phase rather than liquid phase (Ahmed & Semmens, 1992). Figure 2.5 illustrates how micropores behave in hydrophilic membranes, where the pores are filled with liquid. In contrast, hydrophobic membrane pores are liquid free.
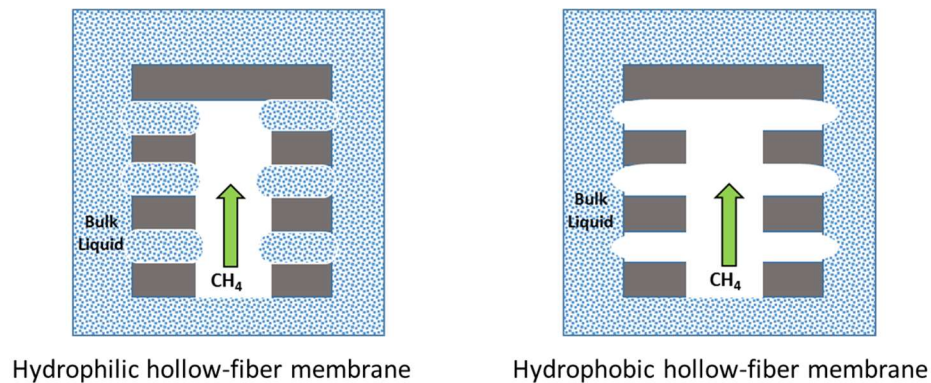
Figure 2-5. Hydrophilic and hydrophobic hollow-fiber membrane behavior (Nerenberg, 2012).

Gas transfer in MBfRs is driven by the concentration gradient across the membrane barrier (Martin

& Nerenberg, 2012). One of the key characteristics of the hollow-fiber membranes used in MBfRs

is bubble-less gas diffusion (Nerenberg, 2005). Therefore, high pressure can be applied to the

membranes to increase the mass transfer of a gaseous substrate through the biofilms, which will

have a positive impact on the reactor's treatment performance. Moreover, MBfRs have a unique

property: the gaseous substrate (electron donor) and electron acceptors are delivered to the biofilms

in a counter-diffusional manner (Martin & Nerenberg, 2012) (Figure 2.6). However, this type of

diffusion may potentially create a substrate-limited boundary due to excessive bulky biofilm

formation, which could impact the overall denitrification performance (Martin et al., 2013).
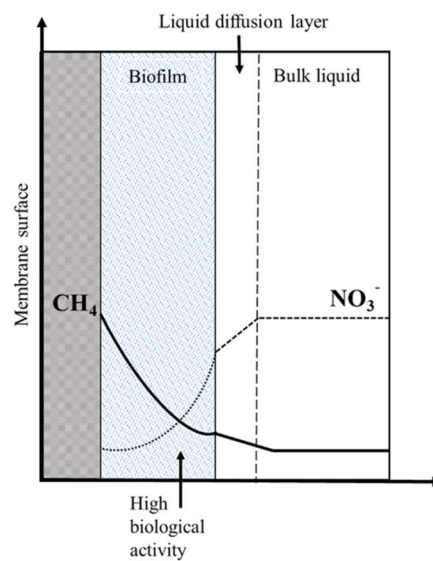
Figure 2-6. Counter-diffusion of the substrate gradients in MBfR biofilm (Martin et al., 2012).

The (methane) transfer or diffusion through the hollow-fiber membranes can be estimated

according to Eq. (2.8) (Mallevialle et al., 1996; Pavissich et al., 2014).

$$J_{CH_4} = K_{mem} \left(\frac{P_{CH_4}}{H_{CH_4}} - C_{CH_4} \right), \tag{2.8}$$

where J is the specific mass flux (g/m^3-s), K_{mem} is the overall mass transfer coefficient (m/s), P_{CH4} is the methane partial pressure in the membrane (kPa), H_{CH4} is the methane Henry's law coefficient (m^3-kPa/g), and C_{CH4} is the methane concentration at the membrane surface (g/m^3). Moreover, the overall mass transfer coefficient (K_{mem}) can be represented by the summation of resistance to mass transfer in the layers of the gas boundary, the membrane, and the liquid diffusion (Mavroudi et al., 2006). Eq. (2.9), expresses the mathematical relationship:

$$R_{total} = \frac{1}{K_{mem}} = \frac{1}{k_G} + \frac{1}{k_M} + \frac{1}{k_L}, \qquad (2.9)$$

where R_{total} is the total resistance, and K_G, K_M, and K_L represent the mass transfer coefficients in the gas, membrane, and liquid layers, respectively. Since the gas diffusion resistance in the liquid diffusion layer is significantly greater than the resistance in either the gas or the membrane, it is normally ignored. Therefore, K_{mem} will only be equal to K_L (Qi & Cussler, 1985).

2.5.2 Biofilm Formation on the Surface of the Membranes

A biofilm can be defined as a compact collection of microorganisms implanted in a polysaccharide group in an aquatic environment (Momba et al., 2000). Alternatively, a biofilm may be described as a thin layer containing immobilized cells that form in an organic polymer matrix having a microbial foundation (O'Toole, 2000). The formation of a biofilm includes several physicochemical steps, in which a single planktonic bacterium attaches to the membrane's outer surface via electrostatic interaction or chemically-based bonding (Gottenbos et al., 2000). Subsequently, the anchored bacterium begins to attach to other microorganisms via polysaccharide groups, forming small microcolonies that form the biofilm layer (Momba et al., 2000), as shown in Figure 2.7.
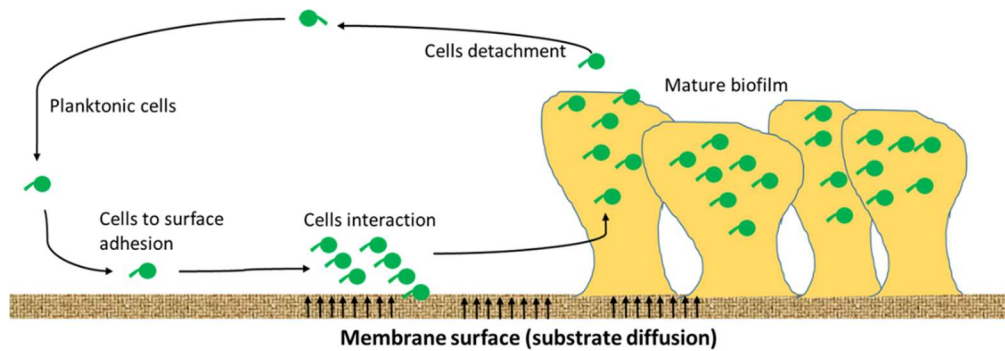
Figure 2-7. Biofilm formation steps on a membrane surface.

One of the techniques used to investigate biofilm morphology is the scanning electron microscope (SEM). Figure 2.8 displays an image of a biofilm that has been built on a hollow-fiber membrane outer surface, where the biofilm morphology is heterogeneous along the length of the membrane. One of the important operating parameters in MBfRs is biofilm thickness, which is positively correlated with time, where the biofilm reaches a steady constant thickness (Dos Santos & Livingston, 1995). However, there are several factors that affect biofilm thickness and, consequently, will have an impact on the MBfR's overall performance because the dual substrate diffusion will be limited due to mass transfer inhibition (Kwok et al., 1998; Liu & Tay, 2002; Modin et al., 2008).

Hydraulic shear force has been reported as a primary factor influencing biofilm structure (Liu & Tay, 2002; Ohashi & Harada, 1994). The effect of shear force in a hydrogen-based MBfR for denitrification has been reported by Celmer et al. (2008), where they applied different shearing forces, reported in revolutions per minute (100, 200, & 300 rpm) in a 3 L MBfR. It was observed that at high rpm mixing conditions, the denitrification rate was the highest with simultaneous biofilm thickness reduction (~ 800 µm); by increasing the shear force, the biofilm thickness was observed at (~300 µm). This reduction in biofilm thickness positively correlating with an increase

in the shear force was also observed by others (Ohashi & Harada, 1994; Kwok et al., 1998; Rittman, 1982).

In addition to the impact of shear stress on biofilm structure (thickness and density), substrate loading has been observed to influence biofilm thickness. In a study done by Peyton (1996), substrate loading rates showed a proportional relationship with biofilm density (X_f), and subsequently biofilm thickness (L_f) up to ~ 30 µm in a pure culture (*Pseudomonas aeruginosa*), where glucose was used as the sole substrate. In addition, Rittmann and McCarty (2001) derived a formula to calculate biofilm thickness at steady state from an active biomass mass balance at any location along the biofilm via Eq. (2.10).

$$L_f = \frac{J\,Y}{X_f\,b_f},$$
(2.10)

where J is the substrate flux diffusing to the biofilm (g/m^2-h), Y is the growth yield (g active biomass /g substrate), and b_f is the total biofilm specific loss rate (1/d), assuming that biofilm density multiplied by biofilm thickness is constant at any given time (Rittmann & McCarty, 2001).

Biofilm control is essential in order to limit excessive detachment of the biofilm layer, especially in the exterior region of the biofilm, which might affect microbial activity mainly due to substrate gradient (Lackner et al., 2008). Hence, controlling the thickness of a biofilm is important for improving the performance of biofilm-based bioreactors, such as MBfRs.
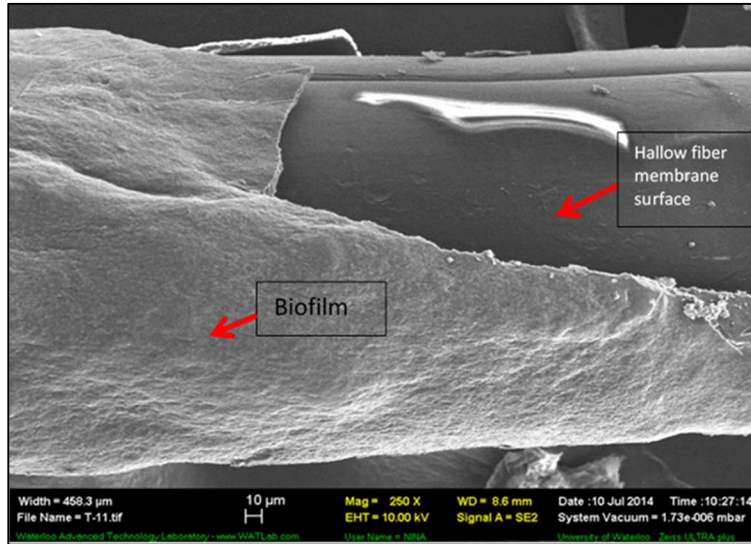
Figure 2-8. SEM image for biofilm formed on a hollow-fiber membrane surface.

As mentioned previously, biofilms in MBfRs have a counter-diffusional substrate delivery, where the optimum microbial activity occurs almost at the midpoint of the biofilm, subjected to the concentration of substrates (e.g., methane and nitrate). The relative microbial activity can be presented by Monod terms, as expressed in Eq. (2.11) for both the electron donor (diffused from the membrane lumen) and the electron acceptor (diffused from the bulk liquid).

$$relative\ activity = \frac{[S_{CH_4}]}{K_{s\,(CH_4)} + [S_{CH_4}]} \cdot \frac{[S_{NO_3}]}{K_{s\,(NO_3)} + [S_{NO_3}]}, \tag{2.11}$$

where S is the concentration of electron donor and acceptor (g /m^3), methane and nitrate, respectively, and K_s is the half-saturation concentration coefficient of the electron donor and acceptor (g/m^3). Thus, microbial activity will be at a maximum when Monod terms equal one. In contrast, as the substrates become limited, the microbial activity will descend to zero (Pavissich et al., 2014)

Chapter 3

Hypoxic Nitrate Reduction in A Membrane Biofilm Reactor Under High Pressure and Concentration of Methane

A version of this chapter, co-authored by Wael Alrashed, Jangho Lee, Joonhong Park, and Lee, H.S., accepted for to publication in Chemical Engineering Journal.

Contributions statement: Wael Alrashed fabricated the bioreactors, performed all laboratory experiments and analyses, sampling for microbial analysis, and contributed to data interpretation and manuscript preparation. Jangho Lee and Joonhong Park conducted the microbial community analysis. Under the supervision of Lee, H.S.

3.1 Introduction

The utilization of methane gas oxidation coupled to denitrification (MOD) as a process for removing nitrogen from water and wastewater have been investigated as this process is both economical and eco-friendly. Therefore, in order to meet governmental regulations, biological nitrogen removal has been investigated thoroughly by varying bioreactor configurations and various electron donors. This was conducted with a view to not only optimize nitrogen removal, but also to minimize the carbon foot-print and costs. Several previous studies have investigated autotrophic denitrification using a hydrogen-based membrane biofilm reactor (MBfR) on groundwater and wastewater (Rittmann et al., 2002; Nerenberg et al., 2005; Terada et al., 2006; Rittmann, 2007; Celmer et al., 2008; Tang et al., 2012; Valencia, 2012; Li, 2014; Zhao et al., 2014). This is because hydrogen is a universal electron donor which anaerobic microorganisms use to reduce many oxidized substrates, including contaminants (Rittmann, 2004; Lee & Rittmann, 2000). In addition, researchers have utilized methane based-MBfR to evaluate its potential for denitrification ((Modin et al., 2008; Luo et al., 2015Lai et al., 2016; Zhang et al., 2016). Modin et al., (2008) used a laboratory based MBfR, where the volume and the membrane surface area were 800 ml and 28.3 cm^2 respectively, to which methane and oxygen were regularly supplied to the MBfR. The authors reported high levels of nitrate removal (93 mg N/ m^2-h) and attributed the removal efficiency to the utilization of a bubble-less gas transfer membrane, in addition to controlling the gas substrate in the MBfR. In another study, Shi et al. (2013) operated an MBfR for two years and investigated nitrogen removal via the utilization of a consortium of anammox and denitrifying anaerobic methane oxidizing microorganisms with methane as a

gaseous substrate, reporting nitrate and ammonium removal at 86 and 27 mg N/ m^2-d respectively. Moreover, they applied high methane pressure, reporting 1.2 atm in batch operation and 1.5 atm in a sequential batch reactor. The aqueous methane has not been quantified during the continuous mode operation; it was quantified only in batch mode. Thus, there is no direct indication of the amount of methane discharged into the atmosphere while applying such high methane pressure, contrary to this study. In fact, a systematical evaluation of dissolve methane in MBfRs effluent has not been documented in the literature, although methane gas is one of the greenhouse gases that should be mitigated (Yusuf et al., 2012; Paustian et al., 2001). The literature lacks any quantitative methodology of quantifying or estimating the O_2 intrusion to MBfRs systems. Moreover, the O_2 permeation impacts has not been reported in MBfRs that utilized methane as the only gaseous substrate for denitrification.

The objectives of this study was to experimentally assess the denitrification performance under various high methane pressures and hydraulic retention times (HRT), while monitoring the dissolved methane concentration in the MBfR. Secondly, to characterize the microbial population (employing metagenomics) as a method to distinguish the methane oxidation and denitrification pathways in the MBfR. The third, is to provide evidence that hypoxic – micro-aerobic environment could exist in a constantly pressurized MBfR with 99.9% methane. Moreover, the biofilm morphology was examined to have an insight on the biofilm growth patterns on the polyethylene hollow fiber membrane outer surface.

3.2 Methodology

3.2.1 MBfR Configuration and Operation

The MBfR was constructed using a Plexiglas tube, with the following dimensions: (length of 30 cm, 1.1 cm outer diameter, and working volume of 86 mL) as illustrated in Figure 3-1. Two membrane modules were prepared with gas-permeable hydrophobic microporous polyethylene fiber (MHF 200TL, Mitsubishi Rayon, Japan), each module consisting of 8 membrane fibers, giving a total specific surface area of 35 m^2/m^3. The hollow-fiber membranes were bundled together using a hydrophobic silicone sealant (Model 908570, Loctite, USA) that cured for 24 h in dry conditions.

The MBfR was inoculated with a consortium of methanogens (*Methanobacterium spp.*) and denitrifying bacteria (50 mL) that had been enriched in serum bottles using methane as the sole electron donor and carbon source for over 12 months. The MBfR was fed with the nitrate medium bottle, and was initially operated in batch mode, and methane gas (99.0%, Praxair, Canada) was supplied to the membrane modules as the sole electron donor and carbon source. The composition of the medium, synthetic nitrate mineral solution (NMS), was as follows: (per Liter of deionized water, mg): $NaNO_3$, 184; $FeSO_4 \cdot 7H_2O$ 1; $CaCl_2 \cdot 2H_2O$ 1; $MgSO_4 \cdot 7H_2O$ 200. In addition, the phosphate buffer composition was Na_2HPO_4, 434; KH_2PO4 128, maintaining the pH value within the 7 ± 0.5 range. Furthermore, 1 mL of trace element solution was added to each liter of medium. The components of the trace solution are (mg/l): $ZnSO_4.7H_2O$ (100), $MnCl_2.4H_2O$ (30), H_3BO_3 (300), $CoCl_2.6H_2O$ (200), $CuCl_2.2H_2O$ (10), $NiCl_2.2H_2O$ (10), $Na_2MoO_4.2H_2O$ (30) and Na_2SeO_3 (30). The medium was autoclaved for 20 min at 121˚C, cooled to room temperature, and purged with N_2 gas (99.0%, Praxair, Canada) for 45 min. Then it was connected with a N_2 gas bag (1 Liter Tedlar - Sigma-Aldrich, USA), and fed to the MBfR

28

with a peristaltic pump. The liquid in the MBfR was circulated at a rate of 10 mL/min using a peristaltic pump (Masterflex L/S economy variable speed Drive, RK-07554-80). The MBfR was operated at a constant temperature of 24 ± 1 °C, and the influent and effluent pH was assessed on a regular basis, ranging from 7.2 to 7.4.

After operating the MBfR in batch mode for a period of 151 days and confirming reproducible denitrification performance in batch mode, the MBfR was switched to continuous mode. To evaluate the impact of HRT and methane pressure on nitrate reduction, the MBfR was run in continuous mode for 180 days. Firstly, the methane pressure was fixed at 7 psig and then the HRT was altered (12, 8 and 4), with a nitrate loading rate of (40, 60 and 120 g/m^3) respectively. Then, the methane pressure was fixed at 5 and 2 psig respectively. During these runs, the MBfR was operated in a stable temperature at ~ 24 ± 1 °C. Table 3-1 summarizes the MBfR operating conditions. After confirming steady-state nitrate concentration in the MBfR effluent these operating conditions were changed.

Table 3-1. Operating conditions in the MBfR including time-intervals.

CH_4 pressure Kpa (psig)	HRT (h) 12	HRT (h) 8	HRT (h) 4
48.2 (7.0)	Day 178 -192	Day 193–207	Day 208–220
34.5 (5.0)	Day 221–242	Day 243–257	Day 258–270
13.7 (2.0)	Day 271–299	Day 300–322	Day 323–337
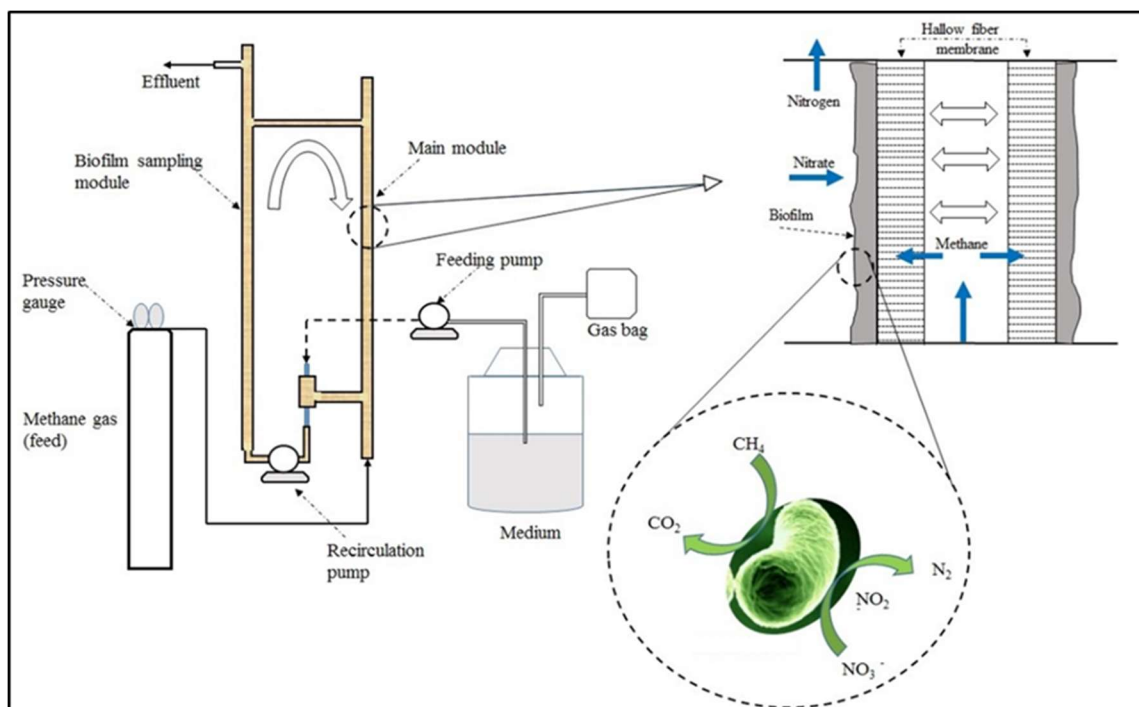
Figure 3.1. Schematic diagram of the membrane biofilm reactor, including a diagram illustrating the potential denitrification pathway in MOD microorganisms.

3.2.2 Nitrate and Nitrite Measurement

Nitrate and nitrite were analyzed with an Ion chromatograph (IC- 1100, Dionex, USA) equipped with an AS9-SC analytical column (Ion- Pac, 4 × 250 mm, Dionex, USA) using 9 mM sodium carbonate as an eluent at a flow rate of 1.00 mL/min. All samples were filtered with syringe filters (pore size: 0.45 µm, VWR International Inc., Canada) before analysis. Samples from the influent and effluent were taken on a regular basis, and measured nitrate and nitrite concentration in duplicate.

N_2O gas was quantified using a gas chromatography (GC-2014, Shimadzu, Japan) equipped with an electron capture detector (ECD) and a molecular sieve column (6 ft × 1/5 in., 85/100 mesh, all tech, USA). The temperatures of the column and the detector were constant at 250 °C and 80 °C respectively, and helium gas was used as the carrier gas (99%, PraxAir, Canada) at a flow

rate of 10 mL/L and a pressure of 21 psig. We regularly sampled gases from the headspace of the MBfR using a gas-tight syringe (Hamilton Gastight Syringe, Hamilton, USA) for N_2O analysis.

3.2.3 Methane Gas and Permeation of Oxygen Measurement

To quantify the dissolved methane concentration in the MBfR effluent using (Eq. 3.1) according to (Yeo & Lee, 2013), liquid samples taken from the MBfR using a syringe were immediately transferred to a vial (20 mL) that had been sparged with N2 gas (99%, Praxair, Canada). The vial was vigorously mixed with a vortex mixer (Fisher STD, USA) for 6 minutes to reach equilibrium between gas and liquid phases. Subsequently, the gas was sampled from the headspace of the vial and gas composition was quantified using a GC equipped with a thermal conductivity detector (TCD) (SRI 310C, SRI instruments, USA).

$$CH_4(aq) = \left[H_{CH_4} \times P_{CH_4} \times MW_{CH_4}\right] + \left[\frac{P_{CH_4} \times V_H \times \rho_{CH_4}}{V_L}\right] \quad (3.1)$$

Where, H_{CH_4} is the Henry's law constant at 25°C (0.0014 mol/L-atm), P_{CH_4} is the methane partial pressure in the 20 ml vial head space, MW_{CH_4} is the methane molecular weight (16 g/mol), V_H is the headspace volume of the vial (10 mL), V_L is the liquid volume of the vial (10 ml), ρ_{CH_4} is the methane density which is $= MW_{CH_4}/$ gas molar volume at 25°C, according to the ideal gas law (24.4 L/mol).

The MBfR was operated under continuous pressure of methane (99%). However, the oxygen permeation through the MBfR tubing system was considered as a minor source of O_2 penetration. Therefore, the O_2 permeation rate was calculated using Eq.3.2

Oxygen permeation rate = (O$_2$ permeability × Area × T × PO$_2$)/Z   (3.2)

Where, Area: surface area of tubing (cm^2), T: time (s), PO$_2$ is the atmosphere's partial pressure of O$_2$, Z: tubing thickness (mm).

3.2.4 Metagenomics Analysis and SEM imaging

To minimize the damages of the membrane biofilms, planktonic samples in MBfR effluent were collected from the steady-state MBfR run at a given condition. The samples were taken in duplicate for each condition to improve the sample representation of the microbial community in a given condition. After effluent collection, the suspension was centrifuged at a speed of 12,000 rpm for 10 minutes (Eppendorf 5424 microcentrifuge, Germany). Then pellets were transferred to micro-centrifuge tubes and directly frozen at -20 °C. Planktonic samples were collected on day 297, at the following operation conditions: methane pressure 2 psig and HRT 12 h. All bio-sampling procedure was performed after sterilizing the sampling tools and the vails in an autoclave at 121 °C for 20 minutes. Genomic DNA (gDNA) of the pellets was extracted by the PowerSoil DNA Isolation Kit (MO BIO Laboratories, Inc., Carlsbad, USA). Sequencing libraries were set according to the protocol of the TruSeq DNA PCR-free Sample Preparation Kit (Illumina, Inc., San Diego, CA, USA). DNA (1 µg), fragmented by the adaptive focused acoustic technology (AFA; Covaries), was end-repaired, followed by selection of DNA size and A-tailing to the 3′ ends of the fragments and ligation of adapters (Head et al., 2014). The DNA was sequenced by Macrogen, Inc. (Seoul, Republic of Korea) using an Illumina Hiseq 1999 (Illumina, San Diego, USA). A total of 5.38 Gb of paired-end reads was obtained by sequencing forward and reverse strands of DNA fragments. The paired-end reads were further merged and filtered using default options of MG-RAST pipeline, including removal of artificial replicates-contained affiliated with *Homo sapiens* DNA (NCBI v36). We filtered out reads containing low

quality bases more than 5 bp with < 15 Phred score. Microbial taxa were assigned using Best

Hit Classification based on the SILVA Small Subunit (SSU) rRNA database (Kougias et al.,

2014; Yang et al., 2014) by filtering with a minimum identity cutoff of 60%, an E-value cutoff of

10−5, and a minimum alignment length of 50 bases. Functions of MOD were annotated by All

Annotations tool based on Genbank database at a minimum identity threshold of 60%, an E-

value cutoff of 10^{-5}, and a minimum alignment length of 17 amino acids (Yergeau et al., 2013).

To analyze the morphology of the biofilm, a composition of the sampled biofilm, a Field

Emission Scanning Electron Microscope (FESEM) (Model Gemini Leo 1530, Carl Zeiss AG,

Germany) along with Energy-Dispersive X-ray (EDX) detector (AMETEK, Inc.) were used.

Two samples of the biofilm-membrane were extracted after nine months of operation, with the

samples being taken from separate locations (the first sample was taken from the upper section

of the membrane, and the other was taken from the lower section) in order to investigate the

uniform biofilm distribution along the membrane. To prepare the biofilm samples for the

FESEM analysis, we dehydrated the bio-samples in an oven at 100°C for 10 minutes to remove

the moisture. Prior to the FESEM analysis, we fixed the precipitates on the SEM stub using a

conductive double-faced adhesive tape and coated it with gold, using the FESEM gold coating

unit Desk II (Denton Vacuum, USA). Argon was used as an inert gas during the gold coating,

and the FESEM works under vacuum (10^{-5}-10^{-7} Pa). Electrons are generated by a field emission

source in FESEM, where the energy is released at ten keV. This beam passes through the

electromagnetic lenses and interacts with the specimen at an approximate depth of 1 μm. As a

consequence of the interference between the beam electron and atoms of the specimen, several

types of electrons are discharged from the specimen. Subsequently, secondary electrons are

received by the EDX detector. Elements in the sample are identified in the EDX spectrum. Then,

the elemental analysis information collected from the software is supplied by the EDAX (Ametek, Inc.).

3.3 Results and Discussion

3.3.1 Nitrate Reduction and Nitrite Accumulation in the MBfR

The MBfR was operated in batch mode for a period of three months in order to have a mature biofilm, acclimating on the external surface of the membrane fiber (Zaho et al., 2014; Lai et al., 2014). Subsequently, a series of batch mode experiments was established, applying a fixed methane pressure of 7 psig and various Hydraulic Retention Times (HRT) in order to evaluate the MBfR performance before moving to the second phase; continuous mode operating. Figure 3-3a-b illustrates the results of the batch mode experiments under the conditions listed in Table 3-2.

Table 3-2. Batch mode operation conditions in the MBfR

HRT (h)	CH$_4$ pressure (psig)	Influent (mg NO$_3^-$-N /L)
12/24	7	15 ± 0.89
12/24	7	23 ± 0.59
12/24	7	30 ± 0.77

The batch mode experiments were done in two stages; the first was 24 h (HRT), in which the methane pressure was regulated at 7 psig, while varying the nitrate concentration in the feed (15, 23 and 30 mg NO$_3^-$-N /L). As expected, at low nitrate concentration, the removal efficiency was almost complete. However, as the concentration increases the removal efficiency of nitrate

declines to ~78% (Figure 3-3a). Furthermore, we explored the impact of decreasing the HRT while controlling the methane pressure with same nitrate concentration as the previous experiment. As shown in Figure 3-3b, the nitrate removal efficiency was ~67% at 15 ± 0.89 mg NO_3^--N /L. However, the removal efficiency appeared unvarying when the nitrate concentration increased the influent (23 ± 0.59, 30 ± 0.77 mg NO_3^--N /L), (58 and 57%) respectively. Accordingly, the denitrification rate was steady at ~ 1.13 mg NO_3^--N /L-h. Additionally, increasing the nitrate concentration in the influent had enhanced the denitrification rate from 0.62 to 1.13 mg NO_3^--N /L-h; implying that the denitrifying methanotrophs consortium metabolism was triggered by the electron acceptor availability in the bulk liquid, irrespective of the abundance of the electron donor (Haroon et al., 2013; He et al., 2015).
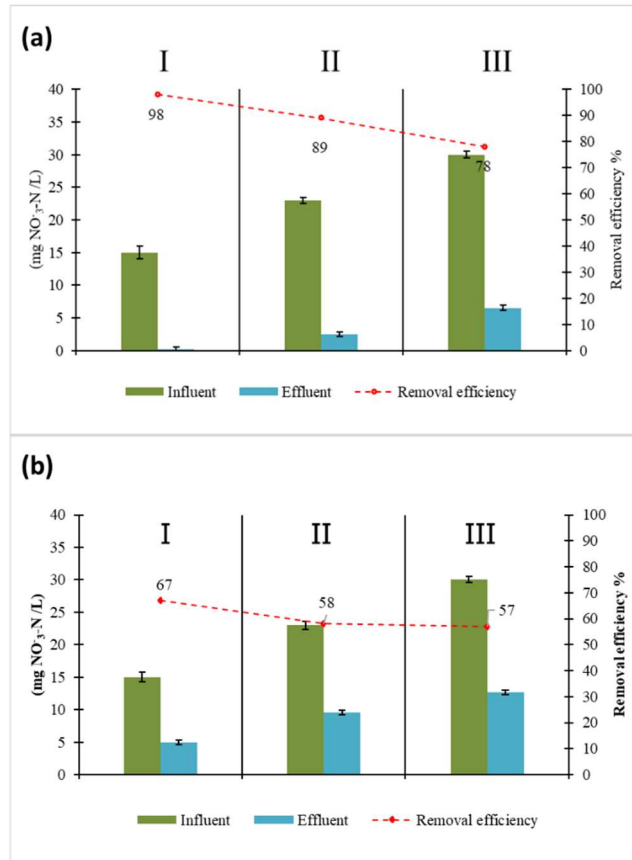
Figure 3- 2. (a) Nitrate influent and effluent concentrations for three different feed concentrations (15, 23 & 30 mg NO^-_3-N /L) are symbolized as (I, II, III) respectively and fixed HRT and CH_4 pressure 12 h & 7 psig respectively. (b) matching operation conditions with HRT of 24 h.

As presented in Figure 3-3a, the nitrate concentration in the effluent was 3.28 ± 0.98 mg N/L, which was the optimum, attained at the highest methane pressure (7 psig) and HRT of (12 h), corresponding to nitrate loading of (~ 42 g/m^3). Furthermore, when the methane pressure was reduced to 2 psig, the nitrate concentration in the effluent was 5.46 ± 1.18 mg N/L, and the statistical test results between the two methane pressures 7 and 2 psig is considered to be extremely statistically significant at a P-value of 0.0001; likewise, between 5 and 2 psig at a P-value of 0.0016. However, that was not the case for 7 and 5 psig, where the statistical results implied that the difference was not

significant. This outcome supports the suggestion that the utilization of very high

methane pressure does not impact the nitrate reduction, rather than overusing the

methane, which will directly impact the operation cost, in addition to releasing methane

gas into the atmosphere. Moreover, in figure 3-3b & c, the HRT was reduced to 8 and 4

h, nitrate loading of (63 and 128 g/m^3) respectively. Thus, as the HRT decreases, we

can observe the same trend of low nitrate removal. That can be attributed to the low

contact time in addition to the slow kinetics of the microbial consortium. The nitrite

concentration was monitored during the nine phases. Table 3-3 outlines the outcomes

where the nitrite was always below 0.2 mg N/L, implying that nitrite did not accumulate

in the MBfR (Chung et al., 2007; Shi et al; 2013). Hence, it can be concluded that

nitrate reduction rather than nitrite reduction was the limiting factor of the

denitrification rate. Intermediate compounds in the denitrification cascade reactions

might have been accumulating in the MBfR. However, N_2O gas was not detected in the

MBfR headspace, which suggest a complete denitrification to N_2. Additionally, the

metagenome analysis had identified the *nos* gene, which is responsible for N_2O

reduction to N_2.

Table 3-3. Nitrite (mg NO^-_2-N/L) concentration in the MBfR effluent for three HRTs
(12,8 and 4 h) and CH_4 pressure (7, 5 and 2 psig)

CH_4 pressure	HRT (h)		
(psig)	12	8	4
2	0.021 ± 0.005	0.07 ± 0.06	0.12 ± 0.005
5	0.017 ± 0.008	0.055 ± 0.07	0.091 ± 0.006
7	0.01 ± 0.009	0.051 ± 0.005	0.085 ± 0.004
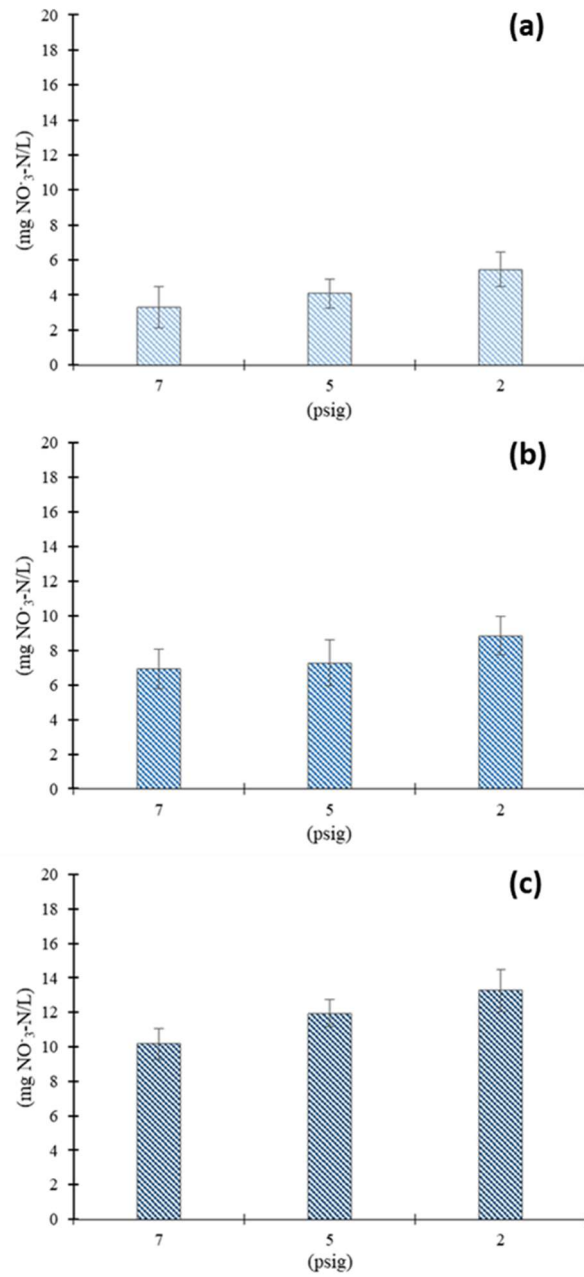
Figure 3- 3. Nitrate concentration in the MBfR effluent for CH_4 pressure (7, 5 and 2 psig), (a) for hydraulic retention time (12h); (b) for hydraulic retention time (8 h); and (c) for hydraulic retention time (4 h)

3.3.2 Dissolved Methane in the MBfR Effluent and Oxygen permeability.

Figures 3-4a, b& c show the dissolved methane concentration in the MBfR effluent for CH_4 pressure (7, 5 and 2 psig) 99.99% methane, alternating the hydraulic retention time for 12, 8 and 4 h respectively. Throughout the whole experiment, aqueous methane had been at a comparatively high concentration. The maximum observed value was 12.9 ± 0.19 mg CH_4/L at methane pressure of 7 psig and HRT of 12 h. Furthermore, when the methane pressure was reduced to 2 psig the dissolved methane was 12.12 ± 0.15 mg CH_4/L. The difference between the two phases was statistically significant at a P-value of 0.0001 of this difference. On the other hand, the lowest dissolved methane concentration was 8.04 ± 0.21 mg CH_4/L at methane pressure of 2 psig and HRT of 4 h. Also, when the methane pressure was at 7 psig at the same HRT (4h), the dissolved methane concentration was 10.12 ± 0.33 mg CH_4/L. Like the maximum HRT of 12 h, there was a significant difference between 7 and 2 psig methane pressure at the lowest HRT (4 h), in which the P-value was 0.0001. This strongly suggests that methane delivery to the biofilm is sensitive to the methane pressure and methane concentration in the feed; the methane concentration was 99.9%. Thus, it can be concluded that methane was not limiting the denitrification rate, because it was abundant in the biofilm. Also, that might be an indication of the inadequate gas delivery of this specific type of bubbleless gas transfer membrane (polyethylene).

During the entire span of the experiment, the MBfR was continuously pressurized with methane gas (99.9%). However, in order to estimate the oxygen permeation to the MBfR, the infused O_2 was calculated according to Eq.3-2. The tubing length was 75 cm,

39

having a thickness of 1.80 mm and a surface area of 73.2 cm^2 and the O$_2$ permeability 20×10^{-10} cm$^3 \times$mm/cm^2-s-mmHg (Masterflex, Norprene A60 G).

$= 20 \times 10^{-10}$ cm$^3 \times$mm/cm^2-s-mmHg) $\times$73.2 cm$^2 \times$ [(160 mmHg) $\times$ (86400) s/1d]/1.8 mm), the maximum O$_2$ permeation was at 1.24 cm^3/d, which is equivalent to 0.74 mg/d. This implies that a micro aerobic methane oxidation can take place in the membrane biofilm at very low dissolved oxygen concentrations, where it was reported that methane can be oxidized at micro-aerobic levels with dissolved oxygen concentrations as low as 0.16 to 1.0 mg/L (Steinle et al., 2017; Kalyuzhnaya et al., 2013).
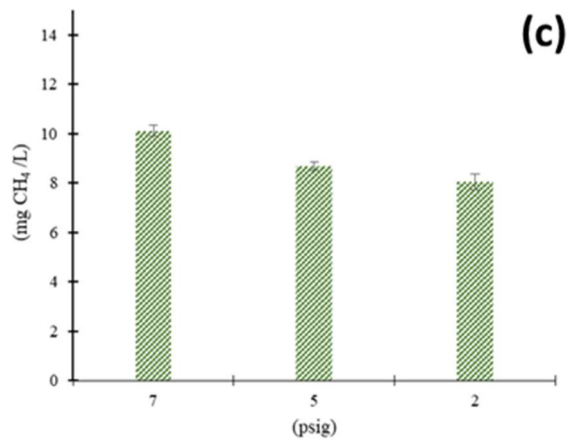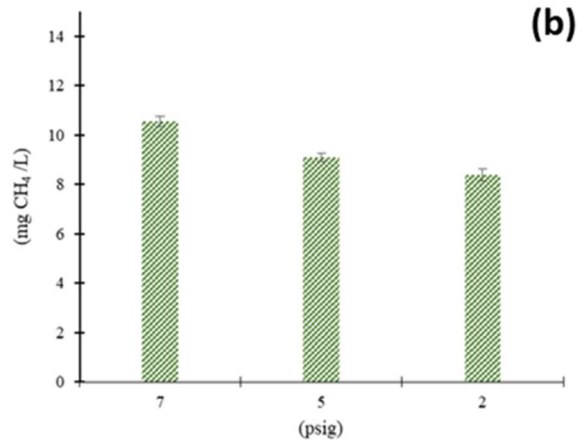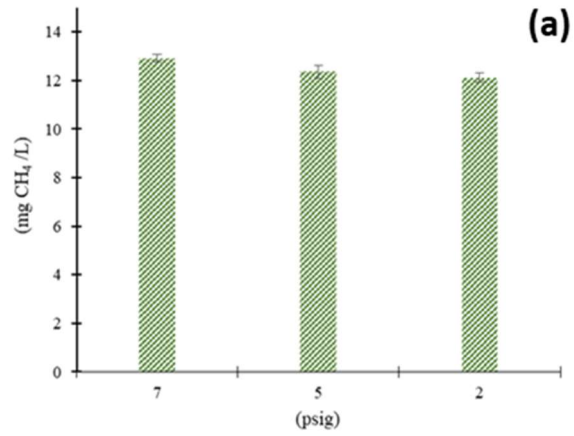
Figure 3-4. Dissolved methane concentration in the MBfR effluent for CH_4 pressure (7, 5 and 2 psig), 99.99% methane, (a) for hydraulic retention time (12h); (b) for hydraulic retention time (8 h); and (c) for hydraulic retention time (4 h).

3.3.3 Metagenomics Analysis and SEM imaging

The community structure of the planktonic samples that were collected from the MBfR are

shown in Fig 3-5a, with a total of 34,195 rRNA sequences. Furthermore, more than 84% of the

whole microbial community was assigned to bacteria, Archaea was at a low level of 0.003% of

the total rRNA sequences, indicating that reverse methanogenesis could not be the main pathway

of methane oxidation (Welte et al., 2016; Timmers et al, 2017). Up to 16% of the rRNA

sequences could not be assigned to any species. Fig 3-9b illustrates the SSU rRNA genes, in

which the *Methylocystaceae* bacterial family has a relative abundance of 21%, that have the

ability to oxidize C1 compounds. In fact, *Methylocystaceae* are associated with aerobic methane

oxidation; yet, the MBfR was kept under continuous 99.99 % methane supply and we confirmed

that there is no gas leak or any means of air infiltration into the reactor via the medium bottle or

the membrane modules (Bowman, 2006; Murrell, 2010). Moreover, *Flavobacteriaceae* and

Xanthomonadaceae come at 8 and 7% respectively. In addition, the functional metagenome in

Fig 3-5b shows the following genes: (*pmo*, *mdh*, *mtdB*, *folD*, and *fdh*), which are linked to

aerobic oxidation of methane (Stein et al., 2011; Chistoserdova et al., 2013; Kalyuzhnaya et al.,

2013; Zhu et al., 2016). In terms of denitrification, the functional genes *(nap/nar)* responsible for

the reduction of nitrate to nitrite were found in *Comamonadaceae* family of the

Betaproteobacteriaat (30%) abundance (Willems et al., 2015). Furthermore, the abundance of

(nap/nar) genes were found in the following denitrifying bacteria: *Brucellaceae*,

Mycobacteriaceae, and *Methylobacteriaceae* at (13, 5 and 5 %) respectively; which have the

ability of coupling the reduction of nitrate with the oxidation of organic compounds (Shen et al.,

2013; Beck et al., 2013; Wilderer et al., 2017; Chu et al., 2017). Additionally, the nitrite

reductase Genes *nir* (Chen et al., 2014), dominated the *Methylocystaceae* family at 27%. In

terms of the nitric oxide, the genes *nor* were found in the following families: *Flavobacteriaceae,*
Comamonandaceae, and Brucellaceae. Likewise*,* the *nos* genes were recognized in the same
group as *nor* genes, which is nitrous oxide reductase (Schreiber et al., 2012). It can be seen that a
diverse bacterial species catalyzing the reduction of nitrate to nitrogen gas, with the coupling of
methane oxidation, in the presence of the functional genes *mdh, mtdB,* and *folD,* imply that
intermediate compounds supported the cascade reactions; yet methanol was not detected in the
MBfR during the experiment. Furthermore, the microbial community can be dynamic over time
in this type of bio-reactors, as Chen et al., (2016) reported that the first inoculum was dominated
by anaerobic methane coupled to denitrification. However, all the Archaea were not detected
later (Chen et al., 2016).
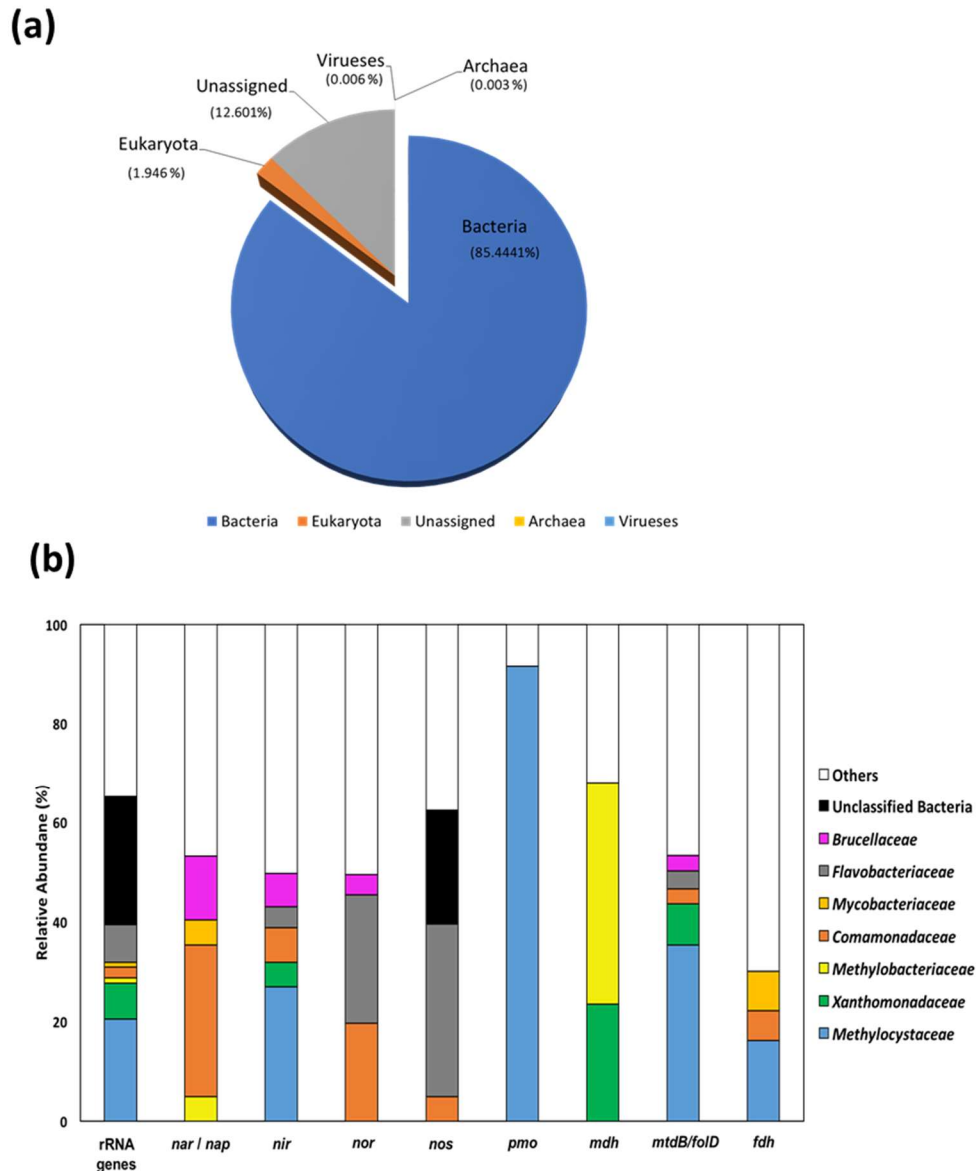
Figure 3-5. The structure of the whole microbial community. (a) The relative abundances were determined with MG-RAST using the best hit classification technique against SILVA Small Subunit (SSU) rRNA database. (b) Methane oxidation coupled to denitrification functional genes relative abundance of SSU rRNA genes; in which "Others" specifies functional genes with 4% for rRNA and 1% or low relative abundance.

The SEM images exhibited that there is no significant difference in biofilm morphology and thickness between the two samples that were extracted from the upper section of the membrane, and the other from the lower section of the membrane as shown in Figure 3-6a, b. However, the sample from the upper section of the membrane showed slightly thicker and denser biofilm structure than the sample from the lower section of the membrane. This can be attributed to proximity to the methane gas supply source, in which the gas feed is connected to the upper end of the membrane, supporting the suggestion of an optimal gas mass transfer close to the gas feed source resulting in enhancing the microbial growth. Moreover, it was observed that the biofilm has a homogeneous distribution along the exterior membrane surface. Additionally, the biofilm layer had a uniform surface, indicating an adequate and regular mixing in the reactor and minimizing the impact of the hydrodynamic shear (Celmer et al., 2008; Martin et al., 2012). Furthermore, the biofilm did not cover the membrane surface completely; this could be due to the sample preparation for the SEM, in which the samples are required to go under a drying phase and a gold coating. Figure 3-6c shows the surface of the gas-permeable hollow fiber, which consists of three layers. The external layer is polyethylene hydrophobic micro-porous with ~ 0.1 μm pore size (Li et al., 2013). Moreover, Figure 3-6d visually shows the biofilm matrix adhered to the membrane surface; and specifically shows diverse shapes of microorganisms (i.e., bacteria colony, a rod-shaped bacterium, and a granular bacteria colony), in which a consortium of methanotrophs and denitrifiers have been cultivated on the membrane external surface for over nine months.
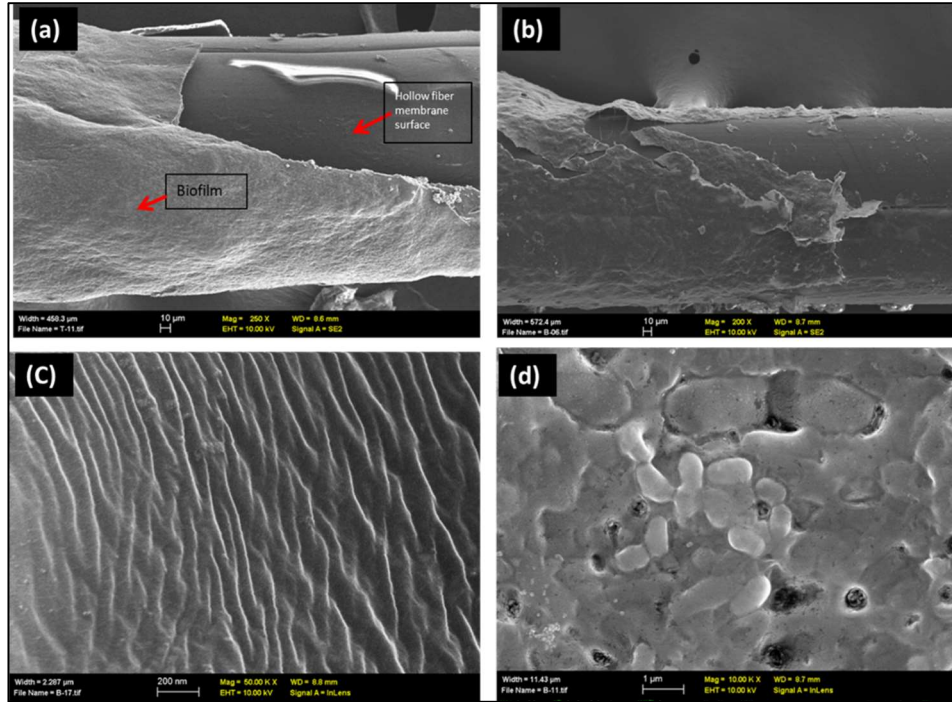
Figure 3-6. (a) SEM image of the upper section of the HF-membrane, (b) SEM image of the lower section of the HF-membrane, (c) SEM image of the exterior surface of the HF-membrane, (d) SEM image of the biofilm matrix adhered to the membrane surface.

The elemental analysis highlighted that carbon was the primary element in the biofilm with an average of 62%, nitrogen was second with 13%, and the rest are (Na, Mg, P, S, and K) shown in the Figure 3-7a. Oxygen was also observed in the biofilm layer, which is logical since the biofilm samples were exposed for a long time. The analysis of the surface of the hollow fiber membrane showed a different element composition as there weren't any microorganisms on the surface; 94 % carbon was detected, which proved that adequate amount of methane was diffused from the membrane lumen, along with nitrogen, oxygen, and silica as shown in the Figure 3-7b.
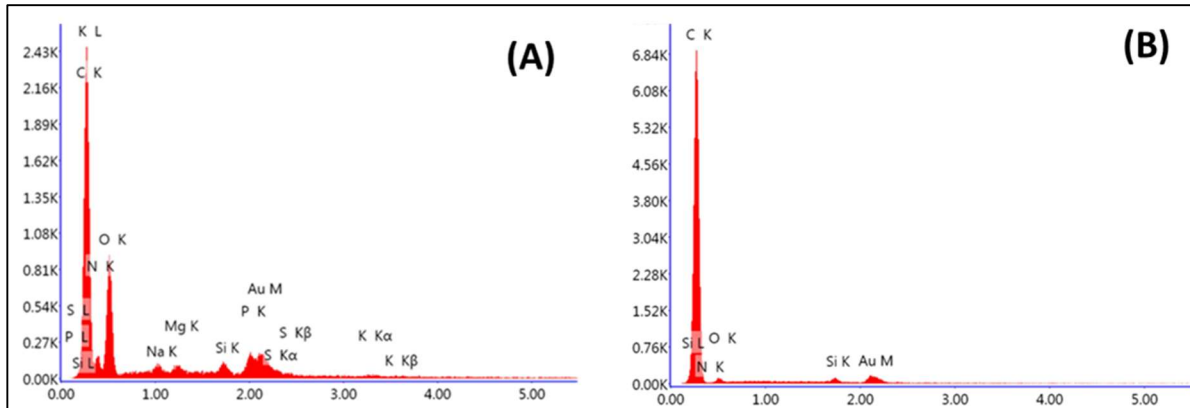
Figure 3-7. (A) MBfR biofilm element analysis, (B) MBfR gas-permeable hollow fiber membrane element analysis.

3.4 Conclusions and Implication of methane-MBfRs for denitrification

The methane based MBfR was investigated for denitrification performance, using methane gas as the sole electron donor and carbon source. Three different methane pressure levels were used in this experiment (2.0, 5.0 and 7.0 psig). The results found that at the low methane pressure of 2 psig, and HRT of (12, 8, and 4 h) nitrate concentration in the effluent was 5.5 ± 1.18, 8.8 ± 1.15, and 13.3 ± 0.91 mg N/L respectively. Moreover, the nitrate removal efficiency was positively correlated to the increase in methane pressure and the nitrate concentration at 5 psig methane pressure and HRT of (12, 8, and 4 h) in the effluent was 4.1 ± 0.81, 7.3 ± 1.31, and 11.9 ± 0.79 mg N/L respectively. At 7 psig the nitrate in the effluent was 3.3 ± 0.98, 6.9 ± 1.11, and 10.2 ± 1.23 mg N/L. However, there was no statistical significance between 7 and 5 psig, supporting the suggestion that the utilization of very high methane pressure does not impact the nitrate reduction, rather than over-using the methane, where the dissolved methane ranged between 8.0-13.0 mg CH_4/L in the effluent, which will eventually impact the operation cost of the nitrogen treatment in MBfRs. Also, this implies that there wasn't a significant issue regarding the methane gas transfer through the membrane to the

47

biofilm. In addition, leakage of methane gas into the atmosphere would contribute to the greenhouse gases impact on the earth's climate change (Howarth et al., 2011; EPA, 2017). The nitrite did not accumulate in the MBfR; it was continuously lower than 0.2 mg N/L. The scanning electron microscope images indicated a successful biofilm growth on the external surface of the hollow membrane with varying biofilm thickness, based on the biofilm position on the hollow-fiber-membrane, where the thickness was varying along the membrane, particularly near the gas source, which means that a more efficient membrane design should be considered in future research. The aerobic oxidation of methane via "intra-aerobic" pathway have been suggested by several studies that utilized methane gas in MBfRs (Lai et al., 2016; Luo et al., 2015), while reporting trivial O_2 intrusion to the MBfRs. This research provides systematic evidence that a microbial consortium consisting *Methylocystaceae* family and particulate methane monooxygenase (*pMMO*) genes are able to oxidize methane utilizing O_2. Additionally, the estimation of O_2 permeation further supports that a syntrophy of heterotrophic denitrification bacteria together with methanotrophic bacteria primarily reduced nitrate to N_2 gas in the membrane biofilm, rather than MOD proceeding via intra-aerobic pathway. Biological nitrogen removal processes have been widely applied to meet the strict environmental regulations. Wastewater treatment plants broadly use an external exogenous electron donor for nitrogen control (e.g., methanol), but this current practice is costly. The MBfRs can well control nitrogen in wastewater more economically. For instance, methane price ranges from \$0.24 -0.3/Kmol e$^-$, while methanol cost is ten-fold higher than methane (\$2.6-2.8/Kmol e$^-$) (Methanex, 2019; OEB, 2019). Moreover, methane is produced in anaerobic digesters of WWTPs. Thus, the MBfRs can utilize the free, on-site methane

48

for MBfR denitrification, substantially reducing chemical costs required for denitrification. Therefore, the methane-based MBfRs have the potential to be employed as tertiary nitrogen removal in WWTPs to minimize the concentration of total nitrogen in wastewater effluent. The infrastructure costs for MBfRs mainly originates from heavy-duty pipeline systems to deliver the biogas to MBfRs. The cost of black steel pipelines which can be used in transferring natural gas is $3.5-4.5/m, with a total length of 70-100 m, would be ~$250-450 with fittings and valves $1,500-2,000 (Ace Peel, Ca, 2020). Hence, it is estimated that the investment cost for MBfR infrastructure would be small, while a demonstration study is needed to determine accurate costs.

Chapter 4

Hypoxic Denitrification in a Membrane Biofilm Reactor Under Low Pressure and Concentration of Methane

4.1 Introduction

Research attention to the process of anaerobic and aerobic oxidation of methane coupled with denitrification has grown in recent years because of the potential for nitrogen control in wastewater treatment (Raghoebarsing et al., 2006; Modin et al., 2007; Ettwig et al., 2010; Welte et al., 2016; Cai et al., 2018; Lai et al., 2016; Lee et al., 2018; Xie et al., 2016). The application of methane oxidation coupled with denitrification in membrane biofilm reactors (MBfRs) has proven to be an effective engineering approach (Rittmann, 2007; Modin et al., 2007; Sun et al., 2013; Shi et al., 2013; Wang et al., 2016; Nerenberg, 2016). Achieving high nitrate removal rates have been one of the challenges in these sophisticated bioreactors. In a recent study, in which a methane based MBfR was employed to treat nitrate in groundwater in aerobic conditions (7 – 9 mg O_2/L), the removal rate has been reported at 0.45 g N/L-d (Luo et al., 2018). Moreover, in the previous study, both acetate and propionate were detected. Hence, it was presumed that methane was oxidized to intermediate VFAs, which was utilized by the heterotrophic denitrifiers as an electron donor to reduce nitrate. In recent studies that utilized methane in a MBfR have investigated high-strength wastewater with elevated nitrate and ammonium concentrations, in order to stimulate the microbial construction of ANME archaea, methanotrophic bacteria that utilizes intracellular O_2, besides anammox bacteria (Cai et al., 2018; Xie et al., 2016). However, this complicated microbial aggregation have been proven to be excessive for achieving high nitrate reduction in domestic wastewater. Even though, nitrate removal in methane-MBfRs have been reported in previous studies (Alrashed et al., 2018; Luo et al., 2018; Sun et al., 2013), still there are two major downsides to be addressed. Firstly, the dissolved methane that are leaked from the MBfR effluent to the atmosphere, which will add up to the environmental concern of the greenhouse gases emissions. Furthermore, the unutilized methane from the MBfR will negatively impact the operation cost and the energy optimization

of a scaleup MBfRs in the field. Thus, it is essential to control the dissolved methane in the

MBfR discharge, to have an optimal working condition for the MBfR in wastewater

applications. Secondly, is the limited information on the MOD pathways that can depict the

microbial community dynamics in the methane based MBfR that are operated under hypoxic

conditions. Such insight will facilitate addressing any operational challenges that might hinder

the MBfR performance in nitrate reduction. The first aim of this study was to achieve high

removal rate of nitrate while maintaining equitable dissolved methane in the effluent by

employing low methane pressure and concentration. The second aim is to characterize the

microbial community composition in the biofilm and the in the planktonic cells. Also, the flux of

the methane that was used for nitrate reduction was assessed in the MBfR. In addition, an in-situ

DO micro-sensor were utilized, to evaluate the hypoxic conditions in the MBfR during the

experiments.

4.2 Methodology

4.2.1 Fabrication and Operation of the MBfR

Acrylic tubes (Plexiglas) were used to fabricate the study's MBfR, with the following

dimensions 30 cm long and 1.10 cm inner diameter, with a total working volume of 75.0 mL.

Two membrane modules were prepared using hydrophobic polyvinylidene difluoride (PVDF)

gas permeable hollow fiber membranes with an outer diameter of 1.2 mm (Econity Co. Ltd.,

South Korea). Each module consisted of 10 membranes, with a total surface area of 188.5 cm^2

(the membrane packing density in the MBfR was 251 m^2/m^3). Next, these hollow fiber

membranes were bundled together with Plexiglas housing tubes (ϕ 0.6 cm and 3 cm length)

using a hydrophobic silicone sealant (Loctite Model 908570, Henkel North America,

Bridgewater, NJ, USA) before being left to cure (Figure 4-1) and (Figure 4-2). After curing, gas

leak tests were performed. The MBfR was inoculated with an effluent from a mother MBfR that had been operated for nitrate reduction with methane gas (99.0 %, Praxair, Canada) as the electron donor for two years, consisting of a type II methanotrophs (*Methylocystaceae* family) (Alrashed et al., 2018). Methane gas (20.0%, Praxair, Canada) and 80% He was supplied to the membrane modules as the sole electron donor and carbon source. To have an accurate methane pressure readings, a digital manometer was used in the experimental setup (see Figure A-4).The medium composition of the synthetic nitrate mineral solution (NMS) per liter of deionized water was as follows: $NaNO_3$, 184; $FeSO_4 \cdot 7H_2O$ 1; $CaCl_2 \cdot 2H_2O$ 1; $MgSO_4 \cdot 7H_2O$ 200. In addition, the phosphate buffer composition was Na_2HPO_4, 434; KH_2PO4 128, preserving a pH value within the 7 ± 0.5 range. Additionally, 1 mL of trace element solution was added to each liter of medium. The composition of the trace solution was as follows (mg/l): $ZnSO_4.7H_2O$ (100), $MnCl_2.4H_2O$ (30), H_3BO_3 (300), $CoCl_2.6H_2O$ (200), $CuCl_2.2H_2O$ (10), $NiCl_2.2H_2O$ (10), $Na_2MoO_4.2H_2O$ (30), and Na_2SeO_3 (30). The liquid medium was fed to the MBfR with a peristaltic pump after a medium glass bottle (VWR, Canada) was autoclaved for 20 min at 120 °C, cooled to room temperature, and purged with N_2 gas (99.0%; Praxair, Canada) for 45 minutes. Then it was coupled with an N_2 gas bag (1 Liter Tedlar - Sigma-Aldrich, St. Louis, MO, USA). To monitor the O_2 concentration inside the MBfR, an in situ microsensor was implicated (PreSens, Regensburg, Germany) having a detection limit of 0.003 mg O_2/L (see Figure A-3). The circulation rate inside the MBfR was set at 10 mL/min via a peristaltic pump to avoid excessive detachment of the biofilm (Masterflex L/S economy Variable-Speed Drive, RK-07554-80; Masterflex, Gelsenkirchen, Germany).
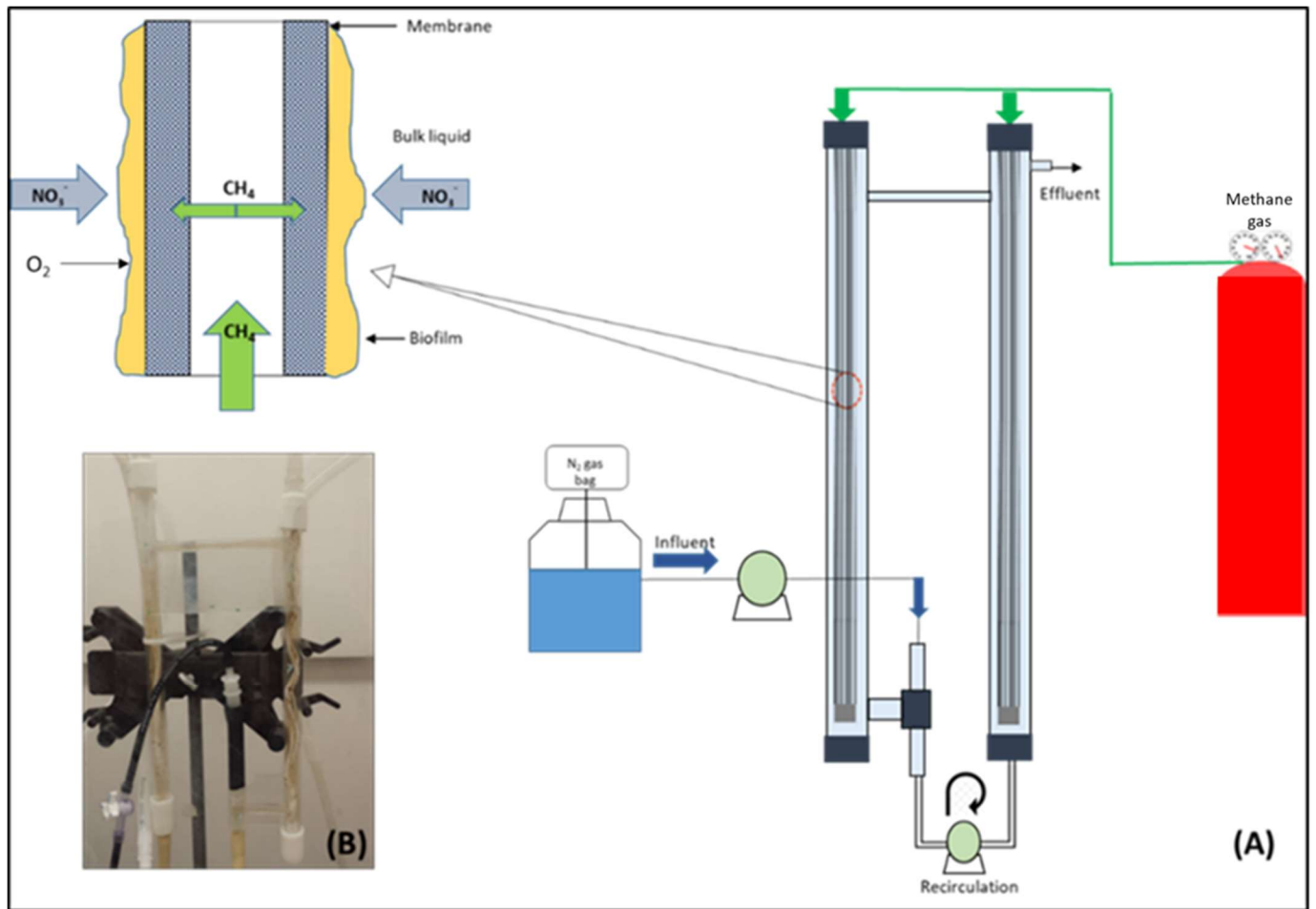
Figure 4-1. (A) Schematic of the membrane biofilm reactor system (MBfR); (B) image of the methane-based MBfR.
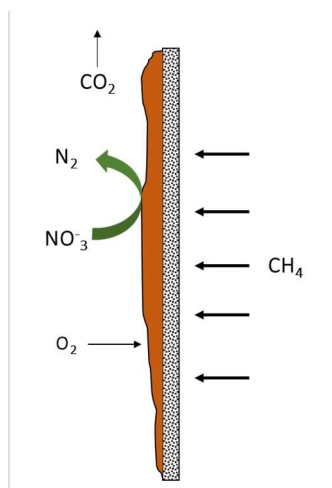
Figure 4-2. Schematic of the proposed syntrophic reactions on the outer surface of the matured biofilm.

4.2.2 Liquid Analysis

Chemical analyses for both nitrate and nitrite were performed using an Ion chromatograph (Dionex ICS-1100, Thermo Scientific, Waltham, MA, USA) equipped with an AS9-SC analytical column (Dionex Ion-Pac, 4×250 mm, Thermo Scientific, Waltham, MA, USA) with 9 mM sodium carbonate as an eluent at a flow rate of 1.00 mL/min. Before analysis, the liquid samples were filtered with syringe filters (PS: 0.450 μm, VWR International Inc., Canada). Samples were regularly collected from the medium feed and the effluent and measured for nitrate and nitrite concentration in duplicate (see Figure A-2). For N_2O gas quantification, a gas chromatograph (GC-2014, Shimadzu, Kyoto, Japan) equipped with an electron capture detector (ECD) and a molecular sieve column (6 ft $\times$ 1/5 in., 85/100 mesh; Alltech, Nicholasville, KY, USA). The temperatures of the column and the detector were constant at 250 °C and 80 °C, respectively, and helium was used as the carrier gas (99%, Praxair, Canada) at a pressure of 144 Kpa. Gas samples were collected regularly from the headspace of the MBfR via a gastight syringe (Hamilton Gastight Syringe, Hamilton, USA).

4.2.3 Quantification of Methane Gas

Methane gas quantification methodology was adapted from Yeo & Lee (2013), where liquid samples taken from the MBfR using a syringe were directly transferred to a 20 mL vial that had been sparged with N_2 gas (99%, Praxair, Canada). The vial was vigorously mixed with a vortex mixer (Fisher Scientific, Pittsburgh, PA, USA) for 5–6 minutes in order to reach equilibrium between gas and liquid phases. Next, the gas was sampled from the headspace of the vial, and the gas composition was quantified using a GC equipped with a thermal conductivity detector (TCD; SRI 310C, SRI Instruments, USA) (see Figure A-1).

4.2.4 Microbiological Population Analysis

In order to have an in-depth understanding of the bacterial community structure and syntropy, microbial community analyses of the biofilm developing on the membrane exterior surface and of the plankton cells in the suspension were investigated. The biofilm samples were sampled via sterile swabs (Puritan Medical Products, USA). Biofilm samples were collected at the end of each experiment after reaching a steady-state phase, sampling was done in duplicate, and the process was performed after sterilizing the sampling tools and the vails in an autoclave at 121 ℃ for 20 minutes. During sampling, 75% alcohol was used to disinfectant the gloves and the working area to avoid any cross contamination. To explore the microbial consortium, 16S ribosomal RNA (rRNA) based sequencing, which is commonly applied for microbial taxonomic analysis and highly conserved in most bacterial and archaeal species (Coenye & Vandamme, 2003), was performed. Thus, RNA and DNA were extracted from the samples using an extraction kit, and Illumina sequencing was performed. Processing and analysis of the data were completed with Mothur software for analyzing microbial communities based on 16S rRNA gene sequences. Together with these analyses, the Basic Local Alignment Search Tool (BLAST) was

used for further confirmation of phylogenetic relationships of the microbial species. BLAST compares retrieved data to sequence databases at an acknowledged statistical significance. The sequencing results showed a relative abundance of sequences at diverse taxonomic levels, displaying the most dominant bacteria, and revealing significant pathways responsible for hypoxic methane oxidation and nitrate reduction.

4.3 Results and Discussion

4.3.1 Evaluation of Nitrate Loading Rate Impact on Denitrification

Initially, the MBfR was operated at batch mode to confirm steady-state nitrate removal. Once a steady state was confirmed, the MBfR operation was switched to continuous mode. The biofilm accumulation and attachment in the methane MBfRs takes long times, ranging from 3 to 10 months (Luo et al., 2018; Alrashed et al., 2018). Moreover, in a supplementary experiment, an MBfR with a volume of 1000 ml was operated to investigate the impact of expanding the membranes 'surface area on enhancing the biofilm density and subsequently improving the denitrification performance (see appendix B) for supplementary information. The main conclusion from the latter experiment was at long membranes (~60 - 80 cm), the gas delivery will have a significant mass transfer issue due to the concentration gradient that resulted from the gas pressure deficiency, especially towards the lower portions of the membrane (Martin et al., 2012).

Figure 4-3 illustrates the biofilm accumulation patterns for the first six months are in. In order to investigate our research hypothesis, which is the capability and sustainability of nitrate removal via MBfR using methane as the sole electron donor and carbon source under hypoxic conditions, the MBfR was operated under three nitrate loading rates (~ 40, 80, and 120 g N/m^3-d), corresponding to an HRT of 12 hours, 8 hours, and 4 hours.
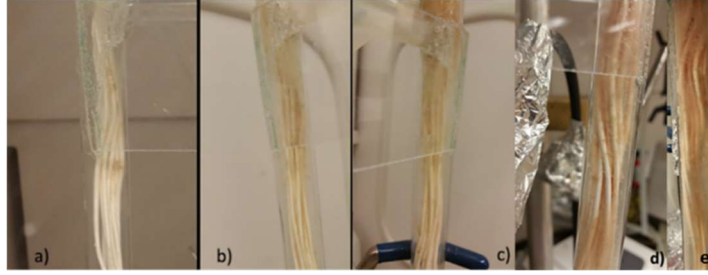
Figure 4-3. Biofilm accumulation on the hollow fiber membrane in the methane-based MBfR at different stages: (a) after 14 days, (b) after 37 days, (c) after 48 days, (d) after 76 days, and (e) after 183 days.

The first stage is illustrated in Figure 4-4a, during which the MBfR was run at an HRT of 12 hours (40 g N/m^3-d) and steady methane pressure of 0.35 kPa (0.05 psig). Because that was the initial stage of operating the MBfR, the denitrification continued to improve. Subsequently, the MBfR was operated in the second stage by reducing the HRT to 8 hours ($\sim$ 60 g N/m^3-d), and the nitrate removal profile is shown in Figure 4-4b. The MBfR was operated for a similar period as in the previous operational stage and reached a steady state at 86% nitrate removal efficiency. This implies that the microbial consortium acclimatizing on the membrane biofilm was growing yet steadily, particularly in the applied operational conditions where methane was the sole supplied organic carbon source. Additionally, operating the MBfR under hypoxic environment might have contributed to this biofilm accumulation pattern, as it was reported by Luo et al., 2018, when the oxygen level increased in the MBfR, the nitrate reduction improved to $\sim$ 0.42 mg N/L-h from 0.02 mg N/L-h. Moreover, they reported a dissolved oxygen concentration of $\sim$ 8.0 mg O$_2$/L, which is substantially high. Moving on to the last stage, the MBfR was operated at an HRT of 4 hours. Figure 4-4c shows the nitrate removal profile at a fixed methane pressure of 0.05 psig and HRT of 4 hours. The steady state was accomplished at $\sim$81% removal efficiency, and the concentration of nitrate in the MBfR effluent was 4.01 $\pm$ 0.68 mg NO$_3^-$-N/L. The

difference between the three loading rates was statistically significant (ANOVA; $P < 0.05$). The same trend of the HRT effect concur with literature, that investigated methane-MBfRs for nitrate reduction (Shi et al., 2013; Xie et al., 2016; Luo et al., 2018). However, they have started operating the MBfRs with high HRTs, up to 5 days for extended time (~300 days), this is in fact is a major factor in any CH_4-MBfR start up, in which the biofilm attachment and successful enrichment can be achieved (Luo et al., 2018). Another important factor is the microbial consortium kinetics, in which a modeling study found that increasing the methane specific utilization rate be able to improve the nitrate removal rate (Lee et al., 2018).
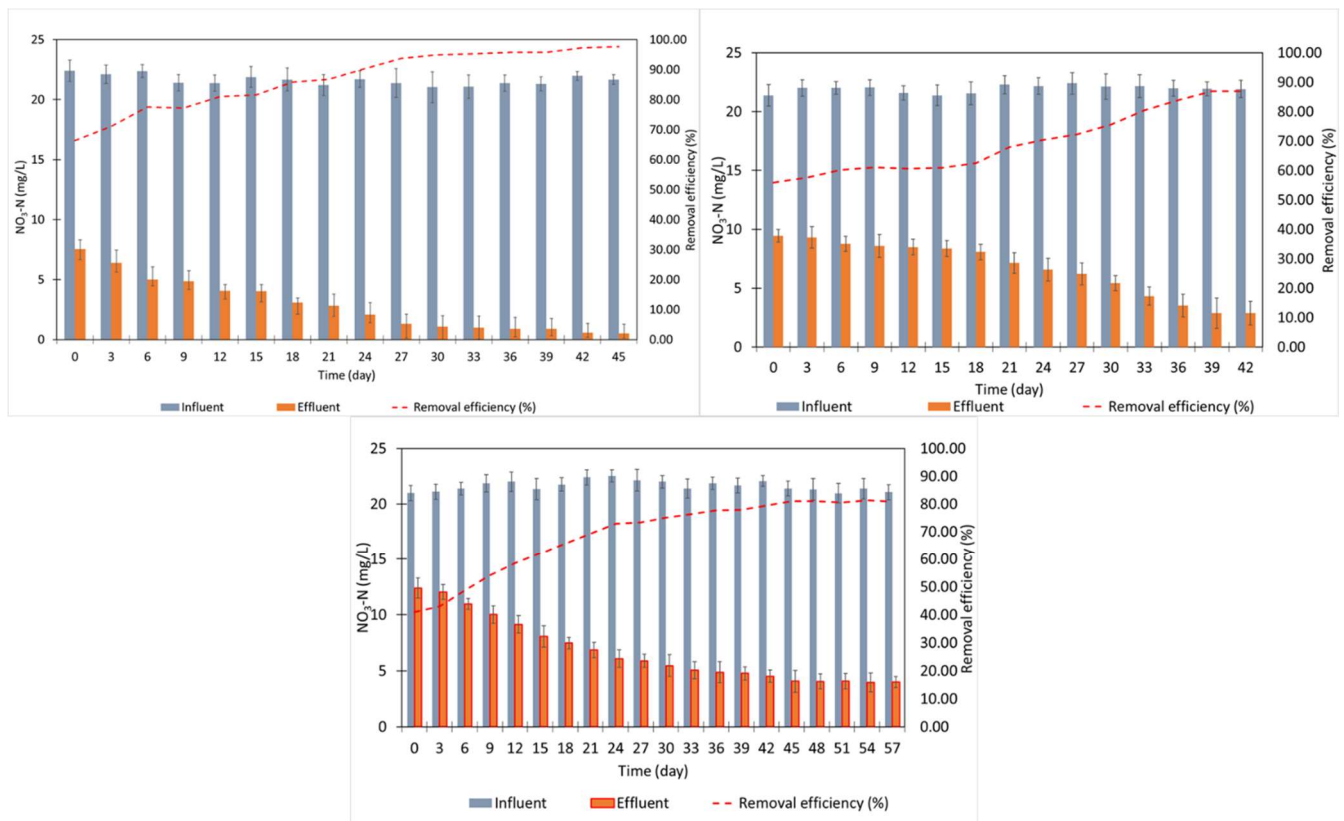
Figure 4-4. Nitrate removal pattern in the methane-based MBfR at methane pressure of 0.35 kPa (0.05) psig, (a) at loading rate of 40 g N/m^3-d, HRT of 12 hours, (b) at loading rate of 60 g N/m3-d, HRT of 8 hours, (c) at a nitrite loading rate of 120 g N/m^3-d, HRT of 4 hours.

4.3.2 Methane Flux Impact on Denitrification in the MBfR

Methane flux and pressure have been proven to correlate with denitrification in MBfRs (Alrashed et al., 2018), in that study, a relatively high methane pressures was applied (7.0 psig), in addition to the high pressures, the methane concentration was 99.9% CH_4. Hence, the present study's proposed hypothesis assumed that low pressure and diluted methane would provide an adequate carbon source and electron donor (methane) for the microbial community to drive the nitrate reduction process to an optimum level. Consequently, a low pressure was applied (0.05, 0.15, and 0.25 psig), respectively. and the methane concentration was diluted to 20% CH_4 instead of 99%. The MBfR was operated at a steady state in three phases, and the findings of the first phase are shown in Figure 4-5a. In this experimental setup, the optimum nitrate removal of 98% efficiency was logged at the highest HRT of 12 hours with a nitrate removal flux of 162.2 mg N/m^2-d. After establishing an almost complete nitrate removal at 12 hours, the MBfR was moved to an HRT of 8 hours with the same operating conditions as the previous stage, and the with a nitrate removal flux of 215.1 mg N/m^2-d. After that, the MBfR was left to run for 2 months at an HRT of 4 hours and a relatively low circulation rate to prevent biofilm detachment due to the sheer force effect (Liu et al., 2002; Telgmann et al., 2004). Eventually, the denitrification steady state was recorded at 80% removal efficiency, with a nitrate removal flux of 404.1 mg N/m^2-d. The difference between the three HRTs was found to be statistically significant at ($P < 0.05$, ANOVA). Moreover, in order to continue monitoring the methane pressure impact, the pressure was increased to 1.03 kPa (0.15 psig). To monitor the nitrate removal profile under the same conditions as the first phase, the nitrate loading rates were varied at 40, 60, and 120 g N/m^3-d, (HRT of 12 hours, 8 hours, and 4 hours), respectively. It can be seen in Figure 4-5b that the denitrification profile had a comparable pattern as the previous

phase (0.05 psig). At an HRT of 12 hours, 8 hours, and 4 hours, the nitrate removal flux was

155.5, 212.1 and 407.5 mg N/m^2-d, respectively. This implies that increasing the methane

pressure by 0.1 psig had a minor effect on the denitrification performance in the MBfRs,

suggesting that the methane-based MBfRs can be operated at minimum operating costs in

wastewater treatment plants, where biogas are produced on-site that contains 50 - 60% methane

(Makisha et al., 2018).

In the last stage, the methane pressure was again increased by 0.1 psig up to 0.25 in order to

confirm the findings from the previous stage. All of the operating conditions were maintained at

as the previous experimental setup. The results displayed in Figure 4-5c showed that the overall

denitrification performance was enhanced to a certain extent. Here, the nitrate concentration was

as low as 0.4 ± 0.85 mg NO$_3^-$-N/L in the MBfR effluent for an HRT of 12 hours, with a nitrate

removal flux of 163.8 mg N/m^2-d. Furthermore, at HRTs of 8 hours and 4 hours, the nitrate

removal flux was 220.1 and 413.0 mg N/m^2-d, respectively. It can be seen that the methane

pressure had an impact on the denitrification performance. In particular, at the HRT of 4 hours,

the nitrate removal flux enhanced from 403.0 to 412.6 mg N/m^2-d, when the pressure was

increased from 0.05 to 0.25 psig. Table 4-1 summarizes the nitrate removal profile at different

methane pressure, the nitrate removal flux is equivalent to 53 - 144 mmol electrons/m^2-d.
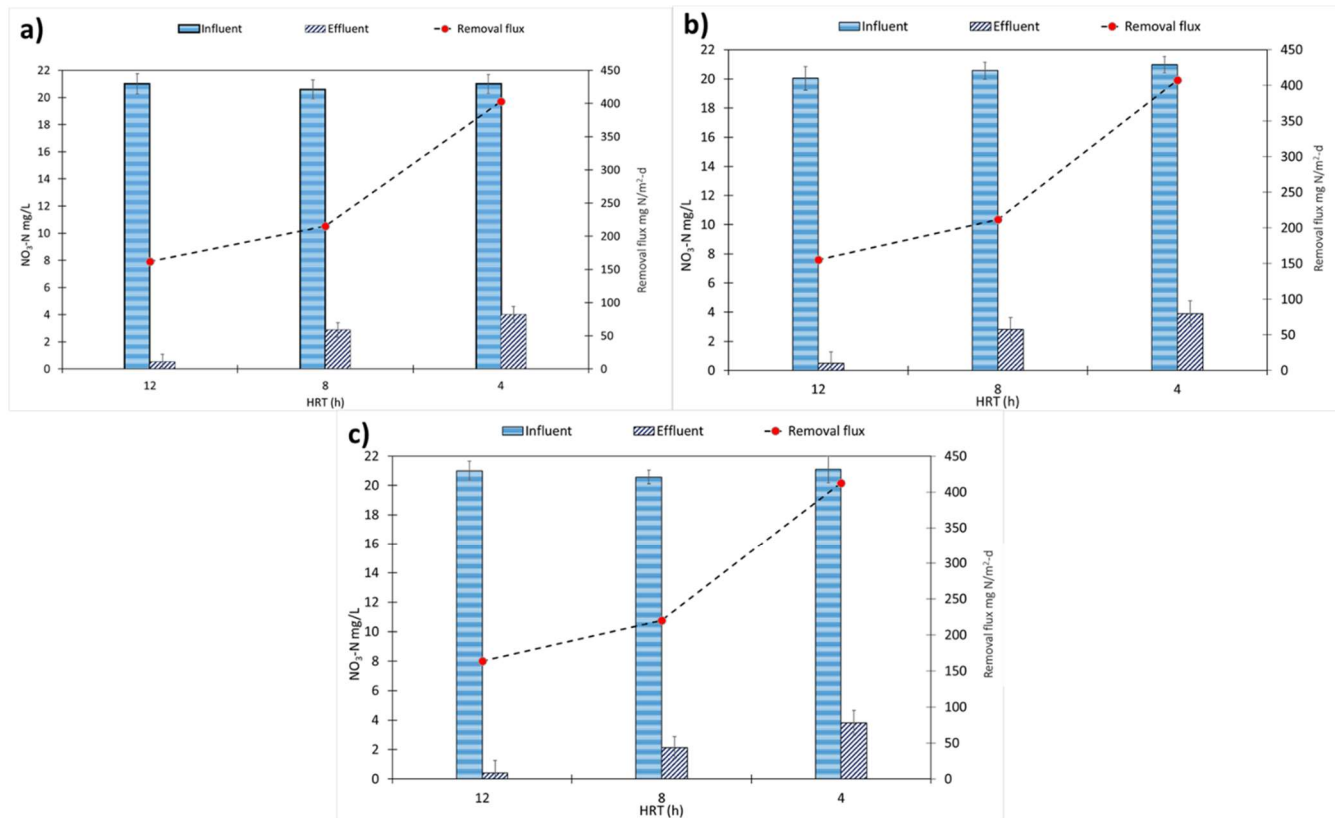
Figure 4-5. Methane pressure impact on denitrification in the methane MBfR, with nitrate loading rates of 40, 60, and 120 g N/m³-d, (HRT of 12 hours, 8 hours, and 4 hours, respectively). a) at 0.35 kPa (0.05 psig), b) at 1.03 kPa (0.15 psig) and c) at 1.72 kPa (0.25).

Table 4-1. A summary of the denitrification profile in the methane-based MBfR at a nitrate loading rate of 120 g N/m³-d and an HRT of 4 hours.

CH$_4$ pressure kPa [psig]	NO$_3^-$-N (influent) (mg/L)	HRT (h)	NO$_3^-$-N Removal flux mg N/m²-d	NO$_3^-$-N Removal flux (mmol e⁻/m²-d)
0.35 [0.05]	20 ± 0.69	4	160.4	57
1.03 [0.15]	20 ± 0.56	4	218.3	78
1.72 [0.25]	20 ± 0.91	4	403.2	144

4.3.3 Assessment of Influent Nitrate Concentration on Denitrification

This experiment was designed to investigate the impact on denitrification performance of increasing the concentration of nitrate feeding the MBfR while also maintaining a stable methane pressure at 0.05 psig (0.35 kPa). The hypothesis was that nitrate reduction would be hindered by the abundance of the primary electron acceptor in the biofilm. Firstly, the nitrate concentration in the influent was 20 ± 0.68 mg NO_3^--N/L. In the second stage, the nitrate concentration was folded to 40 ± 1.06 mg NO_3^--N/L, which was selected bearing in mind that the maximum permissible content for nitrate in drinking water is 10 mg NO_3^--N/L (WHO, 2003). In order to compare the outcomes, both methane pressure and HRT were fixed throughout all of the experiments. Figure 4-6 shows a comparison between the two stages at methane pressure of 0.05 psig and HRT of 4 hours. Figure 4-6a, illustrates stage I, where the nitrate removal flux was 407.0 mg N/m^2-d, with a nitrate concentration in the effluent of 4.01 ± 0.68 mg NO_3^--N/L. Moreover, the removal flux increased to 446.4 mg N/m^2-d when the nitrate influent concentration was 40 ± 1.06 mg NO_3^--N/L. These results document that the MOD microorganisms in the biofilm was not hindered by the abundance of nitrate in the bulk liquid. In fact, it seems that the activity of the microbial population in the biofilm was boosted by the increase of the main electron acceptor. Figure 4-6b illustrates the nitrate removal profile between the two stages at HRTs for 8 hours. It can be seen that the removal flux had a similar trend as the previous, at 215.2 mg N/m^2-d, and increased to 225.5 mg N/m^2-d. This adds to the outcome that the methanotrophs in the biofilm were not challenged under these conditions. Furthermore, when the contact time was increased, the microbial kinetics were capable of completing the nitrate reduction, despite the abundance of the main electron acceptor.
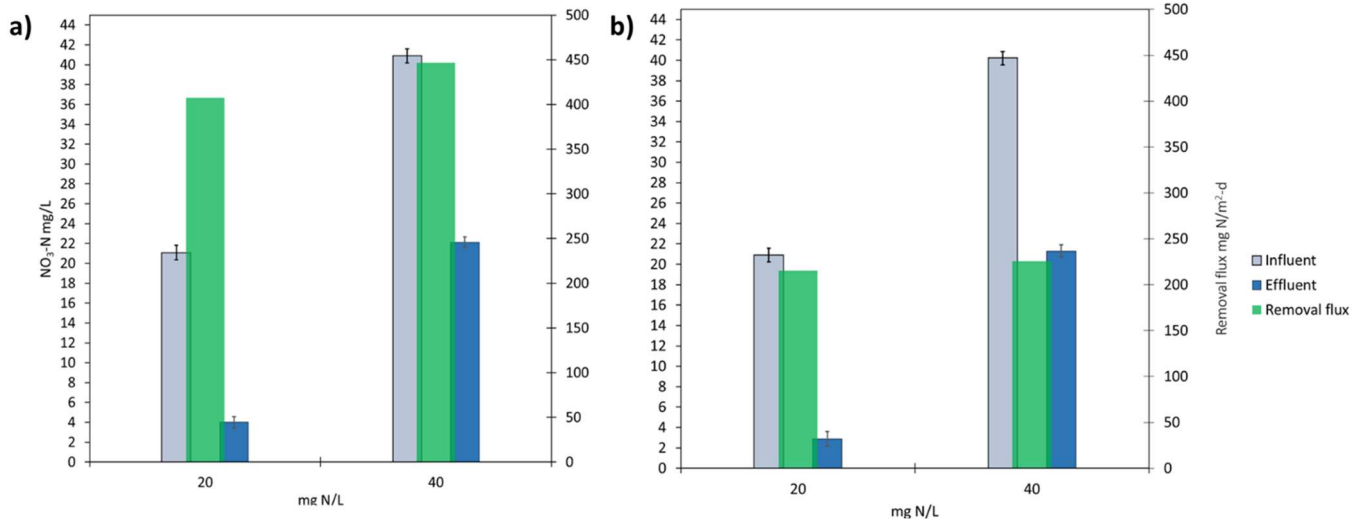
Figure 4-6. Denitrification profile at methane supply pressure of 0.35 kPa (0.05 psig) and influent nitrate concentrations of 20 mg and 40 mg NO$_3^-$-N/L. a) for HRT of 4 hours, and b) for HRT of 8 hours.

4.3.4 Dissolved Methane in the MBfR

Quantification of dissolved methane was performed in all experiments. It was essential to measure the dissolved methane in the MBfR effluent to understand the impact of the methane pressure and flux that were supplied to the membrane. Based on the outcomes of previous research; chapter 3, a diluted methane (20%) was applied to supply gas to the MBfR. The supply gas pressure was reduced, subsequently reducing the flux of methane to the biofilm. As shown in Figures 4-7a, b and c, a direct result of reducing the methane flux is the reduction in methane concentration in the MBfR effluent from 13 mg CH4/L in Alrashed et al. (2018) to a range of 4.0 to 7.0 mg CH4/L. The pressures applied were 0.35, 1.03, and 1.72 kPa (0.05, 0.15, and 0.25), respectively. All measurements were accomplished at a steady state of denitrification so that all the dissolved methane results had matching operational settings. The effect of increasing the methane flux was a build-up of the dissolved methane in the MBfR effluent. The dissolved

methane was recorded at 6.77 ± 0.95 mg CH4/L at the lowest methane pressure of 0.05 psig. The

dissolved methane increased to 6.89 ± 1.02 at 0.15 psig and went up to 7.02 ± 1.08 mg CH4/L at

the highest methane pressure of 0.25 psig. All the dissolved methane concentration in the MBfR

effluent was below the limits of 10 mg CH4/L, that was recommended by the office of surface

mining at the USA department of interior (Eltschlager et al., 2001). The difference between the

three methane supply pressures was found to be significant (ANOVA, $P < 0.05$). Apparently, at

an HRT of 12 hours, the dissolved methane concentration in the effluent was in a close range.

However, as the HRT decreased, the concentration dropped as well, as shown in Figures 4-7a, b

and c.

Figure 4-7b establishes the methane profile at an HRT of 8 hours. The results demonstrate a

positive correlation between the methane pressure and dissolved methane at $r = 0.93$. The

methane in the effluent was found to be the least, 5.11 ± 0.84 mg CH4/L, at the minimum

pressure of 0.05 psig. The methane in the effluent was 6.05 ± 1.11 and 6.24 ± 0.97 mg CH4/L for

methane pressures of 0.15 and 0.25 psig, respectively. The dissolved methane in the effluent was

decreased to 8 hours in comparison to the HRT of 12 hours.

The dissolved methane in the MBfR effluent at an HRT of 4 hours was the lowest concentration

of the conditions, as seen in Figure 4-7c. It had a similar pattern as the prior test for a correlation

between the supplied pressure and the concentration in the effluent. The lowest values of

methane concentration in the operating conditions were 3.34 ± 1.07 mg CH4/L found at

0.05 psig and 4.02 ± 0.88 mg CH4/L at 0.25 psig, dissolved methane data are listed in Table 4-2.

These diluted methane pressures were at the minimums that could be supplied to the MBfR

because a special micro regulator was used to regulate the pressure in order to minimize the

methane delivered to the biofilm. This allowed for examination of the hypothesis that a

minimum methane availability in the biofilm active layer has the ability to support the

methanotrophs and the denitrifiers to optimize the denitrification process.
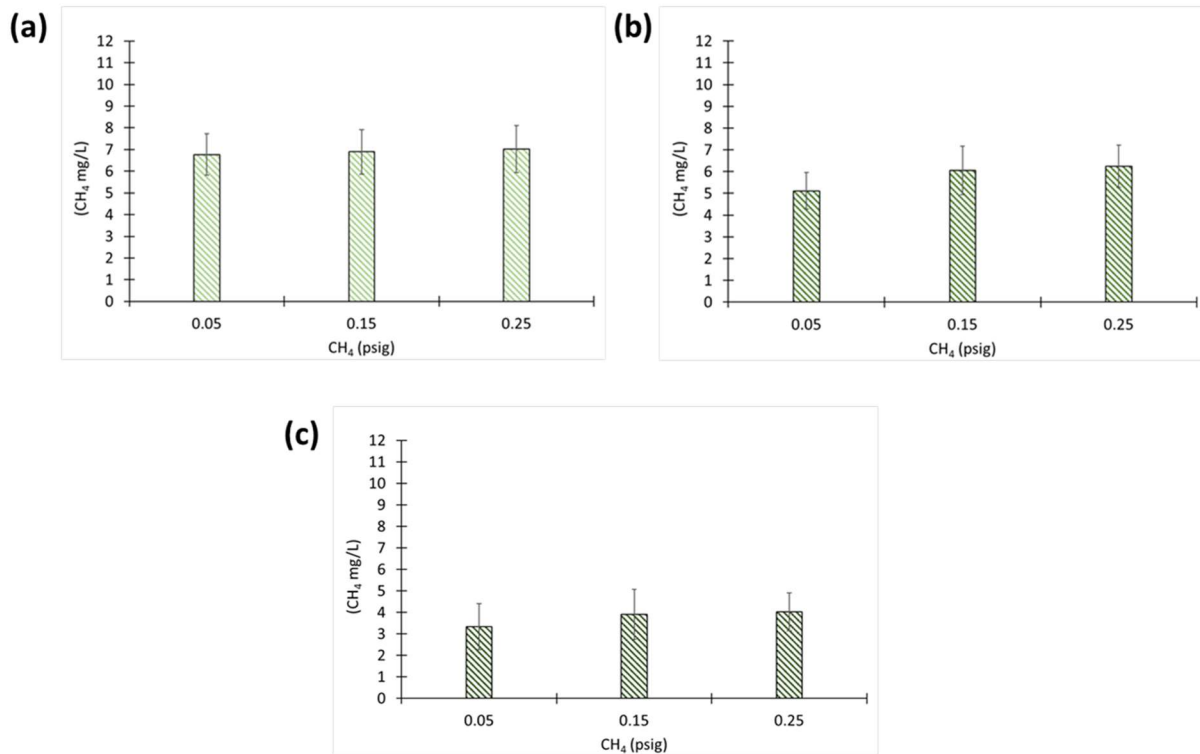
Figure 4-7. Dissolved methane concentration in the methane-based MBfR at methane supply pressure of 0.05, 0.15, and 0.25 psig. (a) at a nitrate loading rate of 40 g N/m3-d, HRT of 12 hours, (b) at a nitrate loading rate of 60 g N/m3-d, HRT of 8 hours and at a nitrate loading rate of 120 g N/m3-d, HRT of 4 hours.

Table 4-2. Dissolved methane profiles at methane pressures of 0.05, 0.15, and 0.25 psig and HRTs of 4, 8, and 12 hours.

20% CH_4 pressure kPa [psig]	HRT (h)	Dissolved CH_4 (mg/L)	HRT (h)	Dissolved CH_4 (mg/L)	HRT (h)	Dissolved CH_4 (mg/L)
0.35 [0.05]	4	3.34 ± 1.07	8	5.11 ± 0.84	12	6.77 ± 0.95
1.03 [0.15]	4	3.91 ± 1.17	8	6.05 ± 1.11	12	6.89 ± 1.02
1.72 [0.25]	4	4.02 ± 0.88	8	6.24 ± 0.97	12	7.02 ± 1.08

In Figure 4-8, both methane flux and the methane utilized in the denitrification process are illustrated. In which methane leakage at HRTs of 12,8 and 4 hours was 90, 120 and 210 mmol electrons/m^2-d, respectively, which is in a range of 19-30% of the total methane supplied to the MBfR. This implies that there wasn't any significant resistance limiting the methane gas transfer from the membrane to the acclimated biofilm. The methane leaking to the bulk liquid may be attributed to the ununiform distribution of the biofilm along the membrane, in which the biofilm density and thickness varies.
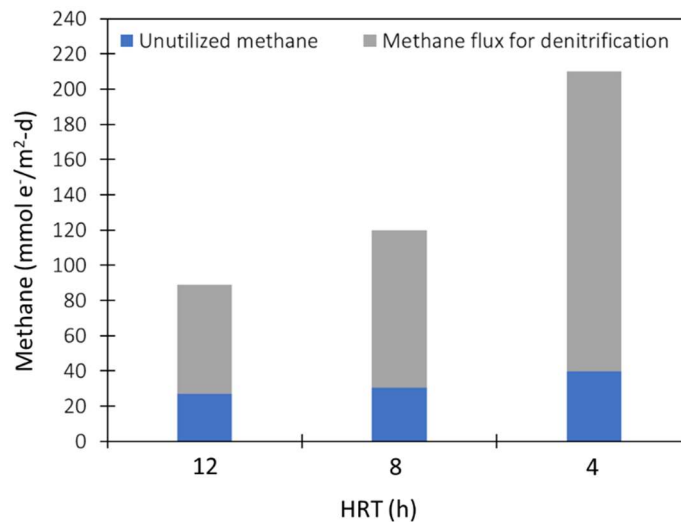
Figure 4-8. Methane flux for denitrification and unutilized methane in the MBfR run at 12, 8, and 4 h HRTs.

4.3.5 Dynamics of the Microbial Community in the MBfR

To have a comprehensive knowledge of the microbial community dynamics of the biofilm and planktonic cells in the MBfR, bio-samples were collected after confirming a nitrate removal steady state to investigate the study hypothesis regarding the resemblances of the abundance of bacterial species in the biofilm and planktonic cells (Douterelo et al., 2017). A comparison of planktonic cell and biofilm microbial communities showed a resemblance at 38% of the

ribosomal DNA of the whole population for the planktonic cells and 37% for the biofilm (Figure 4-9A). This indicates that suspended biomass can represent the main abundant microbial consortium in the biofilm. In fact, this conclusion can resolve the challenge of biofilm sampling issues that researchers face with delicate bioreactors such as MBfR and microbial electrolysis cell (MEC). The 16S rRNA sequencing showed the abundance of methanotrophs and denitrifying bacteria illustrated in Figure 4-9B. Moreover, the anaerobic methanotrophic (ANME) archaea were not identified in the 16S rRNA genes linked with metagenomic libraries. The dominant bacterial sequences distinguished were affiliated with *Methylococcus*, a Type I methanotroph (Wang et al., 2016), at 28% and 53% for HRTs of 8 and 4 hours, respectively. Next was *Hyphomicrobium* at 9% and 7% for HRTs of 8 and 4 hours, respectively (Timmermans et al., 1983). The last bacteria classified in the heterotrophic denitrification category included *Geothrix* at 7% and 3% and *Terrimonas* at 5% and 6% for HRTs of 8 and 4 hours, respectively (Zhang et al., 2010; Shen et al., 2016).

The hypoxic conditions in the MBfR can explain the interactions among the microbial consortium, which was dominated by Type I methanotrophs (*Methylococcus*). This finding is different from the inoculum microbial population that was used for this study. The inoculum was dominated by Type II methanotrophs (*Methylocystaceae* family). Moreover, the significant alteration was the diluted methane, with 20% applied in this research, while it was 99.9% in the previous study (Alrashed et al., 2018). This implies that *Methylococcus* (Type I methanotrophs) thrive at low levels of methane concentration. Also, this indicates how simply the microbial community shifts based on the environmental conditions. The HRT decrease from 8 hours to 4 hours resulted in an approximately twofold increase in the relative abundance of *Methylococcus*. Figure 4-9B, illustrates that the relative abundance of *Methylococcus* was doubled when the

HRT decreased from 8 hours to 4 hours, which could be explained by the increase in the nitrate loading rate from 60 to 120 g N/m^3-d, in addition to the dynamics of the oxygen level in the MBfR at shorter HRTs. Therefore, operating methane-based MBfRs at short HRTs could enhance the denitrification performance in the MBfR.
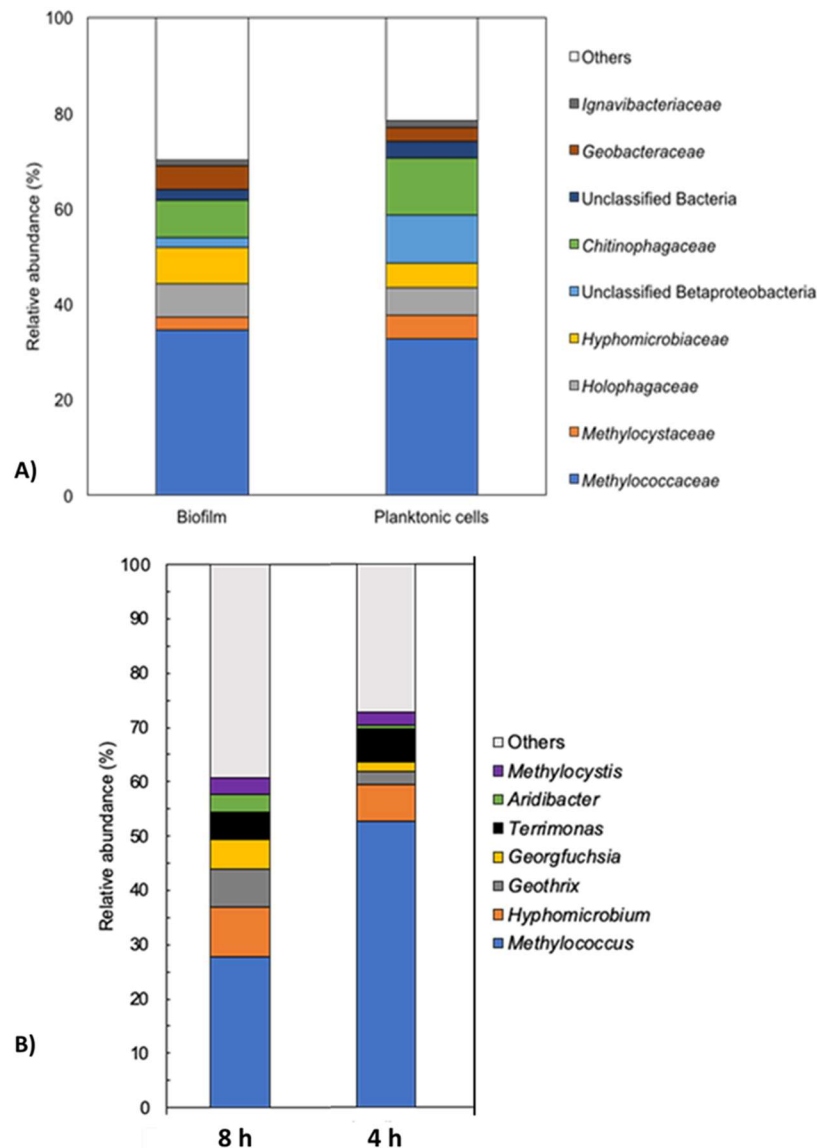
Figure 4-9. Relative abundance of microbial taxa based on 16S rRNA genes in amplicon-based libraries. (A) The microbial populations of biofilm and planktonic cells collected from the MBfR effluent. (B) Microbial community composition of membrane biofilm samples from HRTs of 8 hours and 4 hours. "Others" indicates bacterial genera below 3% relative abundance.

4.4 Conclusion

Denitrification performance was optimal at an HRT of 12 hours and loading rate of 40 g N/m^3-d, while maintaining the methane pressure at 0.05 psig (0.35 kPa). When the HRT was decreased to 8 hours, the removal efficiency dropped to 86.0%, and when the MBfR was operated at an HRT of 4 hours for 2 months, the removal rate came to a steady state at 80.0% at a 120 g N/m^3-d loading rate and nitrate removal rate of 413 mg N/m^2-d. This indicates that the microbial community continued to adapt and accumulate on the outer surface of the membrane. Furthermore, at the same HRT (4 hours), the dissolved methane in the MBfR effluent was 3.34 ± 1.07 mg CH_4/L, indicating that there was an adequate supply of methane to drive the denitrification process even at this very low pressure (0.05 psig). The microbial community in the MBfR was dominated by *Methylococcus*, which is a Type I methanotroph capable of oxidizing methane under hypoxic conditions (Kalyuzhnaya et al., 2013). In this condition, the dissolved oxygen concentration was approximately 0.04 mg/L, which implies the hypoxic methane oxidation pathway. The analysis outcomes showed that denitrifying methanotrophs and ANME archaea were not detected in the 16S rRNA genes. The study results lead to the conclusion that methane-based MBfRs have a potential application for nitrogen removal in wastewater treatment utilizing the on-site produced methane gas at very low pressure and concentration with a trivial methane build-up in the MBfR effluent. Furthermore, this approach could be applied as an eco-friendly and cost-effective alternative to existing tertiary or sidestream nitrogen treatment techniques to prevent harmful effects from the discharged nitrogen to the local environment and bodies of water.

Chapter 5

Nitrite Reduction in A Membrane Biofilm Reactor in Hypoxic Environment Under Low Pressure and Concentration of Methane

A version of this chapter, co-authored by Alrashed, Wael, Lee, Jangho and Lee, H.S., is under preparation for submission to a refereed journal for peer-review and publication.

Contributions statement: Wael Alrashed performed the fabrication of the bioreactor, performed laboratory experiments and analyses, sampling the biofilm, and contributed to data interpretation and manuscript preparation. Lee, J, organized the analysis of the microbial community. Under the supervision of Lee, H.S.

5.1 Introduction

Due to the excessive use of fertilizers in the environment, both nitrite and nitrate have emerged as electron sinks in the majority of water bodies creating sever environmental issue like eutrophication (Bhattarai et al., 2018; Han et al., 2018; Stein et al., 2016). Meanwhile methane gas is known to function as an active electron donor, via both aerobic and anaerobic pathways (Ettwig et al., 2008; Haroon et al., 2013). For the past few years, a number of studies have investigated coupling methane oxidation and nitrite reduction via microbial consortium in sequencing batch reactors (SBR) and membrane bioreactors (MBR) (Allegue et al., 2018; Bhattacharjee et al., 2016; Kampman at al., 2018; Liu at al., 2019; Xie et al., 2018). Allegue et al. (2018) reported nitrite removal of 116 g N/ m^3-d at a hydraulic retention time of 24 hours with abundance of ~50.0% denitrifying methanotroph (*Candidatus Methylomirabilis oxyfera*) in a membrane bioreactor. Furthermore, it was observed that genes capable of oxidizing methane aerobically are found in the *M. oxyfera* genome which enable *M. oxyfera* to oxidize methane aerobically (Ettwig et al., 2010). The utilization of methane in MBfRs have been employed to treat nitrogen species. Shi et al. (2013) operated an MBfR using methane as a gaseous substrate for over 700 days and explored nitrogen removal by applying a consortium of anammox and denitrifying anaerobic methane-oxidizing microorganisms and reported nitrate and ammonium removal at 86 and 27 mg N/ m^2-d, respectively. In a more recent study, a nitrite removal rate was reported at 0.56 g N/L-d, in a methane based MBfR that had a complex microbial community, in which ANME-2D archaea, Anammox and denitrifying anaerobic methane oxidation (DAMO) bacteria was dominant (Xie et al., 2018). Prior to this study, nitrate removal was investigated in a methane-based membrane biofilm reactor (MBfR), at difference methane

concentration, from (20 and 99 %) and pressures ranging from (2.0 – 7.0 psig) and (0.05 - 0.25 psig) (Alrashed et al., 2018; Lee et al., 2019). The results of the previous studies suggested that nitrate reduction appeared to be the rate-limiting step in the denitrification process in the biofilm. Hence, the first aim of this study was to investigate the nitrite reduction in a methane-based MBfR in a hypoxic environment at a comparable operating condition to the MBfR operated to investigate the nitrate removal, along with monitoring of dissolved methane concentration in the MBfR effluent. Additionally, the utilized and leaked methane was characterized, in order to develop an understanding of the diluted methane impact as the main electron donor in the MBfR. The second aim of this study was to compare nitrite reduction performance to nitrate reduction in the MBfR, to better understand the rate limiting step in the denitrification process in the methane based MBfRs. Finally, to explore the microbial community dynamics under various methane pressure and difference nitrite loading rates to advance the understanding of the nitrite reduction pathway in hypoxic conditions.

5.2 Materials and Methods

5.2.1 MBfR Configuration, Inoculation, and Operation

An MBfR was built using Plexiglas tubes (ϕ 1.1 cm and 30 cm in length, working volume 75 mL). Two membrane modules were prepared using hydrophobic polyvinylidene difluoride gas-permeable hollow fiber membranes with an outer diameter of 1.2 mm (Econity Inc., South Korea). Each module consisted of 10 membranes with a total surface area of 188.5 cm^2 (membrane packing density in the MBfR was 251 m^2/m^3); a diagram of the employed MBfR is illustrated in Fig 5-1. Subsequently, these hollow fiber membranes were bundled together with Plexiglas housing tubes (ϕ 0.6 cm and length 3 cm) using a hydrophobic silicone sealant (Model

908570, Loctite, USA) before being left to cure for 24 hours. After confirming that there were no gas leaks in the modules with multiple bubble tests, the MBfR was inoculated with a microbial culture dominated by a Type I methanotrophs (*Methylococcus*) at 53% relative abundance. The nitrite-fed MBfR was operated in batch mode using methane gas (20.0% balanced with N_2, Praxair, Canada) as the sole carbon source and electron donor. The liquid medium was then internally circulated in the MBfR at a rate of 10 mL/min using a peristaltic pump (Masterflex L/S economy variable speed Drive, RK-07554-80) for the purpose of mixing. We continued to operate the MBfR in batch mode until the nitrite concentration was found to be less than 1 mg/L. Thereafter, we began operating the MBfR in continuous mode using a nitrite as the sole nitrogen source.

The chemical composition of the nitrite rich medium included (in mg/L) $NaNO_2$ 98.4, $FeSO_4 \cdot 7H_2O$ 1, $CaCl_2 \cdot 2H_2O$ 1, $MgSO_4 \cdot 7H_2O$ 200, Na_2HPO_4 434, KH_2PO_4 128, and trace minerals (1 mL/L). The trace minerals consisted of (in mg/L) $ZnSO_4.7H_2O$ 100, $MnCl_2.4H_2O$ 30, H_3BO_3 300, $CoCl_2.6H_2O$ 200, $CuCl_2.2H_2O$ 10, $NiCl_2.2H_2O$ 10, $Na_2MoO_4.2H_2O$ 30 and Na_2SeO_3 30 (Modin et al., 2008; Xia et al., 2010). The pH of the nitrite medium was constant at 7.2 ± 0.1. The medium was autoclaved for 20 minutes at 121 ˚C before being cooled at room temperature for 4 hours. The medium was then purged with nitrogen gas (99.0%, Praxair, Canada) for 50 minutes and was immediately connected to the reactor using a N_2 gas bag (1 Liter Tedlar, Sigma-Aldrich, USA). Thereafter, the nitrite medium was fed to the MBfR using a peristaltic pump (Masterflex L/S economy variable speed Drive, RK-07554-80), methane gas was constantly provided through the membrane modules at a given pressure. In order to optimize the nitrite removal flux, the hydraulic retention time (HRT) was varied from 12 to 2 hours, and the methane pressure was changed from 0.05 to 0.35 psig. To experimentally confirm the hypoxic conditions

in the MBfR, a microsensor was employed to monitor the dissolved oxygen in the MBfR

(PreSens, Regensburg, Germany). The MBfR was run at a constant temperature of $24 \pm 1°C$, and

the effluent pH ranged from 7.2 to 7.4 during these experiments.
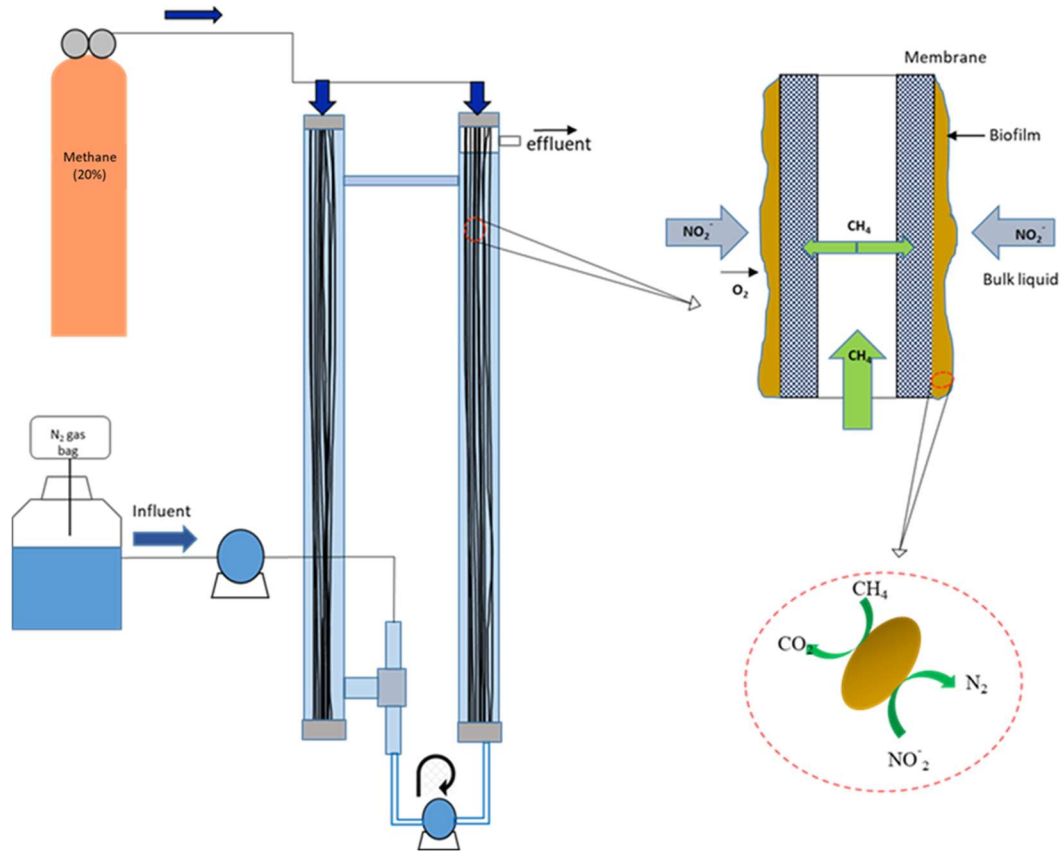
Figure 5-1. Schematic diagram of the nitrite reduction membrane biofilm reactor.

5.2.2 Liquid Analysis

Liquid samples from influent and effluent were taken on regular basis, and nitrite and nitrate

concentration were measured in duplicate. Nitrate and nitrite were analyzed using an ion

chromatograph (IC-1100, Dionex, USA) equipped with an AS9-SC analytical column (IonPac, 4

$\times$ 250 mm, Dionex, USA) with the utilization of 9 mM sodium carbonate as an eluent at a flow

rate of 1.00 mL/min. Prior to the analysis, all samples were filtered with syringe filters (pore size 0.45 μm, VWR International Inc., Canada).

5.2.3 Methane Gas Measurement

In order to quantify the dissolved methane concentration in the MBfR effluent using Eq. 5.1 based on the postulations made by Yeo and Lee (2013), a 10 ml liquid samples taken from the MBfR using a syringe were immediately transferred to a airtight vial (20 mL) that had been sparged with N_2 gas (99%, Praxair, Canada). This vial was then vigorously mixed with a vortex mixer (Fisher STD, USA) for six minutes to attain a state of equilibrium between gas and liquid phases. The gas was sampled from the headspace of the vial, after which the gas composition was quantified using a gas chromatograph equipped with a thermal conductivity detector (TCD) (SRI 310C, SRI instruments, USA).

$$CH_4(aq) = \left[H_{CH_4} \times P_{CH_4} \times MW_{CH_4}\right] + \left[\frac{P_{CH_4} \times V_H \times \rho_{CH_4}}{V_L}\right] \quad (5.1)$$

where H_{CH_4} denotes the Henry's law constant at 25˚C (0.0014 mol/L-atm), P_{CH_4} refers to the methane partial pressure in the 20 ml vial head space, MW_{CH_4} signifies the methane molecular weight (16 g/mol), V_H represents the headspace volume of the vial (10 mL), V_L denotes the liquid volume of the vial (10 ml), and ρ_{CH_4} is the methane density MW_{CH_4}/gas molar volume at 25˚C, in consonance with the ideal gas law (24.4 L/mol). Detailed information on this procedure to quantify dissolved methane is provided in the literature (Yeo et al., 2015).

5.2.4 Microbial Community Analysis
To gain in-depth insight on the microbial community structure, microbial community analyses were carried out on the biofilm growing on the membrane outer surface. Bio-samples were

collected at the end of each experiment. The biofilm samples were collected using sterile swabs (Puritan Medical Products, USA). The samples were obtained at the end of each experiment, sampling was done in duplicate, as described in section 4.2.4. To avoid any possible cross contamination a 75% alcohol was used to disinfectant the gloves and the working area. To explore the microbial communities, sequencing was performed based on 16S ribosomal RNA(rRNA), which is widely used for microbial taxonomic analysis and highly conserved in most bacterial and archaeal species (Coenye & Vandamme, 2003). In order to achieve this, RNA and DNA were extracted from the samples using an extraction kit, and Illumina sequencing was performed. Processing and analysis of the data was completed via Mothur software to analyze the microbial communities based on 16S rRNA gene sequences. Basic Local Alignment Search Tool (Blast) was also used, which compares the retrieved data to sequence databases at an acknowledged statistical significance, for further confirmation of the phylogenetic relationship of the microbial species. The sequence result shows the relative abundance of sequences at diverse taxonomic levels (e.g., class and genus), displaying the most dominant bacteria and revealing the significant pathways responsible for methane oxidation and nitrite reduction.

5.3 Results and Discussion

5.3.1 The Impact of Methane Flux on Denitrification in the MBfR

The MBfR was operated under four methane supply pressures of 0.35, 1.03,1.72 and 2.41 kPa (0.05, 0.15, 0.25 and 0.35) psig, respectively. Increasing the availability of methane (i.e., the electron donor) improves the denitrification performance, but remaining methane will be lost as "dissolved methane" in MBfR effluent. In the previous study, when a high methane pressure was applied (13.7, 34.5, and 48.2 kPa) in the MBfR for denitrification (Alrashed et al., 2018), the dissolved methane in MBfR effluent increased up to 13 mg CH_4/L. This indicates methane

leakage to bulk liquid and requirements of optimal methane pressure for meeting denitrification efficiency simultaneously minimizing dissolved methane concentration in the effluent.

In the first phase, the MBfR was operated at four different HRTs at 0.35 kPa methane pressure. The nitrite removal efficiency was 98% at HRT 12 h (nitrite removal flux 158 mg N/m^2-d). Nitrite removal gradually decreased to 94, 84, and 72%, with decreasing HRT for 8h, 4h and 2 h respectively. Table 5-1 summarizes the nitrite concentration and removal flux in at individual HRTs at a constant methane pressure of 0.05 psig. It was observed that at this low methane pressure, the nitrite removal flux became as high as 754 mg N/ m^2-d (HRT 2h), although effluent nitrite concentration was 5.72 mg N/L.

Table 5-1. Nitrite Concentration Profile and Removal Flux in the MBfR at HRTs of 12, 8, 4, and 2 h; Methane Pressure of 0.05 psig; and Influent Concentration 20 ± 1.2 mg N/L

20% CH$_4$ pressure kPa (psig)	HRT (h)	NO$^-_2$-N (influent) (mg/L)	NO$^-_2$-N (effluent) (mg/L)	NO$^-_2$-N removal flux [mg N/m^2-d]
0.35 (0.05)	12	20 ± 0.52	0.51	157.9
0.35 (0.05)	8	21 ± 0.8	1.21	245.8
0.35 (0.05)	4	20 ± 0.5	3.08	415.9
0.35 (0.05)	2	21 ± 0.2	5.72	754.3

In the second phase, methane pressure was increased to 1.03 kPa. The higher methane pressure improved nitrite removal rate in the MBfR. Nearly complete nitrite reduction was observed without any significant difference at a significant level of 0.05 at HRTs 12 and 8 hours. Table 5-2 shows the maximum nitrite removal flux increased by 812 mg N/ m^2-d at a methane pressure of 0.15 psig, supporting the impact of methane pressure on nitrite reduction.

Table 5-2. Nitrite Concentration Profile and Removal Flux in the MBfR at Hydraulic HRTs of 12, 8, 4, and 2 h; Methane Pressure of 0.15 psig; and Influent Concentration 20 ± 1.2 mg N/L

20% CH_4 pressure kPa (psig)	HRT (h)	NO_2^--N (influent) (mg/L)	NO_2^--N (effluent) (mg/L)	NO_2^--N removal flux (mg N/m²-d)
1.03 (0.15)	12	20 ± 0.71	0.09	164.1
1.03 (0.15)	8	21 ± 0.4	0.18	253.2
1.03 (0.15)	4	20 ± 1.05	2.76	447.3
1.03 (0.15)	2	21 ± 0.9	4.88	812.6

At methane pressure 1.72 kPa (0.25 psig), denitrification rate was further improved. When the MBfR was operated at an HRT of 4 hours, nitrite removal efficiency was 94% with effluent nitrite concentration 1.15 ± 0.94 mg NO_2^--N/L. For HRT 2 hours, the nitrite concentration in the MBfR effluent was 3.02 ± 0.73 mg NO_2^--N/L, and the maximum nitrite removal flux was 863 mg N/m²-d. (see Table 5-3).

Table 5-3. Nitrite Concentration Profile and Removal Flux in the MBfR at HRTs of 1, 8, 4, and 2 h; Methane Pressure of 0.25 psig; and Influent Concentration 20 ± 1.2 mg N/L

20% CH_4 pressure kPa (psig)	HRT (h)	NO_2^--N (influent) (mg/L)	NO_2^--N (effluent) (mg/L)	NO_2^--N removal flux (mg N/m²-d)
1.72 (0.25)	12	20 ± 0.65	0.031	164.07
1.72 (0.25)	8	21 ± 0.1	0.07	262.9
1.72 (0.25)	4	21 ± 0.3	1.15	482.2
1.72 (0.25)	2	21 ± 1.0	3.024	863.04

Finally, at the highest methane pressure 2.41 kPa (0.35 psig), nitrite removal efficiency slightly increased to 97% (effluent nitrite 1.15 mg N/L) at HRT 4 hours, and the maximum nitrite removal reached to 884 mg N/ m^2-d at HRT 2 hours (Table 5-4).

Table 5-4. Nitrite Concentration Profile and Removal Flux in the MBfR at HRTs of 12, 8, 4, and 2 h; Methane Pressure of 0.35 psig; and Influent Concentration of 20 ± 1.2 mg N/L

20% CH$_4$ pressure kPa (psig)	HRT (h)	NO$^-_2$-N (influent) (mg/L)	NO$^-_2$-N (effluent) (mg/L)	NO$^-_2$-N removal flux (mg N/m^2-d)
2.41 (0.35)	12	20 ± 0.65	0.001	162.4
2.41 (0.35)	8	21 ± 0.1	0.002	239.8
2.41 (0.35)	4	21 ± 0.3	0.041	489.3
2.41 (0.35)	2	21 ± 1.0	2.35	884.2

The nitrite removal flux was as low as 160 mg N/m^2-d at methane pressure of 0.05 psig and HRT of 12 hours, and the maximum removal flux was 880 mg N/m^2-d at methane pressures of 0.35 psig, and HRT of 2 hours (Figure 5-2). These results highlight the significance of methane gas delivery (the primary electron donor) to drive the nitrite reduction in the membrane biofilm (Martin et al., 2012). Despite the low concentration of methane in the MBfR (20.0 %), increasing pressure inside the hollow membrane still had a positive impact on the nitrite reduction, and achieved the maximum nitrite flux was as high as 884 mg N/m^2-d (233.2 mg N/L-d). Since the utilization of methane for nitrogen removal in micro-aerobic/ hypoxic conditions is a new research topic, there are limited studies on nitrite removal in methane-MBfRs. Nitrite reduction was evaluated in a methane-MBfR with a synergy of anammox bacteria and anaerobic methane

oxidation archaea, having nitrite removal rate of 173 mg N/L-d (Xie et al., 2018). Also, Shi et al.

(2013) have reported the occurrence of nitrite reduction coupled to methane oxidation in batch

test at 147 mg N/L-d, using a consortium of anammox and denitrifying anaerobic methane

oxidation microorganisms in a methane based MBfR. However, both studies did not consider

dissolved oxygen effects on denitrification in the MBfRs.
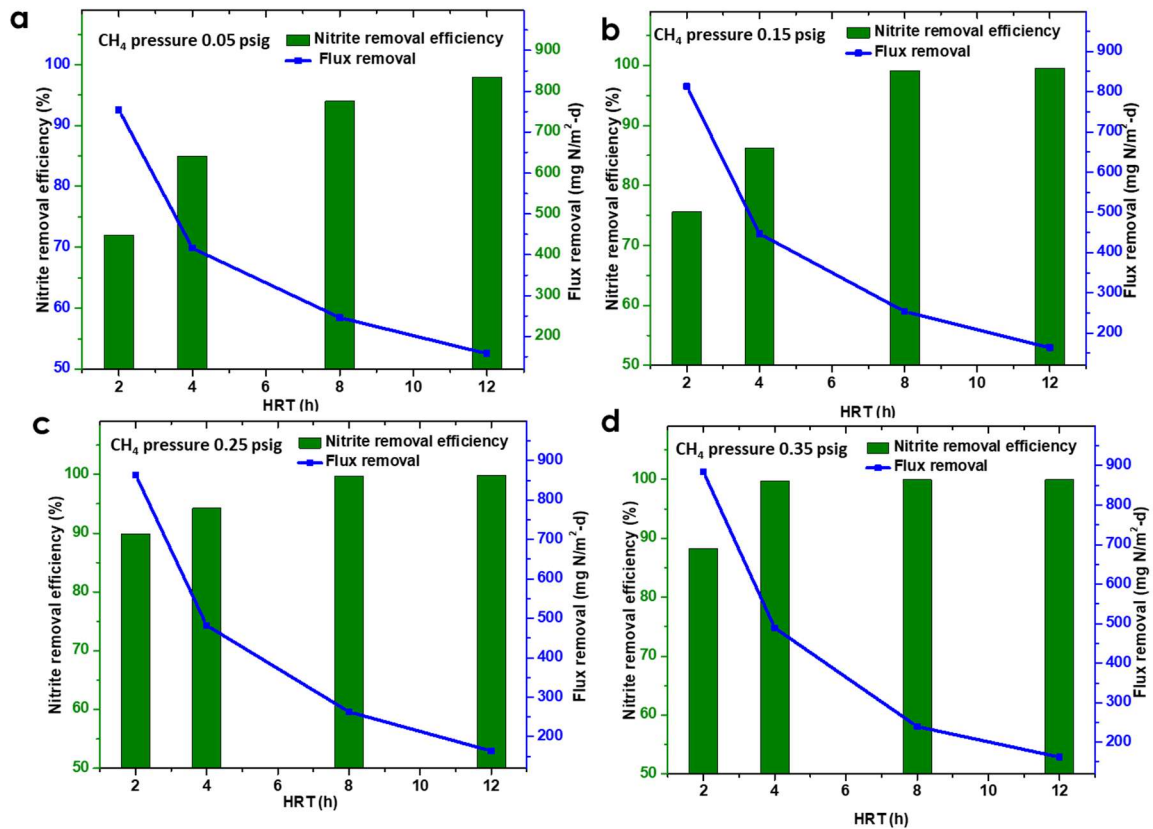
Figure 5-2. Nitrite removal flux and removal efficiency in the MBfR at HRTs of 12, 8, 4, and 2 h. (a) methane supply pressure at 0.05 psig; (b) methane supply pressure at 0.15 psig; (c) methane supply pressure at 0.25 psig and (d) methane supply pressure at 0.35 psig.

5.3.2 Effect of Nitrite Concentration on Denitrification Performance

In order to investigate the rate-limiting step of the denitrification process in the methane-based

MBfR at high nitrite concentration in the MBfR influent. The MBfR was operated using two

different nitrite concentrations. Starting from 20 mg NO_2^--N/L, the concentration was increased up to 40 mg NO_2^--N/L. This high concentration was selected to determine whether a breaking point would occur to hinder the denitrification process in the MBfR due to the electron acceptor competition for electrons from organic intermediates within the biofilm, or if the MBfR will demonstrate a contrary behavior, where the microbial activity will be enhanced according to the electron acceptor concentration in the bulk liquid (Martin et al., 2012). Also, to monitor the membrane durability when the flux of the electron acceptor is elevated in the bulk liquid.

Figure 5-3a depicts the first phase outcomes, in which the nitrite concentration was fixed at 20 mg NO_2^--N/L; additionally, methane pressure was also set at 0.35 kPa (0.05 psig) so that the increased nitrite in the feed was the only altered variable, providing a clear prospective on the robustness of this type of bioreactor for nitrite reduction at elevated concentrations. After running the MBfR at different HRTs. The results demonstrated that at the lowest HRT of 2 h, the nitrite removal flux was at 740.0 mg N/m^2-d. However, when the nitrite concentration was elevated to 40 mg NO_2^--N/L, the removal flux was 674 mg N/m^2-d at HRT 2 h, which implies that the MBfR was challenged at this low HRT of 2 h. On the other hand, at higher HRTs (8 h), with 40 mg NO_2^--N/L in the feed, the removal flux was almost twice as high as the (20 mg NO_2^--N/L) phase (see Figure 5-3a, b). The results suggest that increasing the main electron acceptor flux in the bulk liquid had slightly enhanced the denitrification performance in the biofilm by increasing the electron acceptor gradient in the biofilm (Martin et al., 2012; McCarty and Rittmann, 2001), although it was hindered at lower HRTs (see Table 5-5).
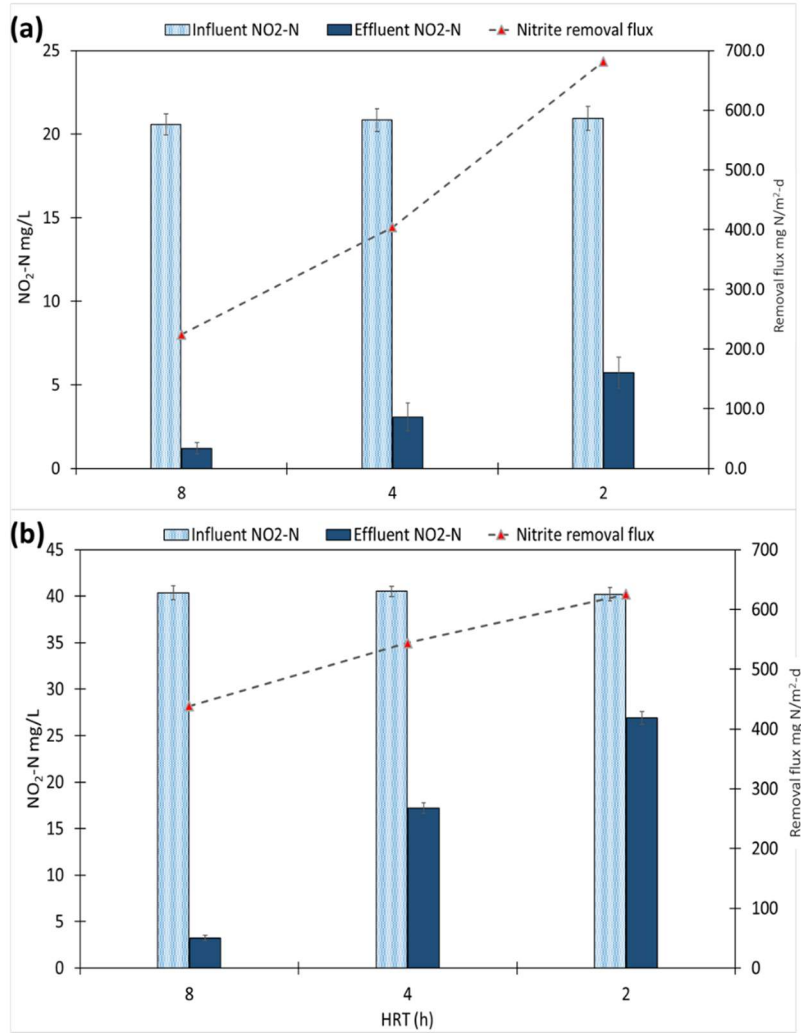
Figure 5-3. Nitrite concentration in the MBfR effluent at influent and removal flux and fixed methane pressure of 0.05 psig (0.35 kPa) for 8, 4, and 2 h HRTs. (a) at influent concentration of 20 mg NO_2^--N/L. (b) at influent concentration of 40 mg NO_2^--N/L.

Table 5-5. Nitrite Removal Profile in Methane-MBfR at Nitrite Concentration in the Influent 20, 40, NO_2^--N/L at Methane Pressure 0.35 kPa and an HRT of 8,4 and 2 hours.

CH$_4$ pressure kPa (psig)	HRT (h)	Influent NO_2^--N (mg N/L)	NO_2^--N removal flux (mg N/m^2-d)	Influent NO_2^--N (mg N/L)	NO_2^--N removal flux (mg N/m^2-d)
0.35 (0.05)	8	21 ± 0.8	237.0	40 ± 0.3	441.0
0.35 (0.05)	4	20 ± 0.5	403.9	39 ± 0.64	535.0
0.35 (0.05)	2	21 ± 0.2	740.0	41 ± 0.27	674.0

5.3.3 Dissolved Methane in the MBfR

During all operation stages of the MBfR, dissolved methane was monitored in the effluent to investigate the research hypothesis that reducing methane gas flux through the membrane could achieve nitrite bioreduction, while the dissolved methane concentration could be kept low in the MBfR effluent. All measurements were accomplished at steady states for different methane pressures, HRTs, and nitrite concentrations. At methane pressures of 0.35, 1.03,1.72 and 2.41 kPa (0.05, 0.15, 0.25 and 0.35) psig at fixed HRT 12h increasing the methane flux led to a build-up of dissolved methane in the MBfR effluent (Figure 5-4a). The dissolved methane was low at 5.94 mg CH$_4$/L at methane pressure 0.05 psig, but it increased to 9.6 mg CH$_4$/L at methane pressure 2.41 kPa (0.35 psig) At HRT 8 h, the dissolved methane concentrations were as follows: 5.04, 6.41, 6.78, and 7.89 mg CH$_4$/L for 0.05, 0.15, 0.25, and 0.35 psig, respectively was recorded (Figure 5-4b). All four stages exhibited significant differences ($p < 0.05$), and the dissolved methane was positively correlated to the methane pressure. In fact, all the dissolved

methane concentration in this study was below the level guidelines (10 mg/L) set by the office of surface mining of the Interior Department in the USA (Eltschlager et al., 2001). In comparison, no guidelines was found in any Canadian agency regarding the maximum allowable limits on the discharged dissolved methane.

The next two HRT conditions exhibited the same pattern. It is evident that the methane concentrations in the MBfR effluent dropped with increase of nitrite loading rate and decrease of HRT. Figure 5-4c illustrates the dissolved methane concentration at nitrite loading rate 120 g N/m^3-d and HRT 4 h, showing dissolved methane concentration from 4.07 to 6.89 mg CH_4/L. Dissolved methane concentration was as low as 2.87 ± 1.04 mg CH_4/L at nitrite loading rate HRT 240 g N/m^3-d and HRT 2 hours (Figure 5-4d). Since there are no clear regulations on dissolved methane in water and wastewater effluent, it is a challenge to determine optimal conditions for the MBfR considering effluent nitrite and dissolved methane concentration. This study clearly indicates methane mass transport rate from the membranes to bulk liquid through membrane biofilms are consistently faster than microbial kinetics for methane-utilizing nitrite reduction for all conditions, although dilute methane gas was used for the MBfR. Figure 5-5 illustrates the methane flux to the MBfR, and the amount of methane utilized. At 0.05 psig, the methane that had been supplied to the biofilm ranges from 57–137 mmole e^-/m^2-d, while the utilized methane was 34–89 mmole e^-/m^2-d (Figure 5-5a). At higher methane pressure (0.15 and 0.25 psig), a similar phenomenon was observed where the leaked methane was 22–41 mmole e^-/m^2-d (Figure 5-5b) and 27–58 mmole e^-/m^2-d (Figure 5-5c).
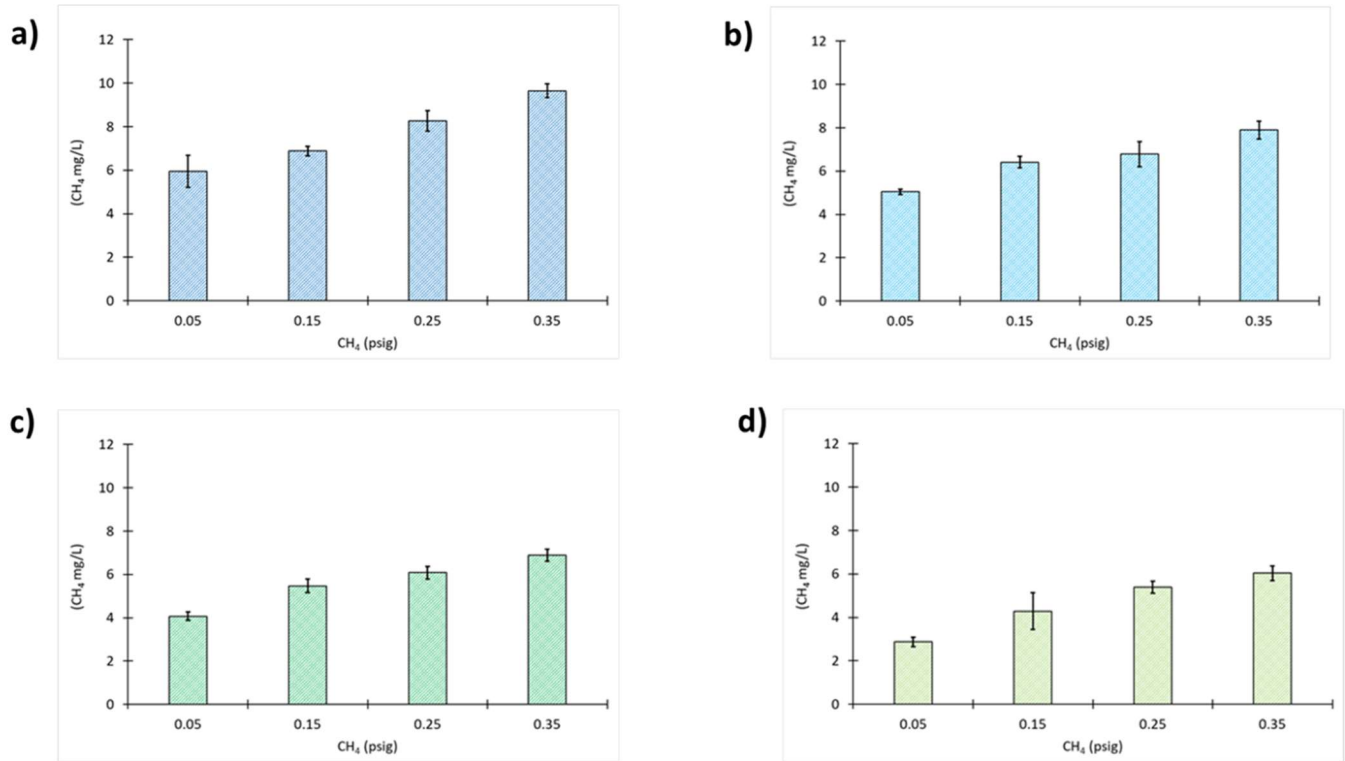
Figure 5-4. Dissolved methane concentration in methane-MBfR at methane supply pressures of 0.05, 0.15, 0.25, and 0.35 psig. (a) Nitrite loading rate of 40 g N/m³-d, 12 h HRT; (b) Nitrite loading rate of 60 g N/m³-d, 8 h HRT; (c) Nitrite loading rate of 120 g N/m³-d, 4 h HRT; (d) Nitrite loading rate of 240 g N/m³-d, 2 h HRT.
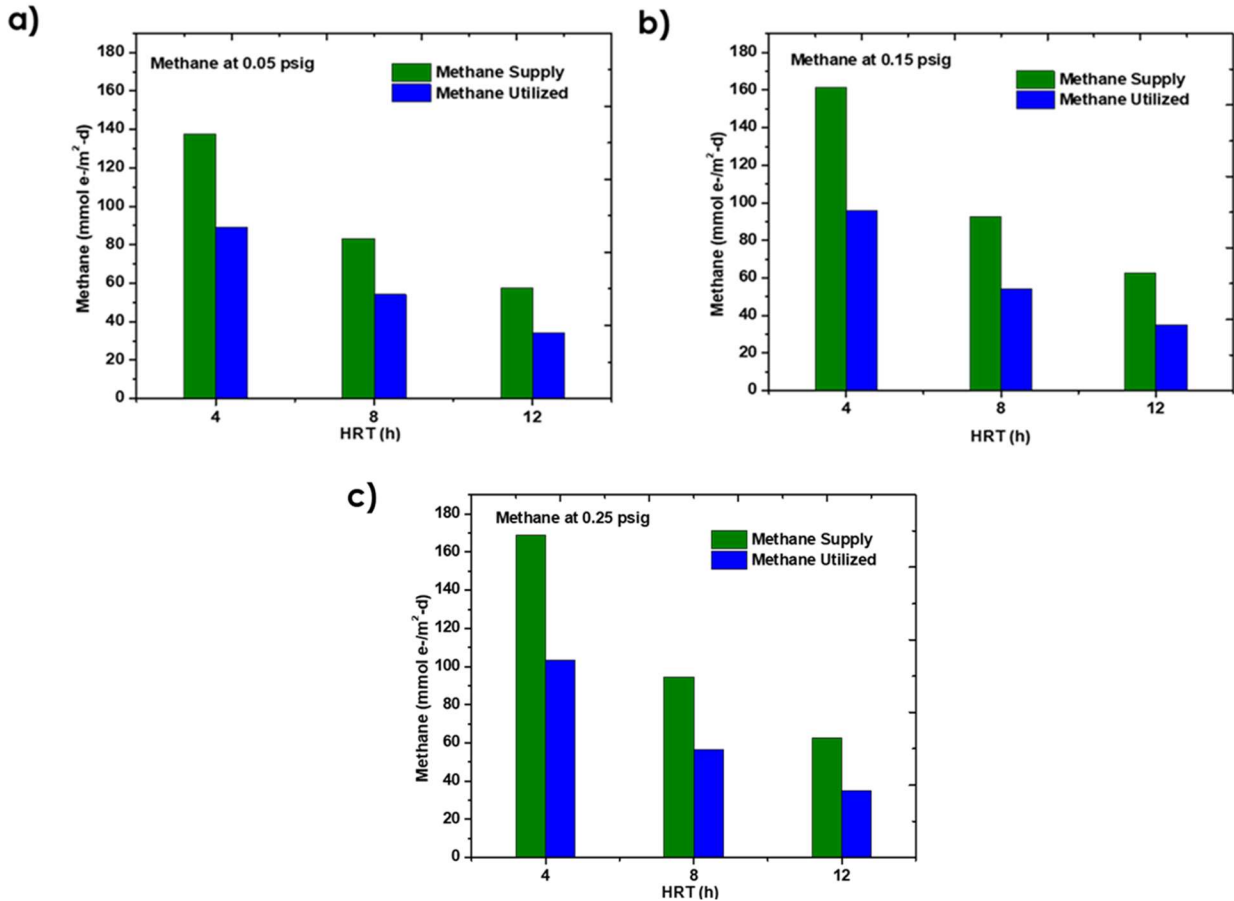
Figure 5-5. Methane flux and utilization for nitrite removal in MBfR (a) at methane pressure of 0.05 psig, (b) at methane pressure of 0.15 psig, and (c) at methane pressure of 0.25 psig.

5.3.4 Evaluating the Removal Performance in the MBfR between Nitrite and Nitrate

In order to further examine the rate-limiting step in the denitrification process, the removal performance of nitrite and nitrate was compared at equivalent operating conditions. Under different HRTs and methane pressures nitrite reduction rate was consistently faster than nitrate. For instance, in Figure 5-6a, the MBfR operated at 0.05 psig and HRT of 12, 8, and 4 h, the nitrite removal fluxes was 158, 246, and 416 mg N/m^2-d, respectively. At the same conditions, the nitrate removal flux was 156, 217, and 384 mg N/m^2-d. At methane pressure 0.15 psig, the nitrite removal flux was as high as 448 mg N/m^2-d, while the nitrate removal flux was relatively

low at 402.7 mg N/m^2-d (Figure 5-6b). The same trend was observed at methane pressure 0.25

psig, as shown in Figure 5-8c. These results imply that nitrate reduction to nitrite would be

sluggish for nitrate reduction to dinitrogen in the MBfR.
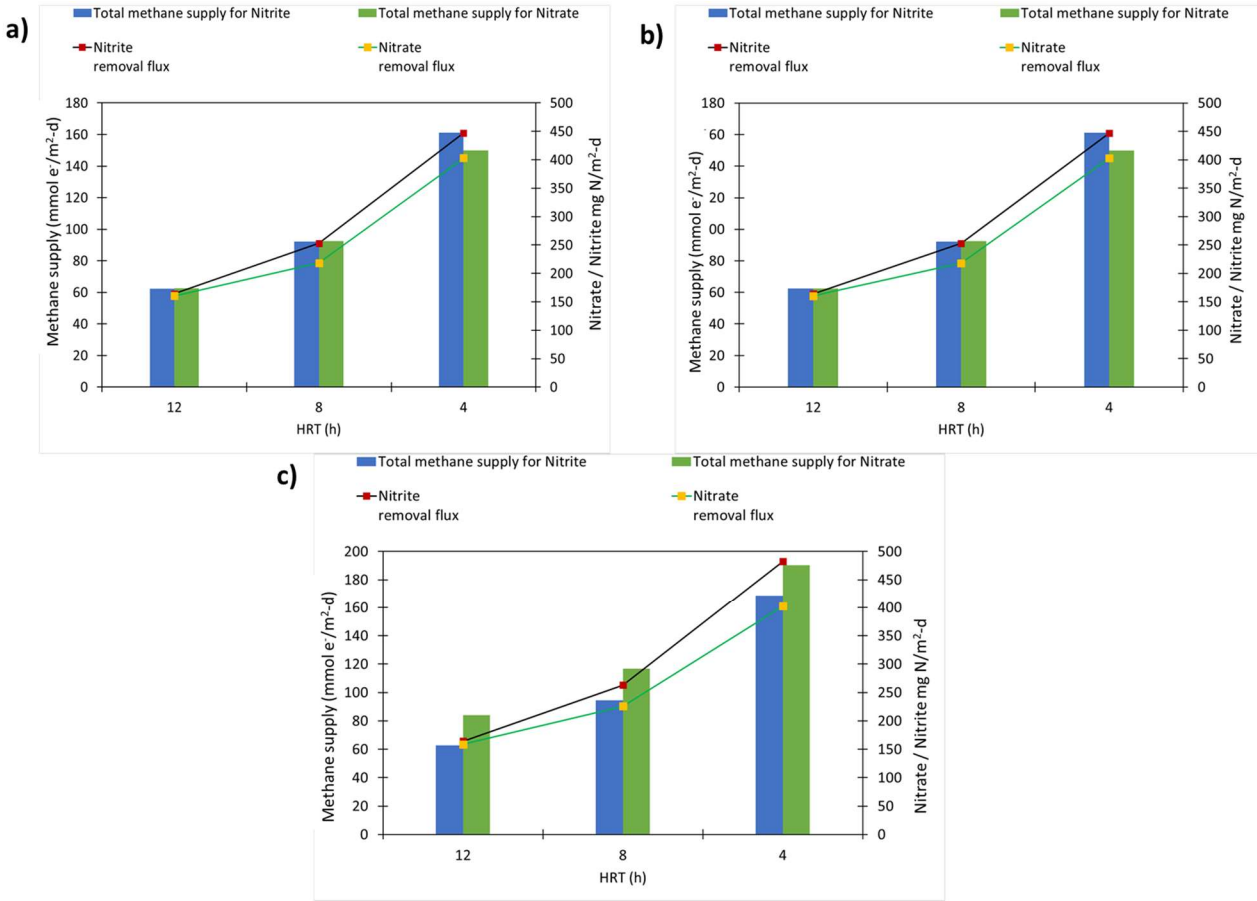
Figure 5-6. Methane flux and nitrate and nitrite removal flux at 12, 8, and 4 h HRTs for (a) methane pressure of 0.05 psig, (b) methane pressure of 0.15 psig, and (c) methane pressure of 0.25 psig.

5.3.5 Microbial Community Dynamics in the MBfR Biofilm

Samples were collected from the biofilm during a range of operating conditions. Figure 5-7 illustrate the 16S rRNA gene sequences of samples collected at different HRTs, (2, 4 and 12 h), in order to investigate the impact of the substrates flux on the microbial community shift. The results depict the presence of *Methylococcus capsulatus*, which is a Type I methanotroph, that can convert methane to methanol via the monooxygenase (MMO) enzyme (Rush et al., 2016; Ward et al., 2004). In fact, it has been reported that methanol is considered as a significant link between methane oxidation and nitrate and nitrite reduction in the environment (Zhu et al., 2016; Kalyuhznaya et al.,2009). However, methanol was not detected in the MBfR, which means that either it was readily consumed by the denitrifiers or the methanol was at a very low concentration and further converted to carbon dioxide as a terminal product. *Methylococcus capsulatus* was found to have the highest relative abundance of 78% for the highest HRT of 12 hours and a methane pressure of 0.35 kPa (0.05 psig). In fact, the population of *M. capsulatus* substantially decreased in the HRTs of 4 and 2 hours samples, at 55% and 33%, respectively. Hence, the *M. capsulatus* population was positively correlated with the methane flux. The available literature does not provide any specific research regarding the findings of this study. The *Methylocystis* genus of the *Methylocystaceae* family was found to have the second highest relative abundance after *M. capsulatus*, at 15% and 13% for HRTs of 2 and 4 hours (Bowman 2006; Webb et al., 2014). Furthermore, the nitrite reductase (*nirK*) was reported to be present in the *Methylocystis* genome (Stein et al., 2011). This result could explain the high nitrite removal flux at the HRT of 2 hours. Additionally, *Methylocystis* population declined to 5.5% for the HRT sample of 12 hours, where the nitrite loading rare was the lowest.
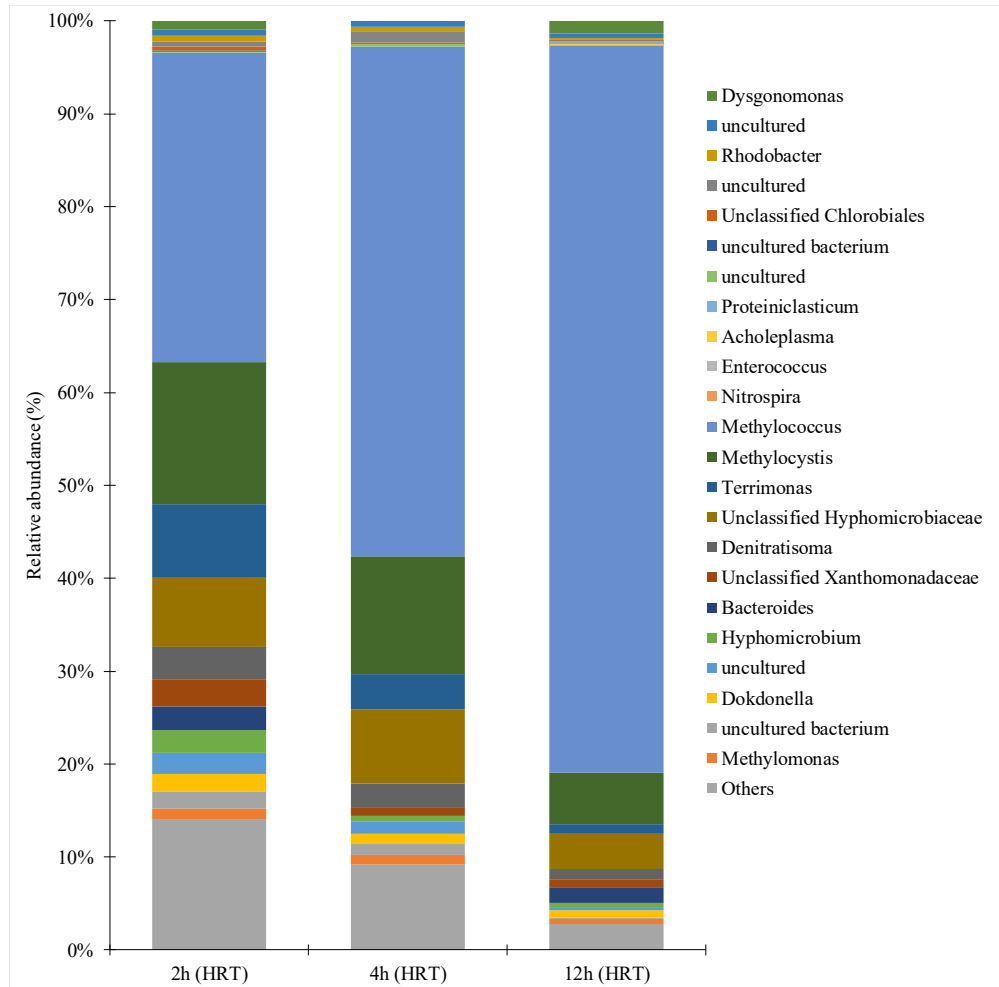
Figure 5-7. Relative abundance of microbes in community composition of membrane biofilm samples for HRTs of 2, 4, 8, and 12 hours based on 16S rRNA gene (Metagenome) libraries; "Others" specifies 1% or lower relative abundance.

In order to derive additional insights into the microbial dynamics in the biofilm, samples were collected from the biofilm at fixed HRTs of 12 hours and varying methane pressures (of 0.05, 0.15 and 0.25 psig) as shown in Figure 5-8. *M. capsulatus* was found to have the highest abundance among the three biofilm samples, at 78% for the lowest methane pressure (0.05 psig). Furthermore, *Terrimonas* which is a bacteria know for heterotopic denitrification, had a relative abundance of (~12 -14%) in the biofilm sample

of 0.15 and 0.25 psig, respectively (Liang et al., 2014; Zhang et al., 2018). In fact, the

nitrite reductase genes (*nir),* which is one of the exclusive nitrite reducers that produce

N_2 as a terminal product, was found in *Terrimonas* in a prior study (Lee et al., 2019;

Zhu et al., 2016). In addition, it was observed that the population had comparable

abundance of *M. capsulatus* between 0.15 and 0.25 psig, at 46% and 43%, respectively.

The increment between the three methane pressures was relatively low, at only 0.1 psig.

Thus, microbial dynamics did not have an impact on the relative abundance of the main

methanotroph (*M. capsulatus*) in the biofilm community when the HRT was fixed at 12

hours. Therefore, it can be inferred that operating the MBfR at such a low methane

pressure would not affect the denitrification performance. Thus, emphasizing the

potential of utilizing extremely diluted methane from a biogas source, which will have a

direct impact on the bioreactors operational cost, in addition to the positive effect on the

environment, by mitigating the release of greenhouse gases.
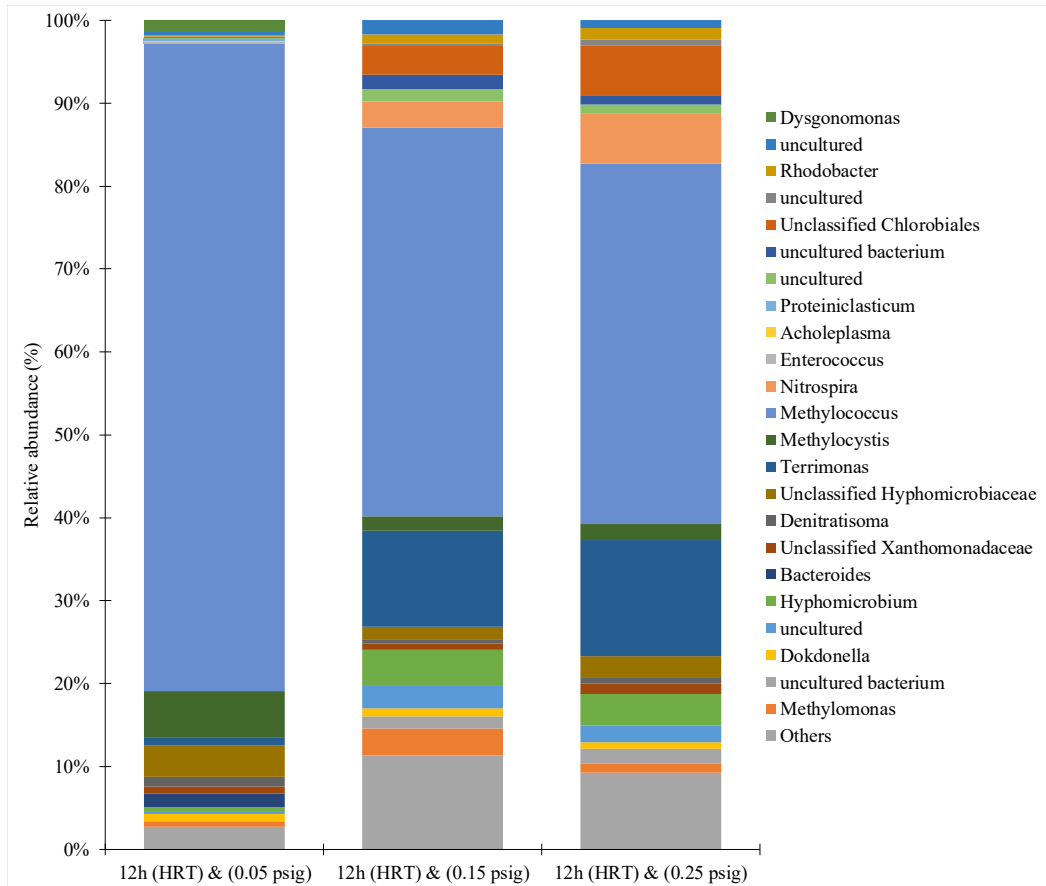
Figure 5-8. Relative abundance of microbes in community composition of membrane biofilm samples for HRT of 12 h and methane pressures of 0.05, 0.15, and 0.25 psig based on 16S rRNA gene (Metagenome) libraries; "Others" specifies 1% or lower relative abundance.

5.4 Conclusions

A dilute methane of 20% at low-pressure approach proved to be efficient in minimizing dissolved methane leakage in the MBfR for nitrite reduction. The results suggest that methane pressure can be utilized as a controllable variable to enhance nitrogen removal efficiency and dissolved methane concentration. The dissolved methane concentration in this study was below the hazardous level guidelines (10 mg/L). The outcomes reveal that low dissolved methane was detected in the MBfR effluent with nitrite removal flux of 885 mg N/m^2-d. Furthermore, the findings suggest that supplied methane concentration could be decreased to 5 –10% in order to

mitigate methane leakage to the environment. The microbial community showed that aerobic methanotrophic bacteria *Methylococcus* (a Type I methanotroph) was identified as the potentially key methane oxidizer in the biofilm, alongside heterotrophic denitrifiers. Moreover, *Methylococcus capsulatus* was detected at high abundance in the biofilm. This supports hypoxic conditions in the MBfR in which dissolved oxygen concentration was at 0.04–0.05 mg O_2/L. This study suggests that nitrite reduction would not be a main rate limiting step in nitrate reduction to dinitrogen in the MBfR biofilm under hypoxic conditions.

Chapter 6

Conclusions and Recommendations for Future Research

6.1 Conclusions

This research delivers a perception on the application of a methane-based MBfR for nitrate and nitrite removal in hypoxic environment. The outcomes of these studies will contribute to improving nitrogen control practices and technologies in water and wastewater treatment sectors such as tertiary nitrogen removal. The microbial community in the MBfRs was examined to explore the dynamics of the microbial community and the syntrophic interactions between methanotrophs and denitrifiers. Although the MBfR was continuously pressurized with methane gas as the sole gaseous substrate, the present study provided a key evidence of the oxygen transmission to the MBfRs possibly via medium bottle, the tubing systems or MBfRs. Thus, a unique application of an in-situ oxygen micro-sensor in the MBfR system was employed to characterize the hypoxic environment. The main conclusions drawn from this study are summarized as follows:

MBfRs were investigated for denitrification performance using methane gas as the sole electron donor and carbon source. The MBfR was operated at varied methane pressures and HRTs. The results revealed that at a low methane pressure of 2.0 psig and a hydraulic retention time (HRT) of 12, 8, and 4 hours, nitrate concentration in the effluent was 5.5 ± 1.18, 8.8 ± 1.15, and 13.3 ± 0.91 mg N/L, respectively. Furthermore, the increase in methane pressure was positively correlated with nitrate removal efficiency. However, there was no statistically significant difference between 7.0 and 5.0 psig, supporting that the utilization of very high methane pressure does not impact nitrate reduction. However, it does overuse the methane, as the dissolved methane ranged between 8 and 13 mg CH_4/L in the effluent, which will eventually

95

impact the operation cost of the nitrogen treatment. In addition, leakage of methane gas into the atmosphere contributes to the greenhouse gas impact on the earth's climate (Howarth et al., 2011; EPA, 2017). The nitrite did not accumulate in the MBfR, where it was below 0.2 mg N/L. The *Methylocystaceae* family of type II methanotrophs was recognized as the main microbial player in oxidizing methane, and it coupled with heterotrophic denitrification bacteria to reduce nitrate to nitrogen gas in the biofilm. The scanning electron microscope (SEM) images showed a successful biofilm growth on the external surface of the hollow membrane.

A methane based MBfR was examined for the hypothesis and environmental conditions that were listed in detail in Chapter 4. Basically, the denitrification coupled to methane oxidation was investigated utilizing a polyvinylidene difluoride (PVDF) gas-permeable membrane at substantially low methane pressures, fluxes, and concentrations. The denitrification performance was optimal at an HRT of 12 hours and a loading rate of 40 g N/m^3-d while maintaining the methane pressure at 0.05 psig (0.35 kPa). When the HRT was decreased to 8 hours, the removal efficiency dropped to 86.0%, and when the MBfR was operated at an HRT of 4 hours for 2 months, the removal rate came to a steady state at 80.0% at a 120 g N/m^3-d loading rate and nitrate removal rate of 413.1 mg N/m^2-d. This indicates that the microbial community continued to adapt and accumulate on the outer surface of the membrane. Furthermore, at the same HRT (4 hours), the dissolved methane in the MBfR effluent was 3.34 ± 1.07 mg CH_4/L, indicating that there was an adequate supply of methane to drive the denitrification process, even at that very low pressure (0.05 psig). The microbial community in the MBfR was dominated by *Methylococcus*, which is a Type I methanotroph capable of oxidizing methane under hypoxic conditions (Kalyuzhnaya et al., 2013). In this condition, the dissolved oxygen concentration was approximately 0.04 mg/L, which implies the hypoxic methane oxidation pathway. The microbial

community analyses also showed that denitrifying methanotrophs and anaerobic methanotrophic (ANME) archaea were not detected in the 16S rRNA genes. These results lead to the conclusion that methane-based MBfRs have a potential application for nitrogen removal in wastewater treatment utilizing the on-site produced methane gas at very low pressures and concentrations and a trivial methane build-up in the MBfR effluent. Furthermore, this approach could be applied as an eco-friendly and cost-effective alternative to the existing tertiary or sidestream nitrogen treatment techniques to prevent eutrophication on the local environment and bodies of water.

Finally, nitrite reduction in hypoxic conditions was studied by running the MBfR in a series of operational conditions, and the nitrite concentration in the MBfR effluent was recorded at 0.51 and 1.21 mg NO_2^--N/L with 12 hours and 8 hours HRT, respectively. This experiment was conducted at the minimum methane pressure level in this study of 0.35 kPa (0.05 psig); with a removal flux was up to 885 mg N/m^2-d, at a relatively low methane pressure of 2.4 kPa. This high removal flux indicate that nitrite reduction might not be the main rate limiting step in denitrification in the biofilm. Despite the low methane pressure used in this study, the dissolved methane in the MBfR was recorded at low levels (4.07 – 6.89) mg CH_4/L. It was also found that increasing the nitrite concentration in the influent by onefold had a slight impact on the removal efficiency, implying that the microbial consortium activity in the biofilm was influenced by concentration gradient of the electron acceptor from the bulk liquid. Thus, the MBfRs could be challenged when treating high concentration of nitrogen species. When the MBfR was operated with methane gas as the sole gas source, the microbial community did not include any anaerobic archaea, and the dominant bacteria were Type I aerobic methanotrophs, which supports the hypoxic methane oxidation coupled to nitrite reduction. The population of *Methylococcus capsulatus* was at 78% for the maximum HRT 12 hours, reducing to 55% and 33% for HRT of

4 hours and 2 hours, respectively.

6.2 Recommendations for Future Work

There are a number of potential research areas that were identified while conducting and analyzing the outcomes of this dissertation. These could be of interest to research groups who are working in the field of nitrogen removal by utilizing methane gas and biogas. The following recommendations are proposed to expand fundamental knowledge and the application of methane oxidation coupled to denitrification in MBfR systems.

- In this study, two types of gas-permeable membranes were investigated in a methane-based MBfR. The first was a hydrophobic microporous polyethylene membrane with an outer diameter of 280 μm. The second type was another hydrophobic fiber made from PVDF with an outer diameter of 1.2 mm. The latter demonstrated better denitrification performance and more well-regulated gas delivery. Hence, it is recommended that various types of gas-permeable membranes be investigated for enhancing methane gas transfer to membrane biofilms in addition to improved biofilm attachment to the membrane outer surface. Moreover, factors such as, efficient methane delivery (optimizing the diffusion coefficient in the membrane) would overcome any substrate limitations and therefore enhancing the denitrification performance. This methane mass transport should be well balanced with biofilm thickness to minimize dissolved methane in MBfR effluent.

- The design that was used in this study was optimized to improve denitrification performance, with two membrane packing densities examined, 35 and 251 m^2/m^3. It would definitely be productive to investigate different MBfR designs and altered membrane packing densities that could improve performance and enhance gas transfer and biofilm growth.

- In future research, it may be possible to focus on the shear force impact on biofilm thickness and the activity of the biomass, monitoring biofilm thickness in real time using an advanced microscopic approach that does not interfere with the environmental conditions inside the MBfR. This study should be well integrated with membrane material study on methane mass transport.

- In this work, two methane gas concentrations were applied to the MBfR. The first was 99.0% CH_4, and the second was with a diluted concentration (20% CH_4). The latter had a direct impact on lowering dissolved methane in the MBfR effluent. In future research, it is recommended to utilize biogas, that is produced from an anaerobic digester, as the methane source to MBfR denitrification.

- In this study, the dissolved oxygen was at trivial concentrations, within 0.045 mg/L by controlling and monitoring the micro-oxygen level in the bulk liquid of the MBfR using a sensitive dissolved oxygen microsensor. However, it is possible that there is an anaerobic zone in the biofilm layers, therefore, it is recommended in future work to design an MBfR in which micro-oxygen probes can access membrane biofilms to experimentally measure DO concentration throughout membrane biofilms at steady-state MBfRs. This approach can prove hypoxic denitrification or anaerobic denitrification in MBfR membranes, and also help assess DO effects on denitrification efficiency and rate.

- The microbial population in this research had an abundance of heterotrophic denitrifiers and aerobic methanotrophs (*Methylococcus*). However, it is recommended in future studies to investigate the microbial community dynamics under various DO concentration, in order to discover alternative methane oxidation pathways and related microbial community with a focus on the functional genes. This would provide an advanced insight of the syntrophic interactions in the microbial community. Moreover, it is suggested to perform an empirical study comparing

various sources of microbial inoculum used for denitrification enrichment in the MBfR to

thoroughly monitor the impact on microbial population diversity and the influence on the

denitrification performance in the MBfRs.

References

A.Mulder, A.A., Graaf, van. De, Robertson, L.A., Kuenen, J.G. (1995). Anaerobic ammonium oxidation discovered in a denitrifying fluidized bed reactor, FEMS Microbiol. Ecol. 16 (3) 177–184.

Ace Peel Hardware. (2020, April). https://www.ace-canada.ca/en

Adham, S., Gillogly, T., Lehman, G., Rittmann, B. E., and Nerenberg, R. (2005). Membrane Biofilm Reactor Process for Nitrate and Perchlorate Removal, American Water Works Association Research Foundation, Denver, Colorado.

Ahmed, T., & Semmens, M. J. (1992). Use of sealed end hollow fibers for bubbleless membrane aeration: experimental studies. Journal of Membrane Science, 69(1-2), 1-10.

Ali, M., Chai, L. Y., Tang, C. J., Zheng, P., Min, X. B., Yang, Z. H., ... & Song, Y. X. (2013). The increasing interest of ANAMMOX research in China: bacteria, process development, and application. BioMed research international.

Allegue, T., Arias, A., Fernandez-Gonzalez, N., Omil, F., & Garrido, J. M. (2018). Enrichment of nitrite-dependent anaerobic methane oxidizing bacteria in a membrane bioreactor. Chemical Engineering Journal, 347, 721-730.

Alrashed, W., Lee, J., Park, J., Rittmann, B. E., Tang, Y., Neufeld, J. D., & Lee, H. S. (2018). Hypoxic methane oxidation coupled to denitrification in a membrane biofilm. Chemical Engineering Journal, 348, 745-753.

AlSayed, A., Fergala, A., Khattab, S., & Eldyasti, A. (2018). Kinetics of type I methanotrophs mixed culture enriched from waste activated sludge. Biochemical engineering journal, 132, 60-67.

Awata, T., Goto, Y., Kindaichi, T., Ozaki, N., & Ohashi, A. (2015). Nitrogen removal using an anammox membrane bioreactor at low temperature. Water Science and Technology, 72(12), 2148-2153.

Background document for development of WHO Guidelines for Drinking-water Quality. (2011). Nitrate and nitrite in drinking-water. WHO Press, Geneva, Switzerland

Beck, D. A., Kalyuzhnaya, M. G., Malfatti, S., Tringe, S. G., del Rio, T. G., Ivanova, N., ... & Chistoserdova, L. (2013). A metagenomic insight into freshwater methane-utilizing communities and evidence for cooperation between the Methylococcaceae and the Methylophilaceae. PeerJ, 1, e23.

Bhattacharjee, A. S., Motlagh, A. M., Jetten, M. S., & Goel, R. (2016). Methane dependent denitrification-from ecosystem to laboratory-scale enrichment for engineering applications. Water research, 99, 244-252.

Bothe, H., Ferguson, S. J., & Newton, W. E. (2007). Biology of the nitrogen cycle. Amsterdam: Elsevier.

Bowman, J. (2006). The methanotrophs—the families Methylococcaceae and Methylocystaceae. In The prokaryotes (pp. 266-289). Springer, New York, NY.

Bq, Liao., Kraemer, JT., Bagley, DM. (2006) Anaerobic membrane bioreactors: applications and research directions. *Crit Rev Environ Sci Technol*. 36:489–530.

Broda, E. (1977). Two kinds of lithotrophs missing in nature. *Z. Allg. Microbiol. 17*, 491–493

Bruning-Fann, C. S., & Kaneene, J. B. (1993). The effects of nitrate, nitrite and N-nitroso compounds on human health: a review. Veterinary and human toxicology, 35(6), 521-538.

Brylev, O., Sarrazin, M., Rou, L., Bˇıelanger, D. (2007). Nitrate and nitrite electrocatalytic reduction on Rh-modified pyrolytic graphite electrodes, Electrochim. Acta 52, 6237.

Cai, C., Hu, S., Chen, X., Ni, B. J., Pu, J., & Yuan, Z. (2018). Effect of methane partial pressure on the performance of a membrane biofilm reactor coupling methane-dependent denitrification and anammox. Science of the Total Environment, 639, 278-285.

Caldwell, S. L., Laidler, J. R., Brewer, E. A., Eberly, J. O., Sandborgh, S. C., & Colwell, F. S. (2008). Anaerobic oxidation of methane: mechanisms, bioenergetics, and the ecology of associated microorganisms. Environmental science & technology, 42(18), 6791-6799.

Camargo, J. A., & Alonso, Á. (2006). Ecological and toxicological effects of inorganic nitrogen pollution in aquatic ecosystems: a global assessment. Environment international, 32(6), 831-849.

Cao, X., Qian, D., & Meng, X. (2013). Effects of pH on nitrite accumulation during wastewater denitrification. Environmental technology, 34(1), 45-51.

Carucci, A., Ramadori, R., Rossetti, S., & Tomei, M. C. (1996). Kinetics of denitrification reactions in single sludge systems. Water Research, 30(1), 51-56.

Celmer, D., Oleszkiewicz, J. A., & Cicek, N. (2008). Impact of shear force on the biofilm structure and performance of a membrane biofilm reactor for tertiary hydrogen-driven denitrification of municipal wastewater. Water research, 42(12), 3057-3065.

Chen, R., Luo, Y. H., Chen, J. X., Zhang, Y., Wen, L. L., Shi, L. D., ... & Zhao, H. P. (2016). Evolution of the microbial community of the biofilm in a methane-based membrane biofilm reactor reducing multiple electron acceptors. Environmental Science and Pollution Research, 23(10), 9540-9548.

Chen, Y., Zhou, W., Li, Y., Zhang, J., Zeng, G., Huang, A., & Huang, J. (2014). Nitrite reductase genes as functional markers to investigate diversity of denitrifying bacteria during agricultural waste composting. Applied microbiology and biotechnology, 98(9), 4233-4243.

Chistoserdova, L., & Lidstrom, M. E. (2013). Aerobic methylotrophic prokaryotes. In The prokaryotes (pp. 267-285). Springer, Berlin, Heidelberg.

Cho, S., Takahashi, Y., Fujii, N., Yamada, Y., Satoh, H., & Okabe, S. (2010). Nitrogen removal performance and microbial community analysis of an anaerobic up-flow granular bed anammox reactor. Chemosphere, 78(9), 1129-1135.

Chu, L., & Wang, J. (2017). Denitrification of groundwater using a biodegradable polymer as a carbon source: long-term performance and microbial diversity. RSC Advances, 7(84), 53454-53462.

Chung J, Nerenberg R, Rittmann B E, (2006) b. Bioreduction of selenate using a hydrogen-based membrane biofilm reactor. *Environmental Science & Technology, 40: 1664–1671.*

Chung, J., Nerenberg, R., & Rittmann, B. E. (2007). Evaluation for biological reduction of nitrate and perchlorate in brine water using the hydrogen-based membrane biofilm reactor. Journal of Environmental Engineering, 133(2), 157-164.

Claus, G., & Kutzner, H. J. (1985). Physiology and kinetics of autotrophic denitrification by Thiobacillus denitrificans. Applied Microbiology and Biotechnology, 22(4), 283-288.

Clifford, D., & Liu, X. (1993). Ion exchange for nitrate removal. Journal (American Water Works Association), 135-143.

Coenye, T., & Vandamme, P. (2003). Diversity and significance of Burkholderia species occupying diverse ecological niches. Environmental microbiology, 5(9), 719-729.

De Filippis, P., Di Palma, L., Scarsella, M., & Verdone, N. (2013). Biological denitrification of high-nitrate wastewaters: a comparison between three electron donors. Chem. Eng, 32, 319-324.

Dinçer, A. R., & Kargı, F. (2000). Kinetics of sequential nitrification and denitrification processes. Enzyme and microbial technology, 27(1), 37-42.

Dodds, W. K., Smith, V. H., & Lohman, K. (2002). Nitrogen and phosphorus relationships to benthic algal biomass in temperate streams. Canadian Journal of Fisheries and Aquatic Sciences, 59(5), 865-874

Dos Santos, L. M., & Livingston, A. G. (1995). Membrane-attached biofilms for VOC wastewater treatment. II: Effect of biofilm thickness on performance. Biotechnology and bioengineering, 47(1), 90-95

Douterelo, I., Jackson, M., Solomon, C., & Boxall, J. (2017). Spatial and temporal analogies in microbial communities in natural drinking water biofilms. Science of the Total Environment, 581, 277-288.

Downing, L. S., & Nerenberg, R. (2007). Kinetics of microbial bromate reduction in a hydrogen-oxidizing, denitrifying biofilm reactor. Biotechnology and bioengineering, 98(3), 543-550.

Dubrovsky, N. and Hamilton, P. (2010). Nutrients in the nation's streams and groundwater: national findings and implications. U.S. Geological Survey, Reston, Virginia (Fact Sheet 2010-3078; pubs.usgs.gov/fs/2010/3078/).

Eisentraeger, A., Klag, P., Vansbotter, B., Heymann, E., & Dott, W. (2001). Denitrification of groundwater with methane as sole hydrogen donor. Water research, 35(9), 2261-2267.

Elmidaoui, A., Elhannouni, F., Sahli, M. M., Chay, L., Elabbassi, H., Hafsi, M., & Largeteau, D. (2001). Pollution of nitrate in Moroccan ground water: removal by electrodialysis. Desalination, 136(1), 325-332.

Eltschlager, K.K., Hawkins, J.W., Ehler, W.C., Baldassare, F., 2001. Technical measures for the investigation and mitigation of fugitive methane hazards in areas of coal mining.

Environment Canada, Climate Change Canada - https://www.canada.ca/en/environment-climate-change/services/canadian-environmental-protection-act-registry/proposed-methane-regulations-additional-information.html

Ergas, S.J.; Rheinheimer, D.E. (2004). Drinking water denitrification using a membrane bioreactor. *Water Research, 38*, 3225-3232.

Erisman, J. W., Galloway, J. N., Dise, N. B., Sutton, M. A., Bleeker, A., Grizzetti, B., ... & De Vries, W. (2015). Nitrogen: too much of a vital resource: Science Brief. WWF Netherlands.

Ettwig, K. F., Butler, M. K., Le Paslier, D., Pelletier, E., Mangenot, S., Kuypers, M. M., ... & Gloerich, J. (2010). Nitrite-driven anaerobic methane oxidation by oxygenic bacteria. Nature, 464(7288), 543.

Fangang, M., Fenglin, Y., Shi, B. & Zhang, H. (2008). A comprehensive study on membrane fouling in submerged membrane bioreactors operated under different aeration intensities. *Separation and Purification Technology, 59,* 91-100

Fernández, I., Dosta, J., Fajardo, C., Campos, J. L., Mosquera-Corral, A., & Méndez, R. (2012). Short-and long-term effects of ammonium and nitrite on the Anammox process. Journal of Environmental Management, 95, S170-S174.

Fernández, I., Vázquez-Padín, J. R., Mosquera-Corral, A., Campos, J. L., & Méndez, R. (2008). Biofilm and granular systems to improve Anammox biomass retention. Biochemical Engineering Journal, 42(3), 308-313.

Fewtrell, L. (2004). Drinking-water nitrate, methemoglobinemia, and global burden of disease: a discussion. Environmental health perspectives, 1371-1374.

Fonseca, A. D., Crespo, J. G., Almeida, J. S., & Reis, M. A. (2000). Drinking water denitrification using a novel ion-exchange membrane bioreactor. Environmental *Science & Technology, 34*, 1557-1562.

Galloway, J. N., Townsend, A. R., Erisman, J. W., Bekunda, M., Cai, Z., Freney, J. R., ... & Sutton, M. A. (2008). Transformation of the nitrogen cycle: recent trends, questions, and potential solutions. Science, 320(5878), 889-892.

Galloway, J.N., Schlesinger, W.H., Levy II, H., Michaels, A. and Schnoor, J.L. (1995). Nitrogen fixation: Anthropogenic enhancement-environmental response. Global Biogeochemical Cycles 9: doi: 10.1029/95GB00158. issn: 0886-6236.

Gavazza dos Santos, S., Amâncio Varesche, M. B., Zaiat, M., & Foresti, E. (2004). Comparison of methanol, ethanol, and methane as electron donors for denitrification. Environmental engineering science, 21(3), 313-320.

Ge, S., Peng, Y., Wang, S., Lu, C., Cao, X., & Zhu, Y. (2012). Nitrite accumulation under constant temperature in anoxic denitrification process: The effects of carbon sources and COD/NO3-N. Bioresource technology, 114, 137-143.

Gottenbos, B., Mei, H. C. V. D., & Busscher, H. J. (2000). Initial adhesion and surface growth of Staphylococcus epidermidis and Pseudomonas aeruginosa on biomedical polymers. Journal of biomedical materials research, 50(2), 208-214.

Grabińska-Ńoniewska, A., Słomczyński, T., & Kańska, Z. (1985). Denitrification studies with glycerol as a carbon source. Water Research,19(12), 1471-1477.

Habermeyer, M., Roth, A., Guth, S., Diel, P., Engel, K. H., Epe, B., & Eisenbrand, G. (2015). Nitrate and nitrite in the diet: How to assess their benefit and risk for human health. Molecular nutrition & food research, 59(1), 106-128.

Hallam, S. J.; Putnam, N. J.; Preston, C. M.; Detter, J. C.; Rokhsar, D.; Richardson, P. M.; & DeLong, E. F. (2004). Reverse Methanogenesis: Testing the Hypothesis with Environmental Genomics *Science (Washington, D. C.), 305*, 145.

Haroon, M. F., Hu, S., Shi, Y., Imelfort, M., Keller, J., Hugenholtz, P., ... & Tyson, G. W. (2013). Anaerobic oxidation of methane coupled to nitrate reduction in a novel archaeal lineage. *Nature, 500(7464),* 567-570.

Harrison, J.A. (2003), "The Nitrogen Cycle: Of Microbes and Men," *Vison learning*, Volume EAS-2 (4).

He, Z., Geng, S., Cai, C., Liu, S., Liu, Y., Pan, Y., ... & Hu, B. (2015). Anaerobic oxidation of methane coupled to nitrite reduction by halophilic marine NC10 bacteria. *Applied and environmental microbiology, 81(16)*, 5538-5545.

He, Z., Geng, S., Cai, C., Liu, S., Liu, Y., Pan, Y., ... & Hu, B. (2015). Halophilic anaerobic oxidation of methane coupled to nitrite reduction by marine NC10 bacteria. Applied and environmental microbiology, AEM-00984.

Head, S. R., Komori, H. K., LaMere, S. A., Whisenant, T., Van Nieuwerburgh, F., Salomon, D. R., & Ordoukhanian, P. (2014). Library construction for next-generation sequencing: overviews and challenges. Biotechniques, 56(2), 61-77.

Health Canada. (2013). Nitrate and Nitrite in Drinking Water. Retrieved from http://www.hc-sc.gc.ca/ewh-semt/consult/_2012/nitrite-nitrite/draft-ebauche-eng.php.

Hord, N. G., Tang, Y., & Bryan, N. S. (2009). Food sources of nitrates and nitrites: the physiologic context for potential health benefits. The American journal of clinical nutrition, 90(1), 1-10.

Houbron, E., Torrijos, M., & Capdevilles, B. (1999). An alternative use of biogas applied at the water denitrification. Water science and technology, 40(8), 115-122.

Howard-Williams, C. L. I. V. E. (1985). Cycling and retention of nitrogen and phosphorus in wetlands: a theoretical and applied perspective. Freshwater Biology, 15(4), 391-431.

Howarth, R. W. (2014). A bridge to nowhere: methane emissions and the greenhouse gas footprint of natural gas. Energy Science & Engineering, 2(2), 47-60.

Howarth, R. W., Santoro, R., & Ingraffea, A. (2011). Methane and the greenhouse-gas footprint of natural gas from shale formations. Climatic change, 106(4), 679.

Hu, B., Shen, L., Xu, X., & Zheng, P. (2011). Anaerobic ammonium oxidation (anammox) in different natural ecosystems. Biochemical Society Transactions, 39(6), 1811.

Hu, S., Zeng, R. J., Burow, L. C., Lant, P., Keller, J., & Yuan, Z. (2009). Enrichment of denitrifying anaerobic methane oxidizing microorganisms. Environmental Microbiology Reports, 1(5), 377-384.

Huang, Z., Ong, S.L., Ng, H.Y. (2011). Submerged anaerobic membrane bioreactor for low-strength wastewater treatment: effect of HRT and SRT on treatment performance and membrane fouling, Water Res. 45 705–713.

Islas-Lima, S., Thalasso, F., Gomez-Hernandez, J. (2004). Evidence of anoxic methane oxidation coupled to denitrification. *Water Res. 38*, 13–16.

Jin, R.C., Yang, G.F., Yu, J.J., Zheng, P. (2012). The inhibition of the Anammox process: a review. *Chemical Engineering Journal, 197,* 67e79.

Judd, S. (2010). The MBR book: principles and applications of membrane bioreactors for water and wastewater treatment. Elsevier.

Kalyuhznaya, M. G., Martens-Habbena, W., Wang, T., Hackett, M., Stolyar, S. M., Stahl, D. A., ... & Chistoserdova, L. (2009). Methylophilaceae link methanol oxidation to denitrification in freshwater lake sediment as suggested by stable isotope probing and pure culture analysis. Environmental microbiology reports, 1(5), 385-392.

Kalyuzhnaya, M. G., Yang, S., Rozova, O. N., Smalley, N. E., Clubb, J., Lamb, A., ... & Vuilleumier, S. (2013). Highly efficient methane biocatalysis revealed in a methanotrophic bacterium. Nature communications, 4, 2785.

Kammermeyer, K. (1976). Technical gas permeation processes. Chemie Ingenieur Technik, 48(8), 672-675.

Kampbell DH, Vandegrift SA. (1998). Analysis of dissolved methane, ethane, and ethylene in ground water by a standard gas chromatographic technique. *J Chromatogr Sci. 36*:253–256.

Kampman, C., Piai, L., Temmink, H., Hendrickx, T. L., Zeeman, G., & Buisman, C. J. (2018). Effect of low concentrations of dissolved oxygen on the activity of denitrifying methanotrophic bacteria. Water Science and Technology, 77(11), 2589-2597.

Kapoor, A. and Viraraghavan, T. (1997). Nitrate removal from drinking water—review. J. *Environ. Eng., 123(4),* 317–380.

Kartal, B., Kuenen, J. G., & Van Loosdrecht, M. C. M. (2010). Sewage treatment with anammox. Science, 328(5979), 702-703.

Kartal, B., Maalcke, W.J., de Almeida, N.M., Cirpus, I., Gloerich, J., Geerts, W., den Camp, H.J.M.O., Harhangi, H.R., Janssen-Megens, E.M., Francoijs, K., Stunnenberg, H.G., Keltjens, J.T., Jetten, M.S.M., Strous, M. (2011).Molecular mechanism of anaerobic ammonium oxidation. Nature, DOI: 10.1038/nature.10453.

Kim, J.H., Rene, E.R., Park, H.S. (2008). Biological oxidation of hydrogen sulfide under steady and transient state conditions in an immobilized cell biofilter. *Bioresour. Technol. 99,* 583–588.

Kimura, Y., Isaka, K., Kazama, F., & Sumino, T. (2010). Effects of nitrite inhibition on anaerobic ammonium oxidation. Applied microbiology and biotechnology, 86(1), 359-365.

Knobeloch, L., Salna, B., Hogan, A., Postle, J., & Anderson, H. (2000). Blue babies and nitrate-contaminated well water. Environmental Health Perspectives, 108(7), 675.

Knowles, R. Denitrification. (1982). Microbiological Rev., 46(1), 43-70.

Kougias, P. G., De Francisci, D., Treu, L., Campanaro, S., & Angelidaki, I. (2014). Microbial analysis in biogas reactors suffering by foaming incidents. Bioresource technology, 167, 24-32.

Kwok, W. K., Picioreanu, C., Ong, S. L., Van Loosdrecht, M. C. M., Ng, W. J., & Heijnen, J. J. (1998). Influence of biomass production and detachment forces on biofilm structures in a biofilm airlift suspension reactor. Biotechnology and bioengineering, 58(4), 400-407.

Lackner, S., Terada, A., & Smets, B. F. (2008). Heterotrophic activity compromises autotrophic nitrogen removal in membrane-aerated biofilms: results of a modeling study. *Water research, 42(4),* 1102-1112.

Lackner, S., Welker, S., Gilbert, E. M., & Horn, H. (2015). Influence of seasonal temperature fluctuations on two different partial nitritation-anammox reactors treating mainstream municipal wastewater. Water Science and Technology, 72(8), 1358-1363.

Lai, C. Y., Wen, L. L., Shi, L. D., Zhao, K. K., Wang, Y. Q., Yang, X., ... & Zhao, H. P. (2016). Selenate and nitrate bioreductions using methane as the electron donor in a membrane biofilm reactor. Environmental science & technology, 50(18), 10179-10186.

Lai, C. Y., Yang, X., Tang, Y., Rittmann, B. E., & Zhao, H. P. (2014). Nitrate shaped the selenate-reducing microbial community in a hydrogen-based biofilm reactor. Environmental science & technology, 48(6), 3395-3402.

Lazarova, V.Z., Capdeville, B. & Nikolov, L. (1992). Biofilm performance of a fluidized bed biofilm reactor for drinking water denitrification. *Water Science Tech*, 26 (3-4), 555-566.

Lee, H. S., Tang, Y., Rittmann, B. E., & Zhao, H. P. (2018). Anaerobic oxidation of methane coupled to denitrification: fundamentals, challenges, and potential. Critical reviews in environmental science and technology, 48(19-21), 1067-1093.

Lee, K.-C. & Rittmann, B. E. (2002). Applying a novel autohydrogenotrophic hollow-fiber membrane biofilm reactor for denitrification of drinking water," *Water Res., 36, 2040-2052.*

Li, D., Wang, R., Chung, T.S. (2004). Fabrication of lab-scale hollow fiber membrane modules with high packing density. *Sep. Purif. Technol. 40,* 15.

Li, G., Yu, J., Zhang, Y. H., Gao, L., & Zhang, H. (2013). Study on membrane fouling of a hydrogen-based membrane biofilm reactor treating nitrate-contaminated drinking water. In Applied Mechanics and Materials (Vol. 361, pp. 814-817). Trans Tech Publications.

Li, Y. (2014). An In Situ MBfR System to Treat Nitrate-Contaminated Surface Water (Doctoral dissertation, Arizona State University).

Liang, Y., Li, D., Zhang, X., Zeng, H., Yang, Z., & Zhang, J. (2014). Microbial characteristics and nitrogen removal of simultaneous partial nitrification, anammox and denitrification (SNAD) process treating low C/N ratio sewage. Bioresource Technology, 169, 103-109.

Liessens, j., germonpré, r., beernaert, s., andverstraete, w. (1993). Removing nitrate with a methylothophic fluidized bed: Technology and operating performance. Am. *Water Works Assoc. 85(4)*, 144–154.

Liu, J., Sun, F., Wang, L., Ju, X., Wu, W., & Chen, Y. (2014). Molecular characterization of a microbial consortium involved in methane oxidation coupled to denitrification under micro-aerobic conditions. Microbial biotechnology, 7(1), 64-76.

Liu, T., Hu, S., & Guo, J. (2019). Enhancing mainstream nitrogen removal by employing nitrate/nitrite-dependent anaerobic methane oxidation processes. Critical reviews in biotechnology, 39(5), 732-745.

Liu, Y., & Tay, J. H. (2002). The essential role of hydrodynamic shear force in the formation of biofilm and granular sludge. Water research, 36(7), 1653-1665.

Loosdrecht, V., MCM, & Henze, M. (1999). Maintenance, endogeneous respiration, lysis, decay and predation. *Water Sci. Technol, 39(1):*107–17.

Luo, J. H., Chen, H., Yuan, Z., & Guo, J. (2018). Methane-supported nitrate removal from groundwater in a membrane biofilm reactor. Water research, 132, 71-78.

Luo, Y. H., Chen, R., Wen, L. L., Meng, F., Zhang, Y., Lai, C. Y., ... & Zheng, P. (2015). Complete perchlorate reduction using methane as the sole electron donor and carbon source. Environmental science & technology, 49(4), 2341-2349.

Luo, Z., Li, S., Zhu, X., & Ji, G. (2018). Carbon source effects on nitrogen transformation processes and the quantitative molecular mechanism in long-term flooded constructed wetlands. Ecological engineering, 123, 19-29.

Makisha, N., & Semenova, D. (2018). Production of biogas at wastewater treatment plants and its further application. In MATEC Web of Conferences (Vol. 144, p. 04016). EDP Sciences.

Mallevaille, J., Odendaal, P.E., & Wiesner, M.R. (1996). *Water Treatment Membrane Processes*. New York, McGraw-Hill.

Martin, K. J., & Nerenberg, R. (2012). The membrane biofilm reactor (MBfR) for water and wastewater treatment: principles, applications, and recent developments. Bioresource technology, 122, 83-94.

Martin, K.J., Picioreanu, C., Nerenberg, R. (2013). Multidimensional modeling of biofilm development and fluid dynamics in a hydrogen-based, membrane biofilm reactor (MBfR). Water Res. 47 (13), 4739e4751.

Mavroudi, M., Kaldis, S. P., & Sakellaropoulos, G. P. (2006). A study of mass transfer resistance in membrane gas–liquid contacting processes. Journal of Membrane Science, 272(1), 103-115.

McAdam, E.J. & Judd, S.J. (2008). Immersed membrane bioreactors for nitrate removal from drinking water: Cost and feasibility. *Desalination, 196,* 135-148.

McAdam, E.J., & Judd, S.J. (2006). A review of membrane bioreactor potential for nitrate removal from drinking water. *Desalination, 196,* 135-148.

McGlynn, S. E., Chadwick, G. L., Kempes, C. P., & Orphan, V. J. (2015). Single cell activity reveals direct electron transfer in methanotrophic consortia. Nature, 526(7574), 531-535.

Meng, X., Qian, D., & Cao, X. (2010, June). Nitrite accumulation during wastewater denitrification. In 2010 International Conference on Electrical and Control Engineering (pp. 4721-4724). IEEE.

Metcalf & Eddy., Tchobanoglous, G., Burton, F. L. 1. & Stensel, H. D. (2003). Wastewater engineering: Treatment and reuse (4th Ed.). Boston: McGraw-Hill.

Methanex, Methanex Methanol Price Sheet, https://www.methanex.com/sites. (2019).

Meyer, K.J., Swaim, P.D., Bellamy, W.D., Rittmann, B.E. and Tang. Y. (2010). Biological and ion exchange nitrate removal evaluation. Water Research Foundation, Denver, Colorado (Report No. 4131).

Missimer, T.M., Ghaffour, N., Dehwah, A.H.A., Rachman, R. (2013). Subsurface intakes for seawater reverse osmosis facilities: Capacity limitation, water quality improvement, and economics. *Desalination 322,* 37-51.

Mitsubishi Rayon (2000). Development of a multi-layered composite hollow-fiber membrane. Retrieved from the Mitsubishi Rayon, Inc. website https://www.mrc.co.jp/sterapore.html

Modin, O., Fukushi K., and Yamamoto K. (2008). Simultaneous removal of nitrate and pesticides from groundwater using a methane-fed membrane biofilm reactor. Water Science & Technology. doi: 10.2166/wst.2008.481

Modin, O., Fukushi, K., & Yamamoto, K. (2007). Denitrification with methane as external carbon source. Water research, 41(12), 2726-2738.

Modin, O., Fukushi, K., Nakajima, F., & Yamamoto, K. (2008). Performance of a membrane biofilm reactor for denitrification with methane. Bioresource technology, 99(17), 8054-8060.

Modin, O., Fukushi, K., Nakajima, F., Yamamoto, K. (2010). Nitrate removal and biofilm characteristics in methanotrophic membrane biofilm reactors with various gas supply regimes. Water research. 44, 8 5 – 9 6.

Momba, M. N. B., Kfir, R., Venter, S. N., and Cloete, T. E. (2000). An overview of biofilm formation in distribution systems and its impact on the deterioration of water quality. Water SA, 26, 59–66.

Mosier, A., Syers, J. K., & Freney, J. R. (Eds.). (2013). Agriculture and the nitrogen cycle: assessing the impacts of fertilizer use on food production and the environment (Vol. 65). Island Press.

Murrell, J. C. (2010). The aerobic methane oxidizing bacteria (methanotrophs). In Handbook of hydrocarbon and lipid microbiology (pp. 1953-1966). Springer, Berlin, Heidelberg.

Nerenberg, R. (2005, February). Membrane biofilm reactors for water and wastewater treatment. In Borchardt Conference: A Seminar on Advances in Water and Wastewater Treatment (Vol. 23, p. 25). Ann Arbor. MI.

Nerenberg, R. (2016). The membrane-biofilm reactor (MBfR) as a counter-diffusional biofilm process. Current opinion in biotechnology, 38, 131-136.

Nerenberg, R., Rittmann, B.E., (2004). Hydrogen-based, hollow-fiber membrane biofilm reactor for reduction of perchlorate and other oxidized contaminants. *Water Science and Technology, 49* (11–12), 223–230

Nerenberg, Robert. (2003). *Perchlorate Removal from Drinking Water with A Hydrogen-Based, Hollow-Fiber Membrane Biofilm Reactor*. (Doctoral dissertation). University Microfilms International, Illinois

Newcomer, T. A., Kaushal, S. S., Mayer, P. M., Shields, A. R., Canuel, E. A., Groffman, P. M., & Gold, A. J. (2012). Influence of natural and novel organic carbon sources on denitrification in forest, degraded urban, and restored streams. Ecological Monographs, 82(4), 449-466.

O'Toole, G., Kaplan, H B., Kolter, R. (2000). Biofilm formation as microbial development. Annul Rev Microbial, 54, 49–79.

Ohashi, A., & Harada, H. (1994). Adhesion strength of biofilm developed in an attached-growth reactor. Water Science and Technology, 29(10), 281-288.

Ontario Energy Board, https://www.oeb.ca/rates-and-your-bill/natural-gas-rates (2019).

Ontiveros-Valencia, A., Tang, Y., Krajmalnik-Brown, R., & Rittmann, B. E. (2014). Managing the interactions between sulfate-and perchlorate-reducing bacteria when using hydrogen-fed biofilms to treat a groundwater with a high perchlorate concentration. Water research, 55, 215-224.

Ordaz, A., López, J. C., Figueroa-González, I., Muñoz, R., & Quijano, G. (2014). Assessment of methane biodegradation kinetics in two-phase partitioning bioreactors by pulse respirometry. Water research, 67, 46-54.

Paustian, K., Babcock, B., Hatfield, J. L., Lal, R., McCarl, B. A., McLaughlin, S., ... & Rosenzweig, C. (2001). Agricultural mitigation of greenhouse gases: science and policy options. In 2001 Conference Proceedings, First National Conference on Carbon Sequestration. Washington, DC: Conference on Carbon Sequestration.

Pavissich, J P., Aybar, M., Martin, K J., Nerenberg, R. (2014). A methodology to assess the effects of biofilm roughness on substrate fluxes using image analysis, substrate profiling, and mathematical modelling. Water. Sci. Technol., 69, 1932–1941. (doi: 10.2166/ wst.2014.103).

Petersen, F.C., Pecharki, D., & Scheie, A.A. (2004). Biofilm mode of growth of Streptococcus intermedius favored by a competence-stimulating signaling peptide. *J Bacteriol: 6327-6331*.

Peyton, B. M. (1996). Effects of shear stress and substrate loading rate on Pseudomonas aeruginosa biofilm thickness and density. Water Research, 30(1), 29-36.

Pinar, G., E. Duque, A. Haidour, J.-M. Oliva, L. Sanchez-Barbero, V. Calvo, and J.L. Ramos. (1997). Removal of high concentrations of nitrate from industrial wastewaters by bacteria. Appl. Environ. Microbial. 63(5): 2071-2073

Powlson, D. S., Addiscott, T. M., Benjamin, N., Cassman, K. G., de Kok, T. M., van Grinsven, H., ... & Van Kessel, C. (2008). When does nitrate become a risk for humans?. Journal of environmental quality, 37(2), 291-295.

Raghoebarsing, A. A., Pol, A., Van de Pas-Schoonen, K. T., Smolders, A. J., Ettwig, K. F., Rijpstra, W. I. C., ... & Strous, M. (2006). A microbial consortium couples anaerobic methane oxidation to denitrification. Nature, 440(7086), 918.

Raghoebarsing, A.A., Pol, A., van de Pas-Schoonen, K.T., Smolders, A.J.P., Ettwig, K.F., Rijpstra, I.C., Schouten, S., Sinninghe Damste, J.S., Op den Camp, H.J.M., Jetten, M.S.M., Strous, M. (2006). A microbial consortium couples anaerobic methane oxidation to denitrification. Nature 440, 918–921.

Rezania, B., Cicek, N., & Oleszkiewicz, J. A. (2005). Kinetics of hydrogen-dependent denitrification under varying pH and temperature conditions. Biotechnology and bioengineering, 92(7), 900-906.

Rezania, B., Oleszkiewicz, J.A. & Cicek, N. (2007). Hydrogen-dependent denitrification of water in anaerobic submerged membrane bioreactor coupled with a novel hydrogen delivery system. *Water Research, 41*, 1074-1080.

Rittman, B. E. (1982). The effect of shear stress on biofilm loss rate. Biotechnology and Bioengineering, 24(2), 501-506.

Rittmann, B. E., & Lee, K. C. (2002). U.S. Patent No. 6,387,262. Washington, DC: U.S. Patent and Trademark Office.

Rittmann, B. E., Nerenberg, R., Lee, K. C.,Najm, I., Gillogly, T. E., Lehman, G. E.,and Adham, S. S. (2004). The hydrogen-based hollow-fiber membrane biofilm reactor (HFMBfR) for reducing oxidized contaminants. Water Sci, Technol.: Water Supply, 4(1), 127-133.

Rittmann, B.E. (2007). The membrane biofilm reactor is a versatile platform for water and wastewater treatment. Environ. Eng. Res. 12, 157–175.

Rittmann, B.E.; Huck, P.M. (1989). *Biological treatment of public water-supplies*. In CRC Critical Reviews in Environmental Control. Boca Raton, FL: CRC Press.

Rittmann, B.E.; McCarty, P.L. (2001). Environmental Biotechnology: Principles and Applications. New York: McGraw-Hill Companies, Inc.

Rocher, V., Laverman, A. M., Gasperi, J., Azimi, S., Guérin, S., Mottelet, S., ... & Pauss, A. (2015). Nitrite accumulation during denitrification depends on the carbon quality and quantity in wastewater treatment with biofilters. Environmental Science and Pollution Research, 22(13), 10179-10188.

Rostkowski, K. H., Pfluger, A. R., & Criddle, C. S. (2013). Stoichiometry and kinetics of the PHB-producing Type II methanotrophs Methylosinus trichosporium OB3b and Methylocystis parvus OBBP. Bioresource technology, 132, 71-77.

Rush, D., Osborne, K. A., Birgel, D., Kappler, A., Hirayama, H., Peckmann, J., ... & Sidgwick, F. R. (2016). The bacteriohopanepolyol inventory of novel aerobic methane oxidising bacteria reveals new biomarker signatures of aerobic methanotrophy in marine systems. PloS one, 11(11), e0165635.

Saddoud, A., Ellouze, M., Dhouib, A., Sayadi, S., 2007. Anaerobic membrane bioreactor treatment of domestic wastewater in Tunisia. *Desalination* 207 (1-3), 205-215.

Sahli, M. M., Annouar, S., Mountadar, M., Soufiane, A., & Elmidaoui, A. (2008). Nitrate removal of brackish underground water by chemical adsorption and by electrodialysis. Desalination, 227(1), 327-333.

Santamaria, P. (2006). Nitrate in vegetables: toxicity, content, intake and EC regulation. Journal of the Science of Food and Agriculture, 86(1), 10-17.

Schindler, D. W., Curtis, P. J., Parker, B. R., & Stainton, M. P. (1996). Consequences of climate warming and lake acidification for UV-B penetration in North American boreal lakes. Nature, 379(6567), 705-708.

Schmidt, I., & Bock, E. (1997). Anaerobic ammonia oxidation with nitrogen dioxide by Nitrosomonas eutropha. *Archives of microbiology, 167(2-3)*, 106-111.

Schreiber, F., Wunderlin, P., Udert, K. M., & Wells, G. F. (2012). Nitric oxide and nitrous oxide turnover in natural and engineered microbial communities: biological pathways, chemical reactions, and novel technologies. Frontiers in microbiology, 3, 372.

Scott, M. E. A. (2006). Grand river watershed analysis of nitrate transport as a result of agricultural inputs using a geographic information system. In Masters Abstracts International (Vol. 45, No. 04).

Segers, R. (1998). Methane production and methane consumption: a review of processes underlying wetland methane fluxes. Biogeochemistry, 41(1), 23-51.

Semmens, M. J., Dahm, K., Shanahan, J., & Christianson, A. (2003). COD and nitrogen removal by biofilms growing on gas permeable membranes. Water Research, 37(18), 4343-4350.

Semmens, M.J., (2005). Membrane Technology: Pilot Studies of Membrane-Aerated Bioreactors. *Water Environment Research Foundation and the International Water Association.*

Shen, L. D., Hu, B. L., Liu, S., Chai, X. P., He, Z. F., Ren, H. X., ... & Wang, Y. M. (2016). Anaerobic methane oxidation coupled to nitrite reduction can be a potential methane sink in coastal environments. Applied microbiology and biotechnology, 100(16), 7171-7180.

Shen, L. D., Liu, S., Huang, Q., Lian, X., He, Z. F., Geng, S., ... & Hu, B. L. (2014). Evidence for the Cooccurrence of Nitrite-Dependent Anaerobic Ammonium and Methane Oxidation Processes in a Flooded Paddy Field. Applied and environmental microbiology, 80(24), 7611-7619.

Shen, Z., Zhou, Y., & Wang, J. (2013). Comparison of denitrification performance and microbial diversity using starch/polylactic acid blends and ethanol as electron donor for nitrate removal. Bioresource technology, 131, 33-39.

Shi, Y., Hu, S., Lou, J., Lu, P., Keller, J., & Yuan, Z. (2013). Nitrogen removal from wastewater by coupling anammox and methane-dependent denitrification in a membrane biofilm reactor. Environmental Science & Technology, 47(20), 11577-11583.

Shin, J.H., Sang, B.I., Chung, Y.C., Choung, Y.K. (2008). A novel CSTR-type of hollow fiber membrane biofilm reactor for consecutive nitrification and denitrification. *Desalination, 221* (1–3), 526–533.

Songliu, L. U., Hongying, H., Yingxue, S., & Jia, Y. A. N. G. (2009). Effect of carbon source on the denitrification in constructed wetlands. Journal of Environmental Sciences, 21(8), 1036-1043.

Stein, L. Y., & Klotz, M. G. (2011). Nitrifying and denitrifying pathways of methanotrophic bacteria.

Stein, L. Y., & Klotz, M. G. (2016). The nitrogen cycle. Current Biology, 26(3), R94-R98.

Steinle, L., Maltby, J., Treude, T., Kock, A., Bange, H. W., Engbersen, N., ... & Niemann, H. (2017). Effects of low oxygen concentrations on aerobic methane oxidation in seasonally hypoxic coastal waters.

Strous, M., Heijnen, J.J., Kuenen, J.G. Jetten, M.S.M. (1998). The sequencing batch reactor as a powerful tool for the study of slowly growing anaerobic ammonium-oxidizing microorganisms, Appl. Microbial. Biotechnol. 50 (5) 589–596.

Sun, F. Y., Dong, W. Y., Shao, M. F., Lv, X. M., Li, J., Peng, L. Y., & Wang, H. J. (2013). Aerobic methane oxidation coupled to denitrification in a membrane biofilm reactor: Treatment performance and the effect of oxygen ventilation. Bioresource technology, 145, 2-9.

Sun, F. Y., Dong, W. Y., Shao, M. F., Lv, X. M., Li, J., Peng, L. Y., & Wang, H. J. (2013). Aerobic methane oxidation coupled to denitrification in a membrane biofilm reactor: treatment performance and the effect of oxygen ventilation. Bioresource technology, 145, 2-9.

Syed, M., Soreanu, G., Falletta, P., Be´land, M. (2006). Removal of hydrogen sulfide from gas streams using biological processes – A review. Can. *Biosys. Eng. 48,* 2.1–2.14.

Tang, Y., Zhou, C., Van Ginkel, S. W., Ontiveros-Valencia, A., Shin, J., & Rittmann, B. E. (2012). Hydrogen permeability of the hollow fibers used in H2-based membrane biofilm reactors. Journal of membrane science, 407, 176-183.

Tang, Youneng. (2012). *Biofilm Reduction of Oxidized Contaminants*. (Doctoral dissertation). Arizona state university, Arizona.

Tao, W., He, Y., Wang, Z., Smith, R., Shayya, W., & Pei, Y. (2012). Effects of pH and temperature on coupling nitritation and anammox in biofilters treating dairy wastewater. Ecological Engineering, 47, 76-82.

Telgmann, U., Horn, H., & Morgenroth, E. (2004). Influence of growth history on sloughing and erosion from biofilms. Water Research, 38(17), 3671-3684.

Terada, A., Kaku, S., Matsumoto, S., & Tsuneda, S. (2006). Rapid autohydrogenotrophic denitrification by a membrane biofilm reactor equipped with a fibrous support around a gas-permeable membrane. Biochemical Engineering Journal, 31(1), 84-91.

Thalasso, F., Vallecillo, A., Garcia-Encina, P., & Fdz-Polanco, F. (1997). The use of methane as a sole carbon source for wastewater denitrification. Water Research, 31(1), 55-60.

Timmermans, P., & Van Haute, A. (1983). Denitrification with methanol: fundamental study of the growth and denitrification capacity of Hyphomicrobium sp. Water Research, 17(10), 1249-1255.

Timmers, P. H., Welte, C. U., Koehorst, J. J., Plugge, C. M., Jetten, M. S., & Stams, A. J. (2017). Reverse methanogenesis and respiration in methanotrophic archaea. Archaea, 2017.

Torresi, E., Fowler, S. J., Polesel, F., Bester, K., Andersen, H. R., Smets, B. F., ... & Christensson, M. (2016). Biofilm Thickness Influences Biodiversity in Nitrifying MBBRsImplications on Micropollutant Removal. Environmental science & technology, 50(17), 9279-9288.

Townsend, A. R., Howarth, R. W., Bazzaz, F. A., Booth, M. S., Cleveland, C. C., Collinge, S. K., ... & Mallin, M. A. (2003). Human health effects of a changing global nitrogen cycle. Frontiers in Ecology and the Environment, 1(5), 240-246.

Tribe, L. A., Briens, C. L., & Margaritis, A. (1995). Determination of the volumetric mass transfer coefficient (kLa) using the dynamic "gas out–gas in" method: Analysis of errors caused by dissolved oxygen probes. Biotechnology and bioengineering, 46(4), 388-392.

Trotsenko, Y. A., & Khmelenina, V. N. (2005). Aerobic methanotrophic bacteria of cold ecosystems. FEMS Microbiology Ecology, 53(1), 15-26.

Trotsenko, Y. A., & Murrell, J. C. (2008). Metabolic aspects of aerobic obligate methanotrophy★. Advances in applied microbiology, 63, 183-229.

U.S. EPA demonstration project at Fruitland, (2002). Water Supply and Water Resources Division, National Risk Management Research Laboratory, Office of Research and Development, U.S. Environmental Protection Agency, Cincinnati, Ohio.

Valentine, D.L., Reeburgh, W.S. (2000). New perspectives on anaerobic methane oxidation. *Environ. Microbial. 2 (*5), 477–484.

Vitousek, P.M., Howarth, R.W., Likens, G.E., Matson, P.A., Schindler, D., Schlesinger, W.H. and Tilman, G.D. (1997). Human alteration of the global nitrogen cycle: causes and consequences. *Issue Ecol*. 1: 1–17.

Wang, D. T., Welander, P. V., & Ono, S. (2016). Fractionation of the methane isotopologues 13CH4, 12CH3D, and 13CH3D during aerobic oxidation of methane by Methylococcus capsulatus (Bath). Geochimica et Cosmochimica Acta, 192, 186-202.

Wang, J. H., Baltzis, B. C., & Lewandowski, G. A. (1995). Fundamental denitrification kinetic studies with Pseudomonas denitrificans. Biotechnology and bioengineering, 47(1), 26-41.

Wang, Y., Bott, C., & Nerenberg, R. (2016). Sulfur-based denitrification: effect of biofilm development on denitrification fluxes. Water research, 100, 184-193.

Ward, N., Larsen, Ø., Sakwa, J., Bruseth, L., Khouri, H., Durkin, A. S., ... & Lewis, M. (2004). Genomic insights into methanotrophy: the complete genome sequence of Methylococcus capsulatus (Bath). PLoS biology, 2(10), e303.

Webb, H. K., Ng, H. J., & Ivanova, E. P. (2014). The family methylocystaceae. The Prokaryotes: Alphaproteobacteria and Betaproteobacteria, 341-347.

Wegener, G., Krukenberg, V., Riedel, D., Tegetmeyer, H. E., & Boetius, A. (2015). Intercellular wiring enables electron transfer between methanotrophic archaea and bacteria. Nature, 526(7574), 587-590.

Welte, C. U., Rasigraf, O., Vaksmaa, A., Versantvoort, W., Arshad, A., Op den Camp, H. J., ... & Reimann, J. (2016). Nitrate-and nitrite-dependent anaerobic oxidation of methane. Environmental microbiology reports, 8(6), 941-955.

Welte, C. U., Rasigraf, O., Vaksmaa, A., Versantvoort, W., Arshad, A., Op den Camp, H. J., ... & Reimann, J. (2016). Nitrate-and nitrite-dependent anaerobic oxidation of methane. Environmental microbiology reports, 8(6), 941-955.

Wijeyekoon, S., Mino, T., Satoh, H., & Matsuo, T. (2004). Effects of substrate loading rate on biofilm structure. Water Research, 38(10), 2479-2488.

Wilderer, P. A., Flemming, H. C., & Davids, L. (2017). Microorganisms and Their Role in Soil. In Fundamentals and Applications of Bioremediation (pp. 283-332). Routledge.

Willems, A., & Gillis, M. (2015). Comamonadaceae. Bergey's Manual of Systematics of Archaea and Bacteria, 1-6.

World Health Organization. (2003). Nitrate and nitrite in drinking-water: Background document for development of WHO Guidelines for Drinking-water Quality (No. WHO/SDE/WSH/04.03/56). World Health Organization.

Wu, M. L., Ettwig, K. F., Jetten, M. S., Strous, M., Keltjens, J. T., & Niftrik, L. V. (2011). A new intra-aerobic metabolism in the nitrite-dependent anaerobic methane-oxidizing bacterium Candidatus 'Methylomirabilis oxyfera'.

Wu, M., Luo, J. H., Hu, S., Yuan, Z., & Guo, J. (2019). Perchlorate bio-reduction in a methane-based membrane biofilm reactor in the presence and absence of oxygen. Water research, 157, 572-578.

Xia, S., Zhong, F., Zhang, Y., Li, H., & Yang, X. (2010). Bio-reduction of nitrate from groundwater using a hydrogen-based membrane biofilm reactor. Journal of *Environmental Sciences, 22*(2) 257–262.

Xie, G. J., Cai, C., Hu, S., & Yuan, Z. (2017). Complete nitrogen removal from synthetic anaerobic sludge digestion liquor through integrating anammox and denitrifying anaerobic methane oxidation in a membrane biofilm reactor. Environmental science & technology, 51(2), 819-827.

Xie, G. J., Liu, T., Cai, C., Hu, S., & Yuan, Z. (2018). Achieving high-level nitrogen removal in mainstream by coupling anammox with denitrifying anaerobic methane oxidation in a membrane biofilm reactor. Water research, 131, 196-204.

Yang, Y., Yu, K., Xia, Y., Lau, F. T., Tang, D. T., Fung, W. C., ... & Zhang, T. (2014). Metagenomic analysis of sludge from full-scale anaerobic digesters operated in municipal wastewater treatment plants. Applied microbiology and biotechnology, 98(12), 5709-5718.

Yeo, H., & Lee, H. S. (2013). The effect of solids retention time on dissolved methane concentration in anaerobic membrane bioreactors. Environmental technology, 34(13-14), 2105-2112.

Yergeau, E., Lawrence, J. R., Sanschagrin, S., Roy, J. L., Swerhone, G. D., Korber, D. R., & Greer, C. W. (2013). Aerobic biofilms grown from Athabasca watershed sediments are inhibited by increasing bituminous compounds concentrations. Applied and environmental microbiology, AEM-02216.

Yoon, Seong-Hoon. (2015). *Membrane Bioreactor Processes: Principles and Applications*. New York, CRC Press.

Yusuf, R. O., Noor, Z. Z., Abba, A. H., Hassan, M. A. A., & Din, M. F. M. (2012). Methane emission by sectors: a comprehensive review of emission sources and mitigation methods. Renewable and Sustainable Energy Reviews, 16(7), 5059-5070.

Zeng, J., Liu, X., Song, L., Lin, X., Zhang, H., Shen, C., & Chu, H. (2016). Nitrogen fertilization directly affects soil bacterial diversity and indirectly affects bacterial community composition. Soil Biology and Biochemistry, 92, 41-49.

Zhang, H., Ziv-El, M., Rittmann, B. E., & Krajmalnik-Brown, R. (2010). Effect of dechlorination and sulfate reduction on the microbial community structure in denitrifying membrane-biofilm reactors. Environmental science & technology, 44(13), 5159-5164.

Zhang, X., Zheng, S., Zhang, H., & Duan, S. (2018). Autotrophic and heterotrophic nitrification-anoxic denitrification dominated the anoxic/oxic sewage treatment process during optimization for higher loading rate and energy savings. Bioresource technology, 263, 84-93.

Zhang, Y., Chen, J. X., Wen, L. L., Tang, Y., & Zhao, H. P. (2016). Effects of salinity on simultaneous reduction of perchlorate and nitrate in a methane-based membrane biofilm reactor. Environmental Science and Pollution Research, 23(23), 24248-24255.

Zhang, Y., Zhong, F., Xia, S., Wang, X., Li, J., (2009). Autohydrogenotrophic denitrification of drinking water using a polyvinyl chloride hollow fiber membrane biofilm reactor. *Journal of Hazardous Materials, 170* (1), 203–209.

Zhao, H. P., Ontiveros-Valencia, A., Tang, Y., Kim, B. O., VanGinkel, S., Friese, D., ... & Rittmann, B. (2014). Removal of multiple electron acceptors by pilot-scale, two-stage membrane biofilm reactors. Water research, 54, 115-122.

Zhao, H.W., Mavinic, D.S., Oldham, W.K., And Koch, F.A. (1999). Controlling factors for simultaneous nitrificationand denitrification in two-stage intermittent aerationprocess treating domestic sewage. Water Res. 33(4), 961–97.

Zhou, C., Ontiveros-Valencia, A., Nerenberg, R., Tang, Y., Friese, D., Krajmalnik-Brown, R., & Rittmann, B. E. (2018). Hydrogenotrophic Microbial Reduction of Oxyanions With the Membrane Biofilm Reactor. Frontiers in microbiology, 9.

Zhu, J., Wang, Q., Yuan, M., Tan, G. Y. A., Sun, F., Wang, C., ... & Lee, P. H. (2016). Microbiology and potential applications of aerobic methane oxidation coupled to denitrification (AME-D) process: a review. Water research, 90, 203-215.

Zhu, J., Xu, X., Yuan, M., Wu, H., Ma, Z., & Wu, W. (2017). Optimum O2: CH4 Ratio Promotes the Synergy between Aerobic Methanotrophs and Denitrifiers to Enhance Nitrogen Removal. Frontiers in microbiology, 8, 1112.

Appendices

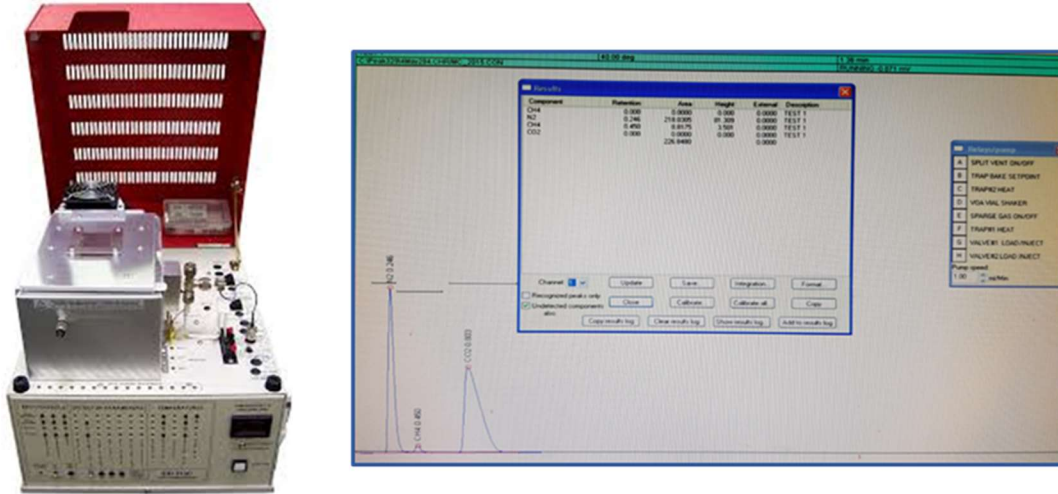## Appendix A

Measurements & Analysis apparatus

Figure A-1. Methane gas quantification in the GC-TCD Peaknet software.
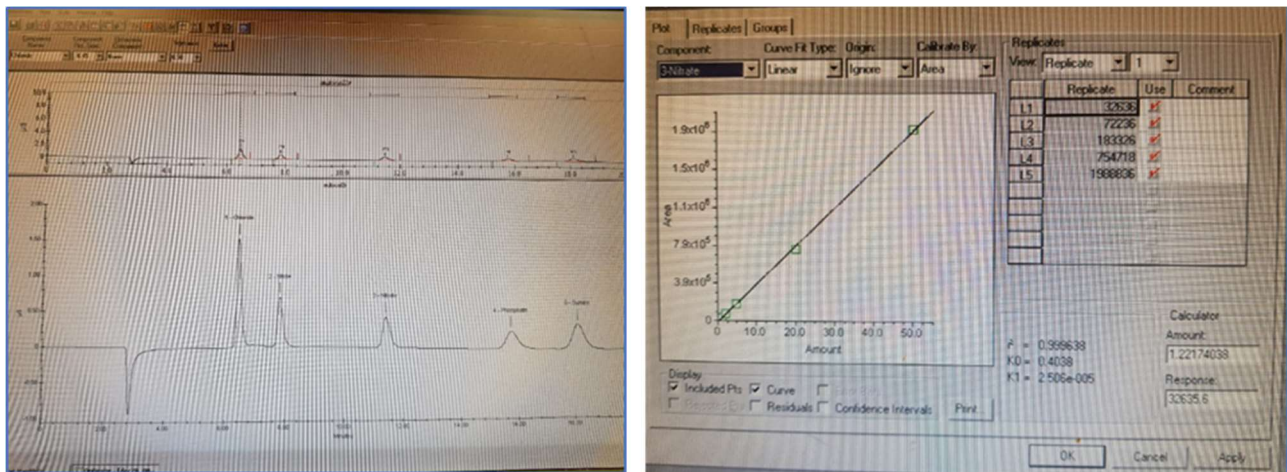

Figure A-2. Data output of the Ion Chromatograph anion analysis (Nitrate and Nitrite). The calibration curve for nitrate in the Ion Chromatograph anion analysis with r^2 value of 0.999
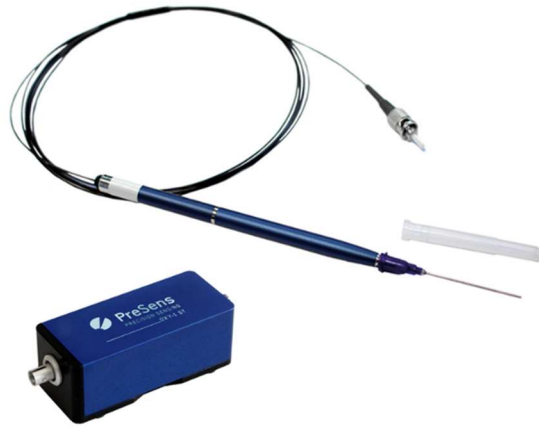
Figure A-3. The dissolved oxygen microsensor and the compact oxygen transmitter.

Figure A-4. Digital manometer (sensitive pressure gauge) used to calibrate the methane pressure.

Appendix B

Supplementary Information

In order to examine the impact of increasing the surface area of the hollow fiber membranes on the denitrification performance, a relatively large MBfR was designed and fabricated. The characterizations and operating conditions are listed in Table B.1. Apparently, the denitrification rate was challenged in this particular design. Moreover, the biofilm accumulation was hindered at this packing density, since the biofilm accumulation didn't show normal distribution along the membranes, compared to the MBfR smaller version (85 ml). Figure B-1shows the nitrate removal profile, where at an HRT of 24 hours, the removal efficiency was recorded at 40.0%. Furthermore, it can be interpreted that the length of the MBfR (55 cm) had contributed to this outcome, since methane gas transfer to the outer layer of the membrane might be challenged towards the lower section of the hollow fiber membranes. A substrate impact experiment was performed to monitor the impact on the denitrification performance, and the results are presented in Figure B-3.
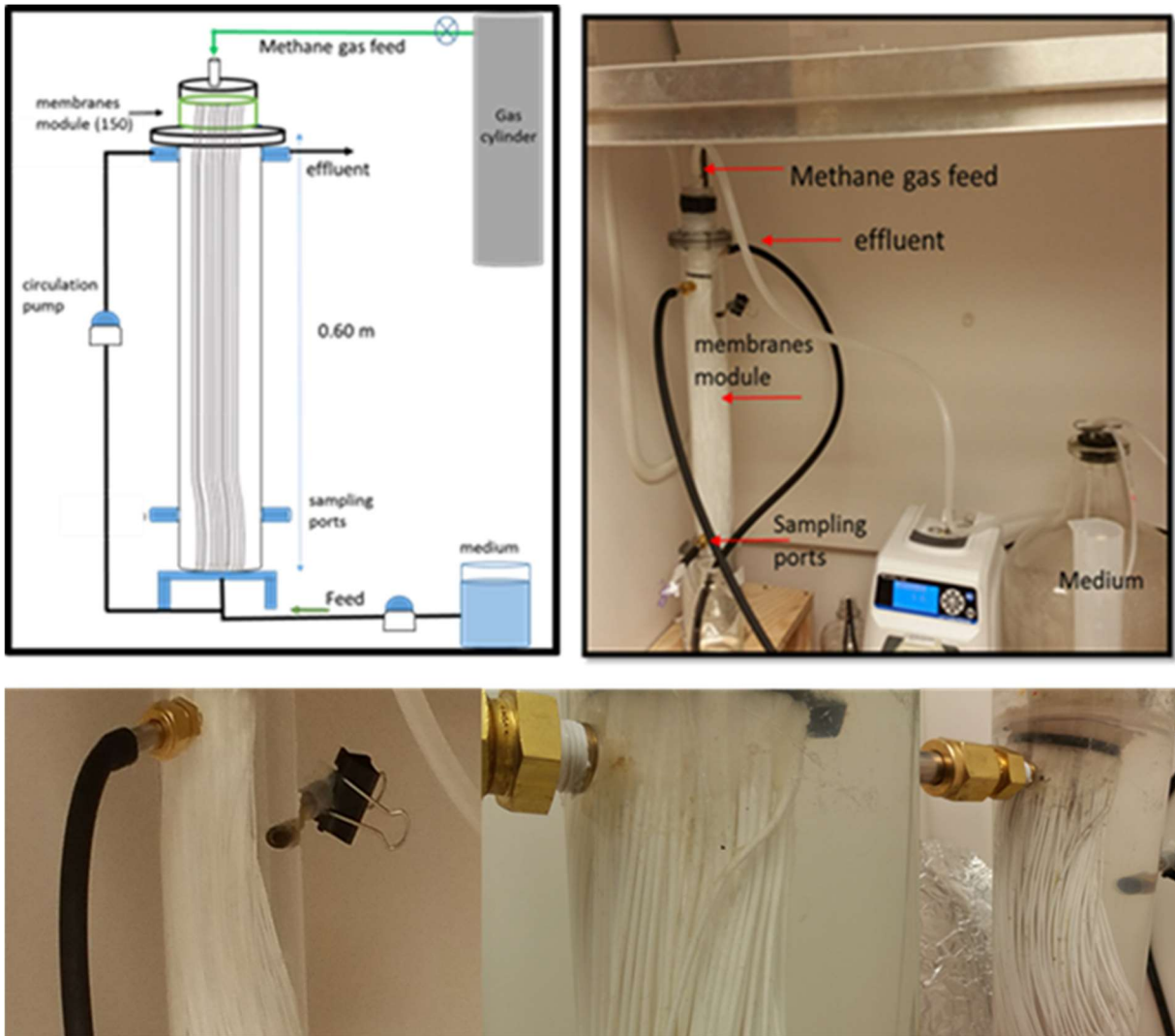
Figure B-1. Schematic diagram of a scale up MBfR (1000 ml in volume) tested for denitrification in batch and continuous modes.

Table B.1. The large MBfR characterizations and operating conditions.

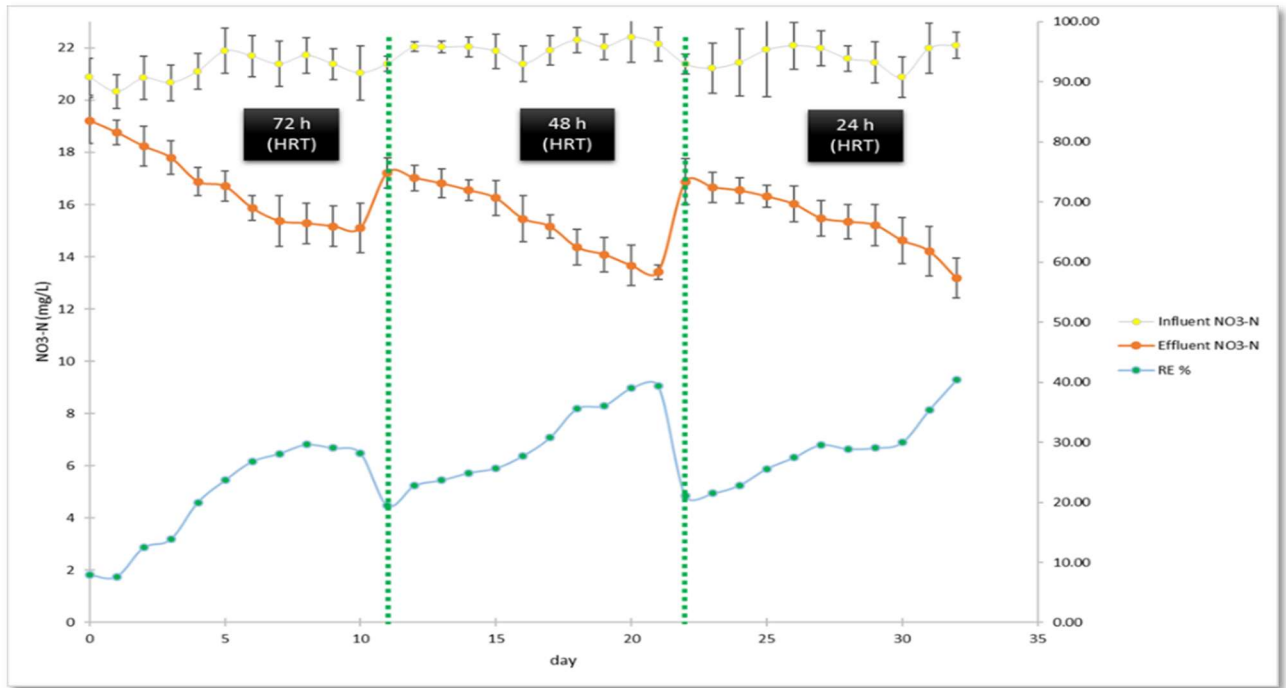| Hollow fiber membrane material	Polyvinylidene difluoride (PVDF) membrane is employed to supply methane	Continuous mode	
		Operating conditions	
HF-Membrane outer diameter (mm)	1.0	**Nitrate influent concentration. (mg NO₃⁻N /L)**	20 ± 0.5
Membranes length (cm)	55.0		
Number of membranes	150	**CH₄ (99 %) pressure**	0.1 (psig)
MBfR volume (ml)	1040		

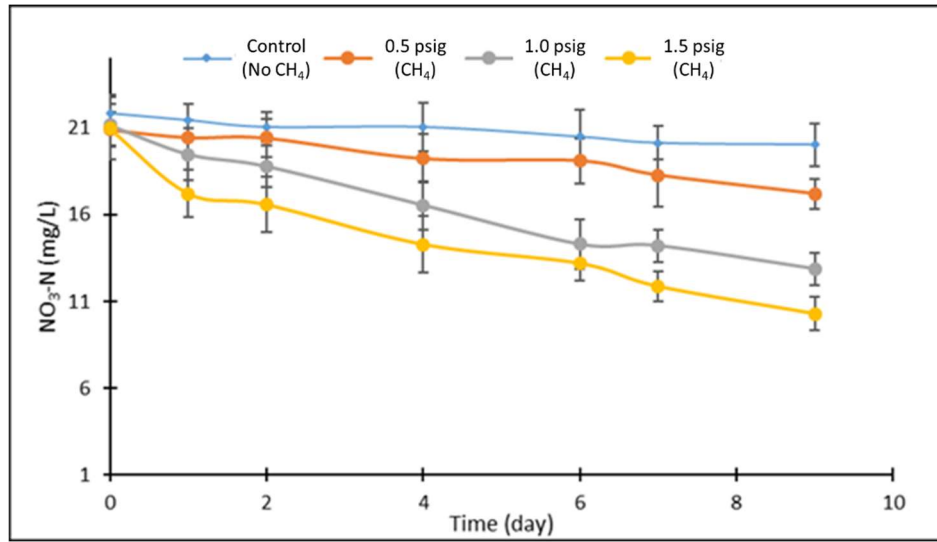**Figure B-2.** Denitrification profile from the scale-up MBfR, at HRT of 72,48 and 24 hours

Figure B-3. Denitrification profile in batch-mode operation at four methane pressures, illustrating the impact of increasing methane availability on the nitrate removal in the Large MBfR.